



National Library of Canada

Cataloguing Branch  
Canadian Theses Division

Ottawa, Canada  
K1A 0N4

Bibliothèque nationale du Canada

Direction du catalogage  
Division des thèses canadiennes

## NOTICE

The quality of this microfiche is heavily dependent upon the quality of the original thesis submitted for microfilming. Every effort has been made to ensure the highest quality of reproduction possible.

If pages are missing, contact the university which granted the degree.

Some pages may have indistinct print especially if the original pages were typed with a poor typewriter, ribbon or if the university sent us a poor photocopy.

Previously copyrighted materials (journal articles, published tests, etc.) are not filmed.

Reproduction in full or in part of this film is governed by the Canadian Copyright Act, R.S.C. 1970, c. C-30. Please read the authorization forms which accompany this thesis.

**THIS DISSERTATION  
HAS BEEN MICROFILMED  
EXACTLY AS RECEIVED**

## AVIS

La qualité de cette microfiche dépend grandement de la qualité de la thèse soumise au microfilmage. Nous avons tout fait pour assurer une qualité supérieure de reproduction.

Si il manque des pages, veuillez communiquer avec l'université qui a conféré le grade.

La qualité d'impression de certaines pages peut laisser à désirer, surtout si les pages originales ont été dactylographiées à l'aide d'un ruban usé ou si l'université nous a fait parvenir une photocopie de mauvaise qualité.

Les documents qui font déjà l'objet d'un droit d'auteur (articles de revue, examens publiés, etc.) ne sont pas microfilmés.

La reproduction, même partielle, de ce microfilm est soumise à la Loi canadienne sur le droit d'auteur, SRC 1970, c. C-30. Veuillez prendre connaissance des formules d'autorisation qui accompagnent cette thèse.

**LA THÈSE A ÉTÉ  
MICROFILMÉE TELLE QUE  
NOUS L'AVONS REÇUE**

MECHANICAL PROPERTIES OF  
ONE-PART URETHANE SEALANTS

Farouk Mohamed Hassan

A Thesis  
in the  
Centre for  
Building Studies  
Faculty of Engineering

Presented in Partial Fulfillment of the Requirements  
for the degree of Master of Engineering (Building) at  
Concordia University  
Montreal, Quebec, Canada

June 1978

© Farouk Mohamed Hassan, 1978

ABSTRACT  
MECHANICAL PROPERTIES OF  
ONE-PART URETHANE SEALANTS

Farouk Mohamed Hassan

An experimental and theoretical investigation has been undertaken on one-part urethane sealants. The factors considered included:

1. strain rate (tension tests)
2. temperature
3. priming
4. workmanship
5. strain level (stress relaxation tests)
6. substrate surface conditions

The experimental results are used to characterize the behaviour of the sealant. In addition, the test results have been organized by applying a Generalized Maxwell model and time temperature superposition technique to successfully yield two master curves which characterize the sealants' properties in a comprehensive format.

Subsequently, one of the master curves is employed in a revised joint design procedure for sealants. This design procedure supercedes existing procedures and may usefully be employed for failures in tension and at low temperature.

ACKNOWLEDGEMENTS

The author wishes to express his sincere gratitude to his thesis supervisors, Drs. S. Mattar and P.P. Fazio for their guidance, stimulus, valuable advice and critical supervision throughout the course of this research work.

The author is indebted to Drs. R. Guy, Y. Haddad and M. Shapiro for their interest and helpful comments.

The financial support of the National Research Council of Canada and La Formation de Chercheurs et d'Action Concertée (FCAC) du Quebec is gratefully acknowledged.

Thanks are extended to the Building Division of the National Research Council for their cooperation.

Thanks are also due to Dr. Sen, Mr. J. Zilkha and Mr. Denis Prud'homme for their help, and to Pam O'Cain for her concerned work in typing this thesis.

TABLE OF CONTENTS

	Page
ABSTRACT	i
ACKNOWLEDGEMENTS	ii
LIST OF TABLES AND FLOW CHARTS	v
LIST OF FIGURES	vi
LIST OF PLATES	ix
NOTATIONS	x
CHAPTER 1 - SEALANTS IN BUILDINGS	1
1.1 Introduction	1
1.2 Sealants in Buildings	2
1.3 Objectives and Scope of this Study	4
CHAPTER 2 - REVIEW OF RESEARCH	6
2.1 Introduction	6
2.2 Performance Characteristics of Sealants	10
2.3 Microscopic Aspects of Elasticity	11
2.3.1 Elasticity in Non-polymeric Solids	11
2.3.2 Elasticity in Polymers	12
2.4 Performance Tests	13
2.4.1 Tension Tests	14
2.4.2 Stress Relaxation Tests	17
2.4.3 Some Problems in Mechanical Testing of Sealants	17
2.5 Models for Viscoelastic Materials	18
2.5.1 Mechanical Models	19
2.5.2 Mathematical Models	20

	<u>Page</u>
2.6 Development to a Master Characteristic Curve	22
CHAPTER 3 - EXPERIMENTAL PROGRAM	29
3.1 Introduction	29
3.2 Preparation of Specimen	29
3.3 Curing of Specimens	34
3.4 Experimental Procedure	34
3.5 Tension Tests	37
3.6 Stress Relaxation Experiments	38
3.7 Glass Transition Temperature	38
CHAPTER 4 - THEORETICAL BASIS OF THE MASTER CURVE	43
4.1 Introduction	43
4.2 The Generalized Maxwell Model	43
4.3 Time-temperature Superposition	47
4.4 Stress Relaxation	48
CHAPTER 5 - TEST RESULTS: ANALYSIS AND DISCUSSION	53
5.1 Introduction	53
5.2 Tension Tests	53
5.3 Analysis of Tension Tests	58
5.4 Glass Transition Temperature	59
5.5 Implication on Joint Design	63
5.6 Stress Relaxation Experiments	64
CHAPTER 6 - IN CONCLUSION	101
CHAPTER 7 - FURTHER RESEARCH	106
REFERENCES	108

LIST OF TABLES

<u>Table</u>	<u>Description</u>	<u>Page</u>
2.1	A Comparison of Canadian Specifications	25
3.1	Description of the Tension Test Program	40
3.2	Description of the Stress Relaxation Test Program	40
5.1	Statistical Analysis of Results	67

LIST OF FLOW CHARTS

<u>Flow Chart</u>	<u>Description</u>	<u>Page</u>
5.1	Suggested Procedure for Joint Design	69

LIST OF FIGURES

<u>Figure</u>	<u>Description</u>	<u>Page</u>
2.1	Engineering stress-strain curves for selected materials, as determined by tensile tests at room temperature	26
2.2	Five regions of viscoelastic behaviour (for polystyrene sample)	27
2.3	Stress distribution pattern in sealant edges at a specific extension (about 40%) of a (13 x 13 mm) joint	27
2.4	The property surface	28
3.1	Schematic diagram of the sealant specimen prior to testing	41
3.2	Differential thermocouple for measurement of temperature difference	42
4.1	Generalized Maxwell model for linear viscoelastic materials. A spring and dashpot system in parallel	52
5.1	Nominal stress-strain for one-part urethane sealant at 60°C	59
5.2	Nominal stress-strain for one-part urethane sealant at 40°C	70
5.3	Nominal stress-strain for one-part urethane sealant at 22.50°C	71
5.4	Nominal stress-strain for one-part urethane sealant at 0°C	72
5.5	Nominal stress-strain for one-part urethane sealant at -20°C	73
5.6	Nominal stress-strain for one-part urethane sealant at -40°C	74
5.7	Nominal stress-strain for one-part urethane sealant at cross head speed 5cm/min.	75



<u>Figure</u>	<u>Description</u>	<u>Page</u>
5.8	Nominal stress-strain for one-part urethane sealant at cross head speed 1cm/min.	76
5.9	Nominal stress-strain for one-part urethane sealant at cross head speed 0.5 cm/min.	77
5.10	Nominal stress-strain for one-part urethane sealant at cross head speed 0.05cm/min.	78
5.11	Nominal stress-strain for one-part urethane sealant at cross head speed 0.01cm/min.	79
5.12	Nominal stress-strain for one-part urethane sealant at cross head speed 0.005cm/min.	80
5.13	Nominal stress-strain for one-part urethane sealant at room temperature for different substrates	81
5.14	Nominal stress-strain for one-part urethane sealant for primed and unprimed substrates	82
5.15	Nominal stress at break-temperature	83
5.16	Strain at break versus temperature	84
5.17	Nominal stress-strain curves from Figure 5.1 reduced to unit strain rate at 60°C	85
5.18	Nominal stress-strain curves from Figure 5.2 reduced to unit strain rate at 40°C	86
5.19	Nominal stress-strain curves from Figure 5.3 reduced to unit strain rate at 22.5°C	87
5.20	Nominal stress-strain curves from Figure 5.4 reduced to unit strain rate at 0°C	88
5.21	Nominal stress-strain curves from Figure 5.5 reduced to unit strain rate at -20°C	89
5.22	Nominal stress-strain curves from Figure 5.6 reduced to unit strain rate at -40°C	90

<u>Figure</u>	<u>Description</u>	<u>Page</u>
5.23	Differential thermal analysis graph	91
5.24	Log $a_T$ versus temperature	92
5.25	Experimentally determined master curve from tensile test results	93
5.26	Experimental relaxation curves of one-part urethane sealants at 60°C	94
5.27	Experimental relaxation curves of one-part urethane sealants at 22.5°C	95
5.28	Experimental relaxation curves of one-part urethane sealants at -20°C	96
5.29	Relaxation modulus versus time at 60°C	97
5.30	Relaxation modulus versus time at 22.5°C	98
5.31	Relaxation modulus versus time at -20°C	99
5.32	Experimentally determined master curve from stress relaxation test results	100

9

LIST OF PLATES

<u>Plate</u>	<u>Description</u>	<u>Page</u>
1.1	Example of a jointing failure in the olympic buildings, Montreal-	6
1.2	Cohesive failure of a joint in the olympic buildings, Montreal	7
3.1	The wooden mould for forming test samples	41
3.2	Tensile loading of test specimen within the environmental chamber	42

NOTATIONS

$a_T$	the shifting factor
$C_1, C_2$	constants
$E$	the elastic modulus
$E_r(t)$	the relaxation modulus
$\underline{E}$	the elastic tensor modulus
$R_t$	constant strain rate
$R(\tau)$	the relaxation kernel
$t$	time
$T$	temperature
$T_0$	reference temperature
$T_g$	glass transition temperature
$\epsilon(t)$	strain at time "t"
$\dot{\epsilon}(t)$	strain rate at time "t"
$\epsilon_0$	initial strain
$\bar{\epsilon}_i$	initial strain in stress relaxation test "i"
$\underline{\epsilon}(t)$	strain tensor at time "t"
$\eta$	the coefficient of viscosity
$\lambda$	the extension ratio
$\sigma_0$	initial true stress
$\sigma_t$	the nominal stress at time "t"
$\sigma(t)$	the "true" stress at time "t"
$\sigma^*(t)$	the theoretical nominal stress at time "t"
$\dot{\sigma}(t)$	stress rate at time "t"
$\underline{\sigma}(t)$	the stress tensor at time "t"
$\tau$	the relaxation time

## CHAPTER 1

### SEALANTS IN BUILDINGS

#### 1.1 Introduction

The technological advances which have revolutionized so many industries in the later half of the twentieth century have also affected building, especially with respect to weather-proof construction. In traditional building, centuries of experience resulted in flashing, weep holes and other design details to catch and divert rain water which leaked into the construction. Moreover, the sealing compounds, then in use, fulfilled the modest expectations admirably. With the development and use of factory-produced components, such as panels, in curtain wall buildings and other industrialized construction, the sealing of joints has become an important problem.

The large dimensions of components have led to absolute and differential movements which impose severe requirements on the sealing compounds, and this problem has been compounded by the diversity of materials with greatly differing properties now on the market. It is not surprising, therefore, to learn that leaky joints are common in contemporary buildings<sup>(1)</sup>. For a dramatic example of a jointing failure, see Plates 1.1 and 1.2 of construction details at the olympic buildings in Montreal, where literally miles of sealants had to be placed at the cost of several million dollars.

---

(1) Dietz, A.G.H., in Introduction to "Building Seals and Sealants", Panek, J. (Ed.), American Society for Testing and Materials, ASTM, STP606, 1976.

Notwithstanding these difficulties, modern sealants have made possible constructions that were previously too difficult to accomplish. In providing continuity between large panels, for instance, sealants have to fulfill all the expectations of the building envelope while accommodating cyclic dimensional changes of up to  $\pm 50\%$  of the joint width. Sealants are used to exclude the external environment, i.e., rain, moisture, pollutants and so on, to protect against mechanical or chemical attack, to exclude noise and to reduce to a minimum air infiltration or exfiltration (an important consideration for energy conservation). The great increase in the number and volume of applications of sealants, in conjunction with the importance of the functions which sealants have to perform in buildings, provides a context for the impetus in the development of new types of sealants with improved physical properties and also for information needs for improved design and application purposes.

## 1.2 Sealants in Buildings

In recent years, the progress in sealant technology has been significant. The new sealants are formulated from synthetic elastomeric polymers which, in an uncured form can be poured or extruded, and as such they are ideal for filling joints and for binding building elements. Their capacity to deform under load is such that they can, when properly designed, accommodate the contraction or expansion of the rigid structures without destroying the bonds. For instance, most of the newly developed sealants can be stretched to at least 100% of their original width under normal service conditions (i.e., at temperatures and rates of deformations

encountered during its life) and on removing the load return roughly to their original width. Because the modern sealants can be poured or extruded, they can also be used in a wide variety of joints encountered in building construction.

Sealants are available in three main forms:

- i) putty - like mastics
- ii) non-cured tapes
- iii) cured gaskets<sup>(2)</sup>

Only sealants in putty-like mastic form are of interest here. These sealants which are fluid at room temperature are available in one- or two-component formulations; one-component formulations having the advantage of not requiring mixing before application and consequently an extended "pot" life. However, the curing agent which is premixed into the base material is sensitive to moisture (hence, the curing process to a rubbery elastomeric material within days) and as such results in limited shelf life. The two-component sealants consist of an accelerator part and the base compound part, and so their curing time, pot life and physical properties can be adjusted although they are at a disadvantage in terms of application when compared to one-part sealants<sup>(3)</sup>. One further differentiation of sealants is of interest for building purposes, viz, self-levelling (which are often employed in horizontal seams and joints) and non-sagging thixotropic (which was used in vertical joints where they stay in place even before curing is complete).

---

(2) Dumasis, A., "Sealants", Reinhold Publishing Corp., 1967.

(3) Ibid

The main types of sealants in use in building construction are based on the following binders: silicones, polysulphides and urethanes, one- and two-components. These sealants provide a variety of characteristics over a wide range of service conditions such as temperature (extremes and fluctuations, diurnal and seasonal), rate of deformation, resistance to weathering, moisture vapour transmission, permeability, etc.

The important mechanical properties of sealants include ultimate tensile strength and elongation, shear strength, fatigue resistance and adhesive strength. Each shape of joint (say, rectangular, trapezoidal or triangular) will induce different strains and stresses in the sealant which fills it. The most common shape of joints in use in buildings is the rectangular one because of its adaptability to various kinds of sealants and also because of the ease of forming them, and as such, is often considered central to the study of sealant performance.

### 1.3 Objectives and Scope of this Study

The excellent performance of modern sealants has attracted the attention of architects, engineers, contractors, maintenance specialists and researchers. It is evident that a study which sets out to meet the expectations of all these different groups (and others besides) would be a Herculean task. The objectives of this study have been dictated by a review of the information needs in the field. Since the performance of both silicones and polysulphides have been examined extensively, only urethane sealants will be studied in this research project. The objectives of the study are:



- (i) To determine the mechanical properties of urethane sealants (complying to CGSB 19-GP-16M, 1977). In this part of the study, which is mainly experimental in nature, the stress-strain-temperature-time aspects of the material will be examined in order to characterize the material. (The effect of priming and substrate material will also be investigated, although not to the same extent).
- (ii) To model the performance of urethane sealants. The applicability of the model to represent the viscoelastic behaviour of the urethane sealant will be evaluated.
- (iii) To study the stress relaxation properties of the urethane sealant. Data from this experimental part of the study will be used in the evaluation of the model.
- (iv) To use the information obtained from this research project and others available in the literature in a design procedure.
- (v) To present a critical review of the literature on the mechanical properties of sealants.



PLATE 1.1 EXAMPLE OF A JOINTING FAILURE  
IN THE OLYMPIC BUILDINGS, MONTREAL



PLATE 1.2 COHESIVE FAILURE OF A JOINT IN  
THE OLYMPIC BUILDINGS, MONTREAL

CHAPTER 2  
REVIEW OF RESEARCH

2.1 Introduction

In the last decade since Karpati's comprehensive literature survey of sealants<sup>(1)</sup>, there has been a considerable amount of research and development in construction sealants. The review undertaken in this thesis takes stock of some of the work done in this fast-developing field and provides a descriptive summary of recently published information on the physical and mechanical properties of sealants. Theoretical aspects of sealants' mechanical behaviour are also examined to provide a basis for understanding the mechanism of their performance and for designing experiments and standard test procedures.

Although this review of research into the behaviour of sealants is general in scope, emphasis is given to tensile tests and stress relaxation experiments which are versatile tools for investigating mechanical performance. Theoretical studies of other visco-elastic materials (such as rubbers and plastics) which illustrate the performance of sealants are also reviewed.

2.2 Performance Characteristics of Sealants

The chemical composition of different sealants varies greatly and, consequently, their thermal and electrical properties are quite different. Their mechanical properties, however, are determined mainly

---

(1) Karpati, K.K., "Literature Survey of Sealants", Journal of Paint Technology, Vol. 40, No. 523, August 1968, pp. 337-347 (also Technical Paper No. 287 of the Division of Building Research, National Research Council of Canada, NRC 10424.)

by the way in which the molecules are packed together. In spite of the difference in their chemical composition, the packing of the molecules is often very similar and so the mechanical properties of the different sealants show great similarity.

There are a variety of tests which provide information about the mechanical properties of materials, the most common being the tensile extension tests at constant strain rate. Figure (2.1) gives the stress-strain curve obtained from such tests at room temperature for samples of different materials. Compared to steel, which can fail at about 30 percent elongation and about  $420 \text{ MN/m}^2$  (60 Ksi), polymers (and sealants, in particular) have a broader range of performance from the brittle polymers with very little elongation prior to failure of those which, like rubber, can be extended 1000 percent, and with strengths from 0 to  $70 \text{ MN/m}^2$  (10 Ksi).

To obtain a more complete representation of the mechanical properties of materials, the stress-strain characteristics should be examined carefully. These characteristics vary with changes in strain rate and temperature. Sealants used in building are subjected to wide temperature variations, both diurnal and seasonal, and the consequent joint movements during their working life. Thus, the influence of temperature and strain rate on the mechanical properties of sealants is of interest to both designers and researchers.

It is evident from the relaxation modulus-temperature curve (Figure (2.2) for polystyrene which is representative of most polymers but with varying temperature scales) that the mechanical properties of sealants vary significantly with temperature. Five regions of mechanical

behaviour can be distinguished, namely, the glassy region with high elasticity but small elongation, the leathery region with no elasticity, the rubbery region with high elasticity and high elongation, and the viscous and liquid regions with no elasticity.

Research on the performance of sealants has dealt, almost exclusively, with the rubbery stage of the five phases of the materials' behaviour. Sealants on the rubbery plateau display elastic behaviour, i.e., their deformation is reversible. On the flow side of the plateau (which occurs with increase in temperature), sealants tend to lose their elastic properties and flow out of the vertical joints. On the glassy side of the plateau, however, sealants stay elastic but the stresses induced during elongation of the material tend to be large and because the joint opening is widest at the lower temperature ranges, failure - adhesive or cohesive - is likely in this region.

In providing continuity between building elements, sealants have to accommodate movements of up to +50% of the original joint width at temperatures ranging from -40°C to +60°C. Moreover, the rate of joint movement is not constant and this implies that sealants in joints will be subjected to variable strain rates. It is, therefore, essential in sealants selection to ensure that they will perform in an optimal manner at all conditions. This implies the selection of a material for which the rubbery plateau coincides with the temperatures prevalent during its service life.

Two limiting factors for the proper functioning of a sealant have been identified and they are its cohesive and adhesive strength.

The cohesive strength is needed to maintain the original shape of the sealant after the repeated movements of the joint and this requires a high modulus of elasticity. However, a high modulus implies high cohesive stresses for a given strain at any section in the sealant and high adhesive stresses at the interface of the sealant and the substrate. This, in turn, may lead to adhesive failure and, hence, the adhesive strength limitation implies a low modulus of elasticity.

### 2.3 Microscopic Aspects of Elasticity

The elastic deformation which crystalline solids, inorganic glasses and metals undergo in response to an applied load is simply a macroscopic manifestation of changes in bond lengths, bond angles between atoms, ions or molecules in the solid.

#### 2.3.1 Elasticity in Non-polymeric Solids

The mechanism of elasticity in non-polymeric solids which results from energy changes at the atomic or molecular levels of the material is reasonably well understood (2,3). The atoms in a perfect crystal, for instance, assume an equilibrium position when external forces are not acting. On application of a tensile force, the distance between atoms is increased until a new equilibrium position is attained. Removal of the deforming force allows the atoms to regain their original positions. The response to the application and removal of forces is instantaneous and complete.

- 
- (2) Ralls, K.M., Courtney, T.H. and Wulff, J. "Introduction to Material Science and Engineering", John Wiley and Sons, 1976.
  - (3) McClintock, F.A. and Argon, A.S. (Eds.), "Mechanical Behaviour of Material", Addison-Wesley, 1966.

### 2.3.2 Elasticity in Polymers

The relationship between atomic and molecule bonding described previously is not applicable for describing the elasticity of polymers because of their characteristic molecular structure. The elastic behaviour of polymers (and sealants) in the rubbery stage stems from the chain structure of the molecule<sup>(4)</sup>. As a polymer is extended, the highly coiled, cross-linked molecules are straightened and aligned; on removal of the load, they coil up once more in order to recover the elastic strain. This process causes thermal agitation of the molecular chain segments and results in time-dependent elasticity (often nonlinear) which cannot be treated in terms of potential energy. The nonlinear nature of rubbery elasticity necessitates an operational definition of stiffness distinct from Young's modulus which is used to characterize linearly elastic materials. One useful means of specifying the elastic modulus is the relaxation modulus,  $E_r$ , (see ordinate of Figure (2.2)) which has been defined as "the ratio of the stress to a small imposed strain after a fixed length of time,  $t$ "<sup>(5)</sup>.

The thermal motion, which is virtually absent in the glassy stage, causes segments of a molecule to rotate according to the valence angles around each link in the chain, thus twisting the molecule into different conformations. The number of possible conformations which are characterized by the distance between the two chain ends is restricted by

---

(4) Trelear, I.R.G., "The Physics of Rubbery Elasticity", Clarendon Press, Oxford, 1958.

(5) Ralls, K.M., et al, Op. Cit. (2).



the length of the molecules or, in the case of cross-linked materials by the length of chains between cross-links. In the kinetic theory of rubbery elasticity, the entropy of a system of polymers has been shown to be dependent on the number of available chains<sup>(6)</sup>. By considering entropy changes accompanying a deformation in terms of three-dimensional Cartesian coordinates, it is possible to relate the shear modulus to the molecular structure of the material.

The dependence of relaxation modulus of polymers on temperature is most marked (Figure (2.2)). The effect of increasing temperature is to enhance the motion of the molecular chain segments. The degree of cross-linking also affects the elastic properties significantly. For lightly cross-linked polymers, the relaxation modulus remains relatively high until the melting (or glass transition) temperature, while totally cross-linked polymers display glassy behaviour until the temperature at which chemical decomposition begins.

Poisson's ratio is often used as a rough guide to the mechanical characteristics of a polymer. In the glassy range (and also for totally cross-linked polymers), Poisson's ratio lies in the same range as metals and ceramics, while above the glass transition temperature it is typically in the range of 0.4 to 0.5, i.e., deformation at constant volume.

#### 2.4 Performance Tests

An examination of the test methods in standards (for example CGSB 19 GP series and ASTM) reveals that they may be divided into two

---

(6) Treloar, I.R.G., Op. Cit. (4)

main categories (see Table 2.1)<sup>(7)</sup>. One set of tests is designed to provide information about sealants for application purposes while the other tests deal with properties after application and curing. A limited number of the performance tests are of interest in this review.

Cyclic tests with simultaneous temperature changes come closest to modelling the service conditions of sealants, however, the period of time during which the specimen is subjected to various conditions is purely arbitrary. Also, complex cyclic tests can only be designed if the material properties are known from tests which use simple loading patterns such as tensile extension at specific strain rates and stress relaxation at constant strains. These are two of the principal test methods which are used to describe the material properties of polymers by means of stress, strain, time and temperature.

#### 2.4.1 Tension Tests

There is considerable agreement among researchers that the tensile test is the most suitable because it encompasses three variables at any given temperature. It has been selected because tensile loads are most likely to cause failure. Moreover, most laboratories are equipped for tensile tests which are easily and quickly performed.

There is a consensus amongst researchers (referred to later) that the primary factors which govern the performance of sealants *qua*

---

(7) Panek, J., "A Review of Sealant Specifications Throughout the World", in Panek, J. (Ed.), "Building Seals and Sealants", American Society for Testing and Materials, ASTM, STP 606, 1976.

material are stress, strain, rate of deformation and temperature. Although the behaviour of sealants is dependent on such variables as humidity, oxygen, radiation, type and condition of substrates, these are considered secondary in characterizing the material. To characterize any sealant, the primary factors are to be found whilst other factors are kept constant. It is evident, however, that permutations and combinations of temperatures and strain rates will result in a large number of different stress-strain curves. This raises the problem of deciding which curves define the material properties explicitly.

A single curve which accommodates the four basic variables resolved the problem of material characterization. Smith <sup>(8)</sup> suggests that dividing the stress and strain at each point on a curve by the strain rate would result in all tensile curves reducing to unit strain rate and should thus provide a single curve at a given temperature. This reduction to a single cumulative curve is known to be valid only if the "true" stress (which is the stress calculated through the minimum cross-section at any time during the test) is known. When these cumulative curves are temperature dependent, they can be further reduced to a single "master" stress-strain-time-temperature' curve by means of the time-temperature superposition technique <sup>(9)</sup>. These

---

(8) Smith, T.L., "Viscoelastic Behaviour of Polyisobutylene under Constant Rates of Elongation", J. of Polymer Science XX (1956), pp. 89-99.

(9) Williams, M.L., Landel, R.F. and Ferry, J.D., "The Temperature Dependence of Relaxation Mechanisms in Amorphous Polymers and other Glass-forming Liquids", J. Am. Chem. Soc., LXXVII, 1955, pp. 3701-3707.

temperature reduced master curves provide an ideal device for comparing polymers at equivalent thermodynamic and rheological states. The master curve, if derived, should permit the direct comparison of rheological and fracture properties of typical elastomers based on combinations of chemical composition and molecular architecture.

In early research on polymers, Smith<sup>(10)</sup> used dumbbell-shaped specimens where a parallel stress-field-hence "true" stress, could be approximated. Most tests approved by standards and specifications associations as well as researchers are based on the practical and simple approach of modelling sealant beads in joints. The test specimen models the complicated stress field (Fig. (2.3)) of the test specimen<sup>(11)</sup> which can thus fail adhesively or cohesively as in a joint. The specimen's high width to length ratio (the dimensions of the sealant bead are 13x13x51mm) amplifies the stress concentration at the edges and "true" stress is not obtained in this type of specimen. Smith<sup>(12)</sup> and, subsequently Karpati<sup>(13,14,14,16)</sup> have modified this approach by multiplying the stress at any strain level by a factor  $(1+c)$  where  $c$  is the strain. This modification is particularly applicable to dumbbell-shaped specimens where the stress

---

(10) Smith, T.L., Op. Cit (8)

(11) Castiff, E., Hoffman, R.F. and Kowalski, R.T., "Predicting Sealant Performance through Computers", Building Research, April/June 1974.

(12) Smith, T.L., Op. Cit (8)

(13) Karpati, K.K., "Mechanical Properties of Sealants: I - Behaviour of Silicone Sealants as a Function of Temperature", J. Paint Technology, Vol. 44, No. 565, Feb. 1972, pp. 55-62.

(14) Karpati, K.K., "Mechanical Properties of Sealants II - Behaviour of a Silicone Sealant as a Function of Rate of Movement", J. Paint Technology, Vol. 44, No. 569, June 1972, pp. 58-66.

(15) Karpati, K.K., "Mechanical Properties of Sealants: III - Performance Testing of Silicone Sealants", J. Paint Tech., Vol. 44, No. 571, Aug. 1972, pp. 75-85.

(16) Karpati, K.K., "Mechanical Properties of Sealants IV: Performance Testing of Two-part Polysulphide Sealants", J. Paint Tech., Vol. 45, No. 580. May 1973. pp. 49-57

field is more uniform<sup>(17)</sup>. Karpati's use of this approach to obtain the "true" stress is based on approximations which avoid such problems as the non-uniform stress field at any section, the inequality of stress at different sections and the stress concentrations at the edges. The errors involved seem to be insignificant, and the approximations are not invalidated by research findings.

#### 2.4.2 Stress Relaxation Tests

Another convenient method of investigating the time dependence of the mechanical properties of sealants is the stress relaxation test. This kind of test is not subject to the experimental errors which plague creep tests where it is not only the length of the specimen that changes but its cross-sectional area as well. In relaxation experiments, the cross-sectional change is negligible and the results lend themselves to studies of the structural changes in polymers. Tobolsky<sup>(18)</sup>, for instance, whilst investigating the molecular structure of polymers by means of changes in the mechanical properties confirmed that a small change in the number of chains causes extensive changes in the mechanical properties of the material.

#### 2.4.3 Some Problems in Mechanical Testing of Sealants

When the modern sealants were first introduced into the building construction market, standard rubber test methods were used to characterize them. Strains of up to 900% on dumbbell specimens

---

(17) Smith, J.L., Op. Cit. (8)

(18) Tobolsky, A.V., "Properties and Structure of Polymers", John Wiley and Sons, 1967.

were reported and this soon caused confusion to designers. The early standard test methods designed for sealants, while improving on existing methods did not predict field performance accurately nor differentiate adequately among performance characteristics of sealants on the market<sup>(19)</sup>.

Cook<sup>(20)</sup>, in evaluating joint designs, proposed the need for more realistic joint specimen lengths which would model actual field joints. Although the tensile tests on prismatic sealant beads do not evade this criticism, the stresses imposed on the material by similar deformations are deemed to be greater in the test specimen than in the field joints and, as such, the standards are conservative. The behaviour of sealants in situ cannot be completely understood by tension tests alone. Stress relaxation experiments can be used to obtain a more complete picture of the performance of sealants with respect to such factors as time effects or strains on the adhesive bonds.

## 2.5 Models for Viscoelastic Materials

The viscoelastic response of real materials have been characterized by mechanical models based on analogies to spring and dash-pot elements which only represent linear viscoelastic behaviour. Due to the shortcomings of these models to predict the actual behaviour of materials (obtained from test results), other approaches, based purely on mathematical models have been introduced to account for the nonlinearity exhibited by some real viscoelastic materials. The

---

(19) Peterson, C.M., "Problems of Testing Sealants", in Damusis A (Ed.), "Sealants", Reinhold Publishing Corp. 1967.

(20) Cook, J.P., "The Effect of Specimen Length on the Laboratory Behaviour of Sealants", Highway Research Board, Jan. 1965.

functions characterizing these models are often expressed in parametric form such that the expressions can be characterized specifically from experimental results.

### 2.5.1 Mechanical Models

The Maxwell model consisting of a spring and dashpot in series and the Kelvin-Voigt model comprising the same mechanical systems in parallel are two simple models which display qualitatively retarded-elastic, creep and relaxation phenomena for an ideal linear viscoelastic material. Unlike the Hookean solid or Newtonian fluid, these models provide only an approximate quantitative representation of real viscoelastic materials. Stress in the material is represented by axial force in the model while axial elongation and velocity represent strain and strain rate.

In the Kelvin-Voigt element, the total axial force is the sum of the spring and dashpot forces, the displacement being the same for both. In the Maxwell element, however, the force is the same in both spring and dashpot, but the displacement (or velocities) are summed. The analogous equations for the continuum as applied to the viscoelastic are:

$$\text{Kelvin-Voigt} - \sigma = E\epsilon + \eta\dot{\epsilon} = E(\epsilon + \tau\dot{\epsilon}) \quad (2.1)$$

$$\text{Maxwell} - \dot{\epsilon} = \frac{1}{E}\dot{\sigma} + \frac{1}{\eta}\sigma = \frac{1}{E}(\dot{\sigma} + \frac{1}{\tau}\sigma) \quad (2.2)$$

where  $E$  is the elastic modulus,  $\eta$  is the coefficient of viscosity and the relaxation time  $\tau$  is given by  $\frac{\eta}{E}$ .

Stress relaxation is best illustrated by the Maxwell element. If strain  $\epsilon_0$  is instantaneously applied at  $t = 0$  and then held constant, the instantaneous response is

$$\sigma_0 = E\epsilon_0 ,$$

and the subsequent behaviour obtained from Equation (2.2) is given by  $\dot{\epsilon} = 0$ . Thus,

$$\sigma(t) = E\epsilon_0 e^{-\frac{t}{\tau}} \quad (2.3)$$

The relaxation time  $\tau$  being the time required for the stress to relax by  $\frac{1}{e}$  from its initial value of  $E\epsilon_0$ . Equation (2.3) is usually employed to describe the general stress relaxation curves.

### 2.5.2 Mathematical Models

The relation between the stress tensor  $\underline{\sigma}(t)$ , the strain tensor  $\underline{\epsilon}(t)$  and time  $t$  for linear viscoelastic materials can be expressed by the Volterra response equation<sup>(21,22)</sup> as follows:

$$\underline{\sigma}(t) = \underline{E} [\underline{\epsilon}(t) - \int_0^t \underline{R}(t-\tau) \underline{\dot{\epsilon}}(\tau) d\tau] \quad (2.4)$$

where  $\underline{E}$  = the elastic tensor modulus.

$\underline{R}(t-\tau)$  = the relaxation function which is usually a positive decreasing function of time

The relaxation behaviour of nonlinear viscoelastic materials has been considered by Distefano and Todeschini<sup>(23)</sup> and expressed for a uniaxial

---

(21) Volterra, V., "Fonctions de Lignes", Gauthier-Villand, Paris, 1913.

(22) Distefano, N., Todeschini, R., "Modelling, Identification and Prediction of a Class of Nonlinear Viscoelastic Material (I)", Int. J. Solids Structures, Vol. 9, 1973, pp. 805-818.

(23) Ibid



case as

$$\sigma(t) = g(\epsilon(t), K_1, K_2, \dots) + \int_0^t h(\epsilon(t), b_1, b_2, \dots) R(t-\tau) d\tau \quad (2.5)$$

In Equation (2.5) the function  $g$  represents the elastic response in a parametric form and the function  $h$  accounts for the nonlinear hereditary effects and is also given in a parametric form.  $K_1, K_2, \dots$  and  $b_1, b_2, \dots$  are unknown constants. The choice of  $g$  and  $h$  are guided by a qualitative knowledge of the viscoelastic behaviour of the material. The relaxation function is assumed to satisfy an  $N^{\text{th}}$  order differential equation with unknown constant coefficients  $a_0, a_1, \dots, a_{N-1}$  of the following form<sup>(24)</sup>.

$$a_0 R + a_1 R^{(1)} + a_2 R^{(2)} + \dots + a_{N-1} R^{(N-1)} + R^{(N)} = 0 \quad (2.6)$$

In simplifying the analysis, Haddad<sup>(25)</sup> assumed that the instantaneous elastic response was linear and could be represented only by the elastic constant  $E$ . Thus, for a stress relaxation test "i" under constant strain  $\bar{\epsilon}_i$ , Equation (2.5) can be modified to give the theoretical stress  $\hat{\sigma}(t)$ ,

$$\hat{\sigma}(t) = E \bar{\epsilon}_i + h(\bar{\epsilon}_i, b_1, b_2, \dots) \int_0^t R(\tau) d\tau \quad (2.7)$$

where  $i = 1, 2, \dots, n$  (denoting the number of relaxation experiments and  $E, \bar{\epsilon}_i$  represents the elastic response of the material. The material constants are determined almost exclusively from experimental data

(24) Ibid

(25) Haddad, Y.M., "Mathematical Modelling in the Realm of Nonlinear Viscoelasticity", Proceedings of Conference, 1977 pp. 847-857.

obtained from relaxation tests. The numerical processes for deriving the roots of the characteristic equations, (which are often real and distinct) are unduly involved and time-consuming. For the instances where the roots are multiple and complex, the modifications complicate matters even more (perhaps a reason for the lack of examples in the published literature with such analyses). Furthermore, such a complicated model cannot be readily used in design.

## 2.6 Development to a Master Characteristic Curve

Although new products of sealants are constantly being introduced into the market, the research identifying their mechanical properties is lagging. The effect of temperature and strain rate on their behaviour has not been considered for most of these products. This should not, however, belittle the importance of the considerable amount of research reported in the literature.

Smith's<sup>(26)</sup> analysis of the viscoelastic properties of polyisobutalene at different temperatures and deformation rates is a precursor of a series of test programs conducted to characterize other polymers; in particular sealants. The generalized Maxwell model (based on the assumption that the material is linearly viscoelastic) which Smith employed to obtain cumulative stress-strain curves per unit strain rate has been used along with the time-temperature superposition principle in the characterization of sealants (see, for example, Karpati's articles

---

(26) Smith T.L., Op. Cit (8)

referred to earlier). Assuming that all relaxation times have the same temperature dependence and that the modulus of each spring in the Maxwell model is proportional to the absolute temperature, the cumulative curves (at unit strain rates) could be shifted along a log time scale so as to superimpose them on each other; hence, the master curves. The superposition at a reference temperature was achieved by means of a shifting factor  $a_T$ , obtained from an empirical formula (WLF equation)<sup>(28)</sup>.

$$\text{Log } a_T = \frac{-C_1(T-T_g)}{C_2+T-T_g} \quad (2.8)$$

where  $C_1$  and  $C_2$  are empirical constants determined from experiments.

Karpati's review<sup>(29)</sup> formed the basis for the subsequent research<sup>(30,31,32,33)</sup> into highly elastic one-part silicone sealants and two-part polysulphide sealants available on the market. One of the highlights of Karpati's work is the development of a three-dimensional property surface to represent the viscoelastic behaviour of two-part polysulphide sealants (Figure (2.4)). The complexity of three-dimension coordinate system to characterize the material was deemed to be impractical. The concept of a failure envelope derived from actual tests provides another tool for characterizing the material independently of time or temperature.

---

(28) Williams, M.L., et al, Op. Cit.(9)

(29) Karpati, K.K., Op. Cit.(1)

(30) Karpati, K.K., Op. Cit.(13)

(31) Karpati, K.K., Op. Cit.(14)

(32) Karpati, K.K., Op. Cit.(15)

(33) Karpati, K.K., Op. Cit.(16)

The link between experiments designed to establish the mechanical properties of sealants at various temperatures and strain rates and actual performance *in situ* forms the subject of some recent tests at the Division of Building Research of the National Research Council of Canada, in Ottawa. Specially designed weathering racks<sup>(34)</sup> which simulate joint movement *in situ*, form part of a current program to study the performance of sealants when exposed to the natural aging process experienced by exterior surfaces of buildings. A parallel study<sup>(35)</sup> already underway is designed to perform extension cycling of sealants in laboratory conditions. The cyclic test program which the daily cycles experienced by building joints in a year in a particular locality may be developed into an evaluation test as and when standard procedures are developed and refined.

---

(34) Karpati, K.K., Solvason, K.R. and Sereda, P.J., "Weathering Racks for Sealants", J. Coatings Technology, Vol. 49, No. 626, March 1977.

(35) Karpati, K.K., "Extension Cycling of Sealants", Proceedings, XIIth Fatipel Congress, May 1974, pp. 455-459.

TABLE 2.1  
A COMPARISON OF CANADIAN SPECIFICATIONS

Specification No.	19GP-3M	19GP-5b	19GP-9M	19GP-13M	19GP-14M	19GP-15M	19GP-16M	19GP-18	19GP-19M
Polymer	polysulfide	acrylic	silicone	polysulfide	butyl	urethane	urethane	silicone	silicone
Type	2 part	1 part	1 part	1 part	1 part	2 part	1 pt/solution	2 part	2 part
Date of Issue	Apr. 1977	Apr. 1971	Apr. 1976	Apr. 1976	Apr. 1976	Apr. 1976	Sept. 1977	June 1970	Sept. 1977
Intended uses:									
Movement capability	25%	7.5%	25%	20%	5%	25%	20%	25%	25%
Including H <sub>2</sub> O immersion	yes	no	no	yes	no	yes	yes	no	yes
Surfaces, glass	OK	OK	OK	OK	OK	OK	OK	OK	OK
Aluminium	OK	OK	OK	OK	OK	OK	OK	OK	OK
Metals	OK	OK	OK	OK	OK	OK	OK	OK	OK
Masonry	OK	OK	OK	OK	OK	OK	OK	OK	OK
Wood	OK	OK	OK	OK	OK	OK	OK	OK	OK
Plastics	OK	OK	OK	OK	OK	OK	OK	OK	OK
Requirements after 14 days at 158°F									
Hardness range	15 to 50	55 max	15 to 50	15 to 50	40 max	15 to 50	15 to 50	50 max	12 to 30
Weight loss max, %	10%	15%	10%	10%	25%	5%	12%	15%	3%
Adhesion in peel (lb/in./width)									
Including H <sub>2</sub> O immersion	yes	no	yes	yes	no	yes	yes	yes	yes
Surface, glass	10+	10+	10+	10+	3.5+	10+	10+	10+	10+
Aluminium	10+	10+	10+	10+	3.5+	10+	10+	10+	10+
Masonry	10+	10+	10+	10+	3.5+	10+	10+	10+	10+
Ultraviolet thru glass	10+	10+	10+	10+	3.5+	10+	10+	10+	10+
Stain Test	yes	none	yes	yes	yes	yes	yes	yes	yes
Recovery, % min	none	none	none	50%	none	none	none	none	none
Cycle Tests									
Including H <sub>2</sub> O immersion	yes	no*	only glass*	yes	yes	yes	yes	only glass*	yes
Surfaces, glass	OK	OK	OK	OK	OK	OK	OK	OK	OK
Aluminium	OK	OK	OK	OK	OK	OK	OK	OK	OK
Masonry	OK	OK	OK	OK	OK	OK	OK	OK	OK
Low Temperature Test Limit, °F									
Blister Test	none	yes	yes	none	yes	yes	yes	none	none

\* See specifications for exact details.

19GP-17 - similar to 19GP-5b but allows 25% weight loss and 6 lb adhesion in peel.

19GP-24 - similar to 19GP-15a but is not generic and allows 10% weight loss.

19GP-25 - similar to 19GP-13a but allows 10% weight loss and 5 lb adhesion in peel.

Source: Parke, J., "A Review of Sealant Specifications throughout the World", in Parke, J. (Ed), "Building Seals and Sealants", American Society for Testing and Materials, ASTM, STP 606, 1976.

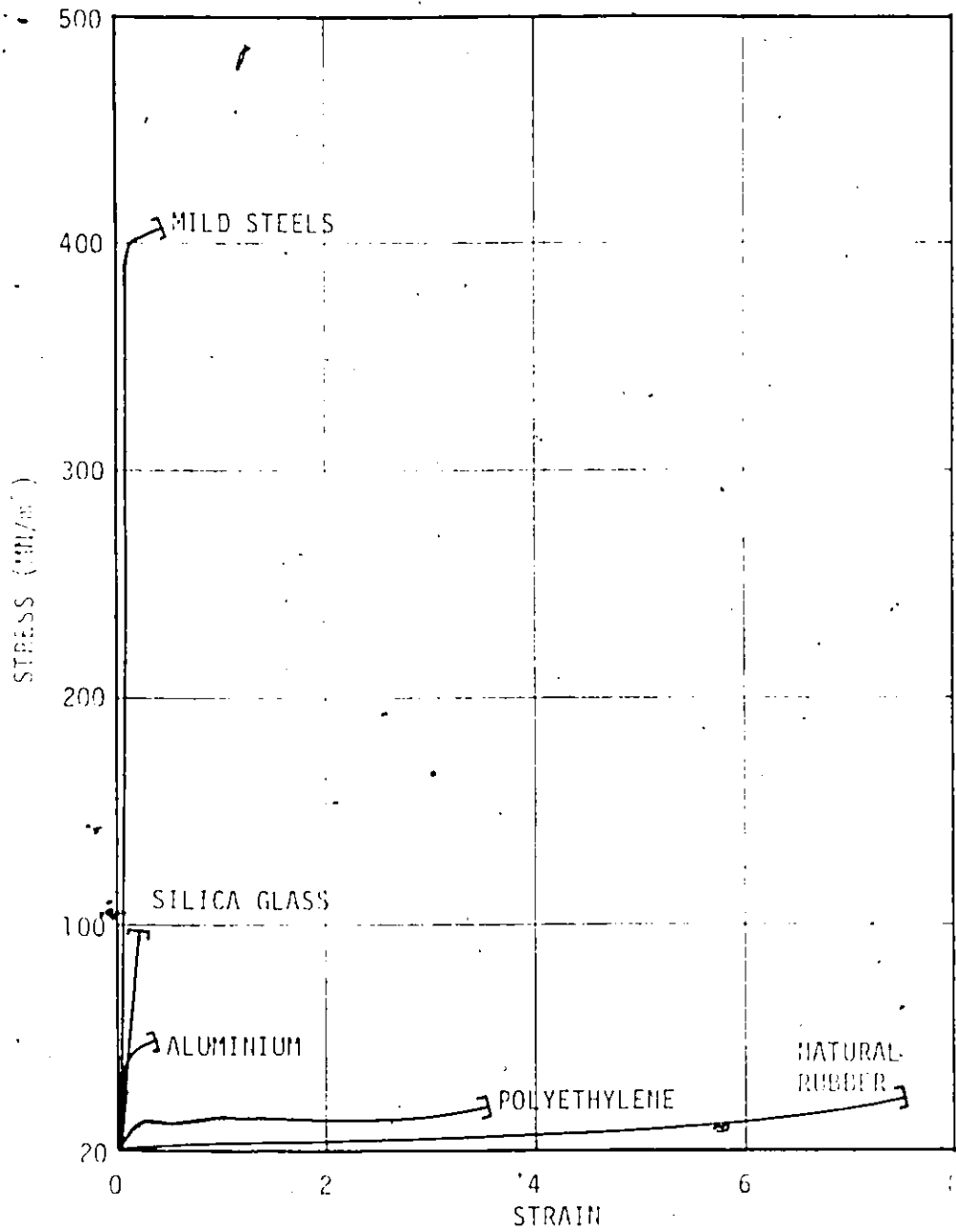


FIGURE 2.1 - Engineering stress-strain curves for selected materials as determined by tensile tests at room temperature (Various sources).

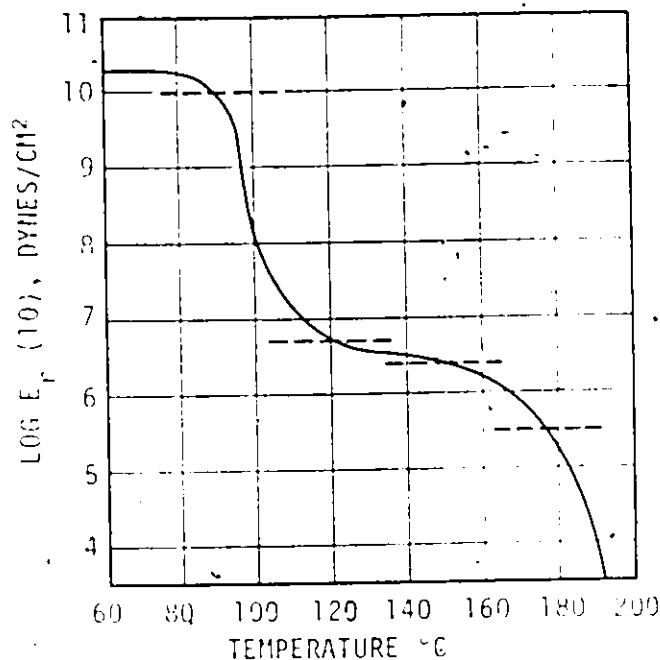
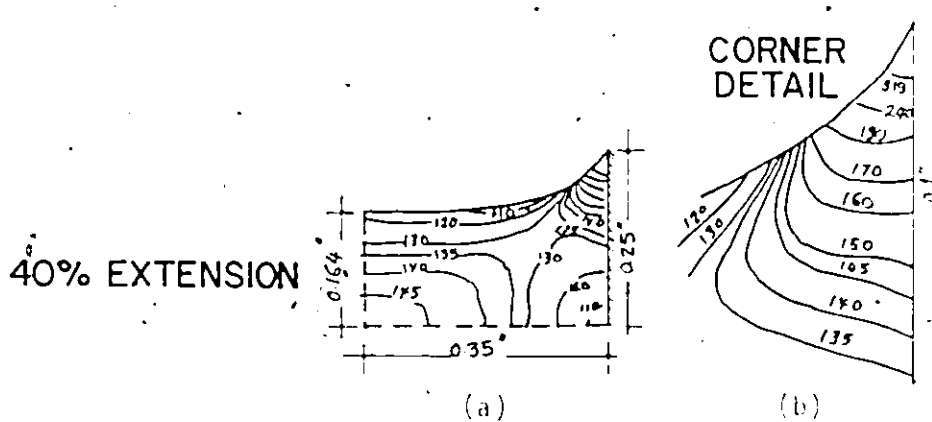


FIGURE 2.2 - Five regions of visco-elastic behaviour (for polystyrene sample) (after Tobolsky)



NOTE: NUMBERS ON CONTOUR LINES ARE STRESSES IN PSI

FIGURE 2.3 - Stress distribution pattern in sealant edges at specific extension (about 40%) of a (13 x 13 mm) joint.

- (a) quarter-section
  - (b) enlarged section of corner detail
- (after Catsiff)

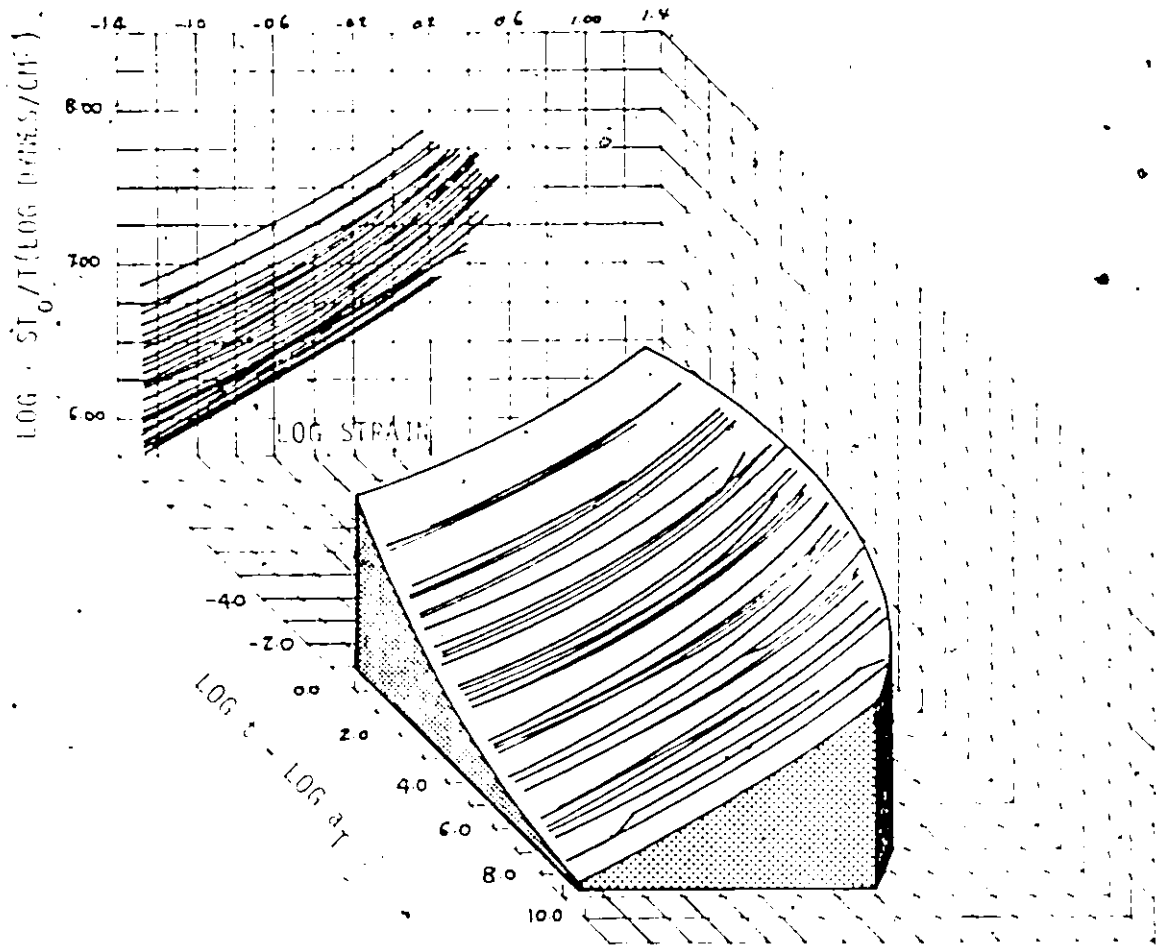


FIGURE 2.4 - The property surface  
(after Farpati)



CHAPTER 3  
EXPERIMENTAL PROGRAM

3.1 Introduction

The objective of the experimental program described in this chapter is to establish the mechanical properties of one-part urethane sealants conforming to CGSB 19-GP-16M at different temperatures, strain rates and with different substrates. The choice of this sealant for testing was based on the paucity of research reported in the technical literature and on the relatively recent introduction of the material into the market (1962).

The experimental program comprised two kinds of tests:

- 1) Tension tests
- 2) Stress relaxation tests

The tension tests follow, in essence, the procedures in the standards (CGSB, ASTM, etc...) and previously published research programs<sup>(1,2,3)</sup>. Because of the viscoelastic nature of the material, a further set of experiments was undertaken to characterize the viscoelastic performance of urethane sealant. These experiments took the form of stress relaxation tests as opposed to creep tests in order to avoid the experimental errors inherent in the creep tests<sup>(4)</sup>.

- 
- (1) Canadian Government Specification Board, "Standards for: Methods of Testing Putty, Caulking and Sealing Compounds", 19-GP-0M, April, 1976.
  - (2) ASTM, "Test for Adhesion and Cohesion of Elastomeric Joint Sealants under Cyclic Movements", Vol. 18, C719, 1977.
  - (3) Karpati, K.K., "Mechanical Properties of Sealants: I-Behaviour of Silicone Sealants as a function of Temperature", J. Paint Technology, Vol. 44, No. 565, Feb. 1972, pp. 55-62.
  - (4) Karpati, K.K., "Literature Survey of Sealants", J. of Paint Technology, Vol. 40, No. 523, August 1968, pp. 337-347 (Also Tech. Paper No. 287 of the Division of Building Research, National Research Council of Canada, NRC 10424).

The experimental program comprises three distinct and disparate stages:

- 1) Specimen preparation
- 2) Curing of specimens
- 3) Tensile or stress relaxation tests

A supplementary experiment to determine the glass transition temperature which is essential in any subsequent analysis of the experimental data was also undertaken.

### 3.2 Preparation of Specimen

The procedure for preparation of samples is the same for both tension and stress relaxation test. The specimen comprises essentially a bead of sealant cast between two prismatic pieces of substrate (of aluminium, glass, wood or mortar) measuring 13 x 25 x 76 mm each (Fig. (3.1)).

The preparation of the surface of the substrates before casting the sealant varies with the type of material. Here, the manufacturers' recommendations were deemed appropriate and followed. The substrates' surface were prepared as follows:

- (1) Plain Aluminium: The pieces were chosen to be free from scratches, bends and other defects. Surface dirt or grease was removed by wiping with a clean paper tissue. The pieces were then wiped with a cloth soaked in detergent to remove any gross oil films on the surface and rinsed with water. They

were subsequently left for 30 minutes in acetone, washed in distilled water and then dried by means of "type 900-L" paper towels. The test surface was finally primed with the recommended primer by means of a brush and left exposed in room conditions (23°C and 35% RH) for one hour before the application of the sealant. In the samples where the effect of nonpriming was investigated, the sealant was cast after cleaning.

(2) Mortar: The mortar pieces were prepared by using 1 part of normal portland cement and 2 parts by weight of clean, well graded fine aggregate (ASTM C33) and sufficient water to produce a flow of 120.5% when tested in accordance with the test for consistency of cement mortar (ASTM C109). After curing 1 day in moist conditions (95 to 100% RH) and 6 days in water at 23.2°C, the test surface was polished by wet grinding using No. 60 silicon carbide. The pieces were oven dried to constant weight at 110°C and then cooled to 23.2°C. The loose dust was removed by brushing with a clean natural bristle paint brush. Only one set of prismatic mortar pieces was primed on the test surface.

(3) Glass: The glass substrate consisted of a wooden piece (25 x 13 x 76 mm) on which was glued a glass piece (4 x 13 x 76 mm) and left to cure for a period of 28 days. The glass face was then prepared in a manner similar to the aluminium pieces.

(4) Wood: The wood pieces (red wood) were brushed clean by a natural bristle paint brush thus removing dust and dirt. They were then conditioned in a dessicator at 50% RH and 23°C for 6 weeks prior to casting the sealant.

The next phase involved the casting of the sealant. This comprised of the following steps:

- a) A piece of wax paper was placed in the wooden mould (Plate 3.1).
- b) The substrate bars were positioned on the wax paper with 13 x 13 x 13mm spacers between them at the ends (Plate 3.1). The 13 x 13 x 13mm end spacers which were placed between the substrate bars to provide the uniformity of sizes of the sealant are covered by wax paper on the sides which may be exposed to the sealant. This sub-assembly of pieces was repeated (up to 9 specimens per mould) as required. The whole assembly was secured by placing a long moveable wooden bar tightly against it and nailed to the mould. Wedges were then driven between the rail and individual pieces which were loose in order to secure them tightly in the mould.
- c) The substrate bars and the end spacers were held down by adhesive tape and thus only 13 x 51 mm cavities remained in which the sealant was applied.
- d) The sealant, in the liquid state, was applied carefully into the cavity by means of a caulking gun thus forming a sealant bead 13 x 13 x 51 mm. Starting from the near edge the sealant

extruded from the gun was cast into the cavity with the tip of the gun advancing towards the farther edge. This process was repeated three times to fill the cavity.

Some problems encountered in the preparation of test samples are outlined below:

- a) Formation of air bubbles: This was by far the most serious problem both in terms of its influence on test results and also because of the number of specimens involved. Sometimes up to 60% of a batch contained air bubbles and if discovered during an experiment, the tests were discontinued or the results were discarded. Most of the air bubbles occurred at the edges and on applying a tensile load caused adhesive failure. Air bubbles in the middle of the sealant bead performed in a manner similar to cracks in materials and invariably affected the test results adversely. This problem is difficult to overcome even with experience, as evidenced by the large number of specimen failures encountered by other researchers<sup>(5)</sup>. However, using an evacuated glove box may solve this problem.
- b) The lack of uniformity of application of the primer of the aluminium samples was also a cause of test failures. This problem is aggravated by the condition of the primer for which the manufacturer recommends immediate use of an opened can.
- c) Uniformity of the sealant bead thickness in different specimens is difficult to achieve by pressing the spatula against the substrate.

---

(5) Private discussions with technicians of DBR/NRC, April 1978.

Standardizing the procedure, however, helps in minimizing the dimensional variations.

d) Impurities and factory batch differences could be detected in the sealants during casting.

### 3.3 Curing of Specimens

a) The specimens which were cast at room temperature and humidity were left in the mould for 24 hours. They were then removed and clamped at the edges by brass clips to maintain the specimens in the desired shape during a curing period of 14 days.

b) The wax paper and end spacers were then removed and replaced by other smaller spacers (6 x 13 x 13 mm) at the edges to expose the ends of the sealant beads to ambient conditions.

c) The specimens were clamped together once again and heat-aged at 70°C in a ventilated oven for 28 days.

### 3.4 Experimental Procedure

The Instron Universal Testing Machine model 1125 was used for both the tension tests and the stress relaxation tests. The machine comprises two major systems: the load weighing system, which measures and records the load on the specimen, and the cross head drive system, which stretches the specimen. The load in the test specimen, is caused by the moving crosshead (operated by threaded screws coupled to a d.c. drive motor, at a constant crosshead speed)

was measured on a 500 kilogram load cell which was mounted to the loading frame. The deformation was assumed to be the same as the movement of the crossheads which is measured automatically.

An environmental chamber was used to permit testing to be performed in a temperature-controlled environment. The temperature that can be achieved in the chamber ranges from about,  $-70^{\circ}\text{C}$  to  $200^{\circ}\text{C}$ . Temperatures below  $23^{\circ}\text{C}$  were obtained by means of liquid nitrogen while higher temperatures were obtained by using heaters built into the chamber. The sensitivity of the load cell to temperature changes was taken into account in the operation of the machine by allowing the load cell to stabilize at the test temperature for two hours prior to the start of the experiment. At the lower temperatures,  $-40^{\circ}\text{C}$  and  $-20^{\circ}\text{C}$ , a long pull rod was used to ensure that the temperature of the load cell itself did not reach  $-29^{\circ}\text{C}$  (this is the critical temperature recommended in "Users' Manual") below which the readings are not valid.

On removing the specimens from the ventilated oven where they were being heat-aged, they were placed on a laboratory bench in order to stabilize for up to four hours at room temperature. The specimens were then mounted in specially designed grips (Plate 3.2). Special features of the design are described below:

- a) The grips were made of high strength "boiler" plate steel, 1" thick and adapted to fit into the universal joint which in turn was mounted on the load cell.

- b) The 1" diameter holes were drilled into the grips in order to minimize the weight which was tared out when calibrating the load cell on the chart.
- c) The jaws were serrated and hardened in order to ensure that the grip on the substrate was as good as possible.

The procedure for setting up the tests was also standardized. The steps followed are outlined below:

- a) One substrate bar was positioned in the bottom set of serrated jaws which was equipped with only one moveable jaw and tightened.
- b) The upper substrate bar was then placed between the jaws of the upper grip and aligned by means of a spirit level to ensure that the specimen was vertical. The jaws were then tightened from both sides (since both are moveable) while constantly checking that the specimen remained vertical. This procedure eliminated as much as possible, such stresses as torsion or shear which might have resulted from misalignment and which would have unduly influenced the test results.

To minimize the effect of any residual misalignment, each test was begun with the sample slightly extended (i.e., with the least extension perceptible on the Instron recorder).

- c) When required, the environmental chamber modified the temperature to the test temperature. Two temperature-measuring devices were used to ensure that stable conditions were achieved within the chamber, i.e.,



- (1) An ordinary mercury thermometer was placed on the inside of the chamber window, and
- (2) a thermocouple was imbedded in the middle of a red wood bar of the same size as a substrate, sealed with epoxy glue and monitored by means of a digital voltmeter.

When both temperatures were stable for more than 10 minutes, the calibration and the tests were allowed to proceed (Note: Tests at a specific temperature were performed consecutively and so the two hours required for stabilizing the load cell was necessary only for the first test.

In subsequent tests, the procedure outlined below was followed).

- d) Adjustments and calibration to the recording instrument were undertaken by following the instruction in the "Users' Manual".

These procedures were identical for both tension and stress relaxation experiments.

### 3.5 Tension Tests

The Instron Universal Testing Machine model 1125 used for the tests comprises a set of automatic control buttons which determine the speed at which the crosshead frame was moved, i.e., the loading of the specimens was at specific constant strain rate. On X-Y plotter, the load was recorded on the X-axis (facing the console) while on the Y-axis the plot was time. This was related to the crosshead movement electronically and the scale could be adjusted automatically by means of buttons which changed the scale proportionally from 1:0.01 to 1:100.

On selecting a crosshead speed (strain rate multiplied by the joint width) and the appropriate proportional chart speed, the test was started. The X-Y plotter recorded automatically the load and deformation changes.

The tension tests were carried out on a number of specimens at different strain rates and temperatures as shown in Table 3.1.

### 3.6 Stress Relaxation Experiments

In these experiments, the test procedure was akin to that of the tension test. However, instead of allowing the test to proceed to failure, the crosshead was stopped at various strain levels and maintained at those levels. The variations of load with time was then monitored for up to 3 hours. The crosshead speed in the stress relaxation experiments was constant (2mm/min). The various levels of strain and temperature for the program of stress relaxation tests are presented in Table 3.2.

### 3.7 Glass Transition Temperature

The Differential Thermal Analysis experiment was performed at the Division of Building Research, National Research Council, Ottawa. A DU PONT 990 thermoanalyzer with 0-50 DTA standard cell (Fig. (3.2)) was used to determine the glass transition temperature which is required for the analysis of the data obtained from the tension tests. Thermocouple A was placed in a previously weighed sample of the urethane sealant. Thermocouple B was placed in an inert reference material,

which was selected so that it undergoes no thermal transformations over the temperature range under examination. The sample and the reference material were then placed close together and cooled to  $-100^{\circ}\text{C}$  using liquid nitrogen. They were subsequently heated at a uniform rate ( $5^{\circ}\text{C}$  per minute). The temperature of the sample and reference material follow the changes in their surrounding temperatures. In the absence of physical or chemical change, the temperature differential,  $\Delta T$  assumes a definite value.  $\Delta T$  versus temperature was recorded on the DU PONT 990 thermoanalyser and the glass transition temperature was determined from the recorded graph.

TABLE 3.1

Description of tension test program

		Crosshead Speed cm/min					
		5.000	1.000	0.500	0.050	0.010	0.005
TEMPERATURE °C	-40.0	*		*0	*	*	*
	-20.0	*	*	*0	*0	*0	*0
	0.0	*	*0	*	*0	*0	*
	22.5	*0	*0	0*X	*0	*0	*0
	40.0	*	*	*0	*	*	*
	60.0	*	*	*0	*	*0	*0

- \* Test done on primed substrate.
- X Test done on different substrates.
- 0 Test repeated because of air bubble, adhesive failure or other defect.

TABLE 3.2

Description of stress relaxation program

		Strain Level				
		0.5	0.4	0.3	0.2	0.1
TEMP. °C	-20.0	*	*	*0	*●	*
	22.5	*	*	*	*	*
	60.0	*	*	*	*0	*0

- \* Test done on primed substrate
- 0 Test repeated because of air bubble, adhesive failure or other defect.
- Test rejected due to inadequate data.

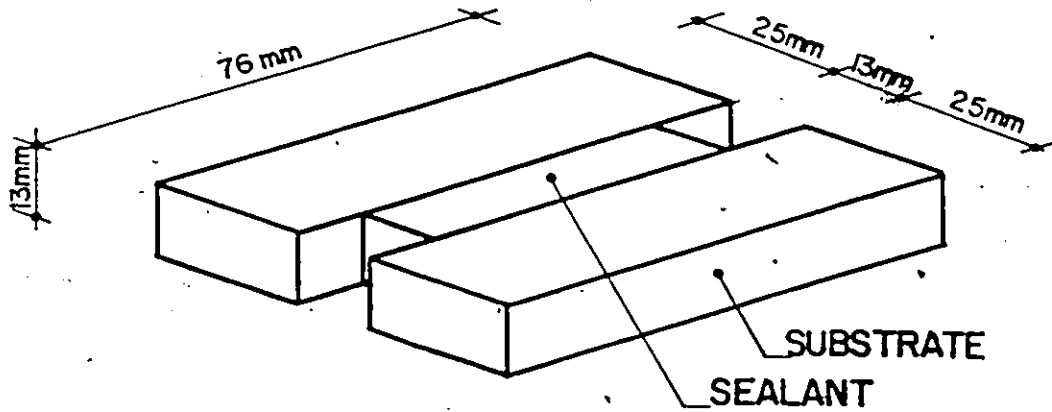


FIGURE 3.1 Schematic diagram of the sealant specimen prior to testing.

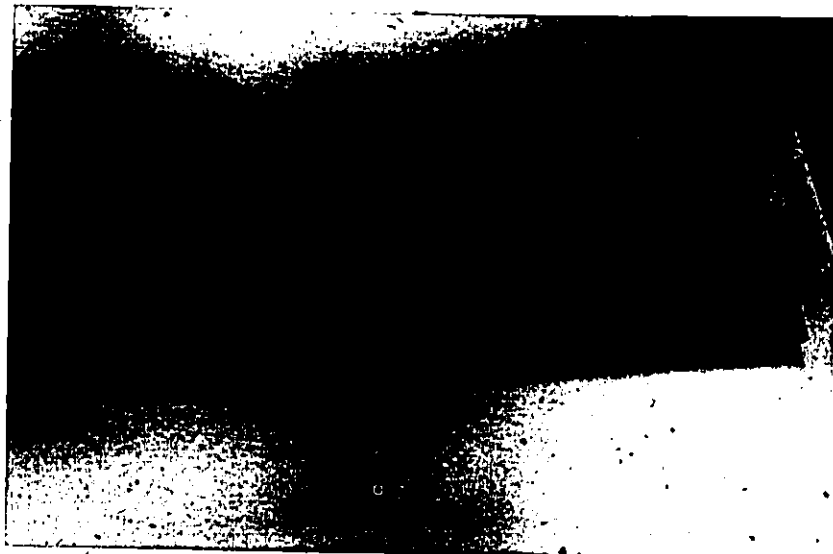


PLATE 3.1 THE WOODEN MOULD FOR FORMING TEST SAMPLES



PLATE 3.2 TENSILE LOADING OF TEST SPECIMEN  
WITHIN THE ENVIRONMENTAL CHAMBER

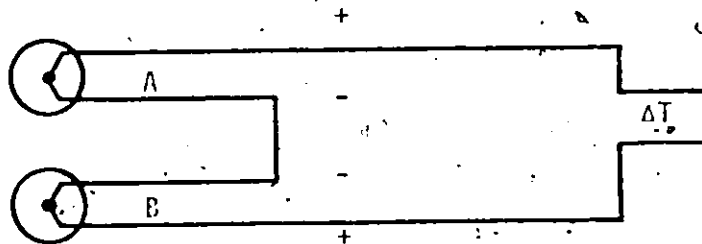


FIGURE 3.2 - Differential thermocouple for measurement  
of temperature difference.

CHAPTER 4

THEORETICAL BASIS OF THE MASTER CURVE

4.1 Introduction

The behaviour of visco-elastic materials has been modelled in two distinctly different ways, they are:

- (i) by mechanical models such as the Maxwell element<sup>(1)</sup>.
- (ii) by mathematical models such as those developed from Volterra's formulations<sup>(2)</sup>.

In the brief review and critique of the models presented earlier (Chapter 2), the complexities and problems involved in the mathematical model are considered to preclude its use in design. The mechanical model, however, has been found useful in explaining the physical processes involved when a viscoelastic material is deformed and also in characterizing the material. Consequently, only the mechanical model will be developed here in order to derive single curves at each temperature. The time-temperature superposition technique will then be used to consolidate the single curves to a master curve which will accommodate the four basic variables (stress, strain, time and temperature) which are required to characterize the material response. In modelling the transient conditions (i.e., stress-strain behaviour to failure), the development will be guided to a considerable degree by Smith's<sup>(3)</sup> and Karpati's<sup>(4)</sup> work, while for the static case the model will be extended to account for the stress relaxation experiments.

- 
- (1) Tobolsky, A.V., "Properties and Structure of Polymers", John Wiley & Sons, 1967.
  - (2) Volterra, V., "Fonctions de Lignes", Gauthier Villard, Paris, 1913.
  - (3) Smith, T.L., "Viscoelastic Behaviour of Polyisobutylene under constant Rates of Elongation", J. Polymer Sci., Vol. XX, 1950, pp. 89-99.
  - (4) Karpati, K.K., "Mechanical Properties of Sealants: IV Performance Testing of Two-part Polysulphide Sealants", J. Paint Tech., Vol. 45 No. 580, May 1973, pp. 49-57.

#### 4.2 The Generalized Maxwell Model

Rheological and fracture properties of polymers when modelled by means of Hookean springs and Newtonian dashpots are linearly visco-elastic. A basic property of Hookean springs is that the incremental extension caused by an increment in load is independent of the previous load or deformation history. Also, the increase in rate of extension of a Newtonian dashpot subject to an increment in load is independent of the past history, and so, any assembly of such springs and dashpots is not history dependent.

The generalized Maxwell model consists of an infinite number of Maxwell elements as shown in Figure (4.1). Consider the fundamental equation for the  $i^{\text{th}}$  Maxwell element.

$$\dot{\epsilon}(t) = \frac{1}{E_i} \dot{\sigma}_i(t) + \frac{1}{\eta_i} \sigma_i(t) \quad (4.1)$$

where

$\dot{\epsilon}_i(t)$  is the strain rate of the  $i^{\text{th}}$  element,

$\sigma_i(t)$  is the "true" stress of the  $i^{\text{th}}$  element,

$\dot{\sigma}_i(t)$  is the "true" stress rate of the  $i^{\text{th}}$  element,

$E_i$  is the modulus of elasticity of the  $i^{\text{th}}$  element,

$\eta_i$  is the coefficient of viscosity of the  $i^{\text{th}}$  element.

Rearranging the terms in Equation (4.1)

$$\frac{d\sigma_i(t)}{dt} + \frac{E_i}{\eta_i} \sigma_i(t) = E_i \frac{d\epsilon_i(t)}{dt} \quad (4.2)$$



The standard integral form for this linear differential equation of the 1<sup>st</sup> order is:

$$\sigma_i(t) = E_i e^{-t/\tau_i} \int e^{t/\tau_i} \dot{\epsilon}_i(t) dt + K e^{-t/\tau_i} \quad (4.3)$$

where  $\tau_i (= \eta_i/E_i)$  is the relaxation time of the Maxwell element and  $K$  is a constant of integration.

Applying the boundary condition  $\dot{\epsilon}_i(t) = R_t$  and  $\sigma_i(t) = 0$  when  $t = 0$ ,

$$\int e^{t/\tau_i} \dot{\epsilon}_i(t) dt = R_t \tau_i e^{t/\tau_i}$$

and  $0 = E_i \cdot R_t \cdot \tau_i + K$

$$\therefore K = -\eta_i R_t \quad (4.4)$$

substituting into Equation (4.3),

$$\sigma_i(t) = R_t \eta_i (1 - e^{-t/\tau_i}) \quad (4.5)$$

rewriting

$$\sigma_i(t) = R_t \cdot \tau_i \cdot E_i (1 - e^{-t/\tau_i}) \quad (4.6)$$

For the case of  $n$  Maxwell elements in parallel (Figure (4.1)), Equation (4.6) can be generalized to the form

$$\sigma(t) = \sum_{i=1}^n \sigma_i(t) = R_t \sum_{i=1}^n \tau_i E_i (1 - e^{-t/\tau_i}) \quad (4.7)$$

Stress relaxation experiments on linear viscoelastic polymers make it quite evident that the "true" stress is best represented by an assembly of Maxwell elements as described in Equation (4.7), in which

the number of elements  $n$  is infinite. The relaxation times  $(\tau_i)$  are so close to each other that the summation of Equation (4.7) may be replaced by a continuous integral of the form:

$$\sigma(t) = R_t \int_0^{\infty} \tau E(\tau) [1 - e^{-t/\tau}] d\tau \quad (4.8)$$

where  $E(\tau)$  is the elastic modulus at relaxation time  $(\tau)$ .

Since the experimental data are often plotted as a function of  $\log t/\tau$  it is a standard procedure to express the integral in terms of  $d \ln \tau$  where  $d \ln \tau = \frac{d\tau}{\tau}$

and so

$$\sigma(t) = R_t \int_{-\infty}^{\infty} E(\tau) \tau^2 [1 - e^{-t/\tau}] d \ln \tau \quad (4.9)$$

Defining the relaxation spectrum  $R(\tau) = \tau \cdot E(\tau)$  within the integral as the contribution to  $E(\tau)$  of relaxation times between  $\ln \tau$  and  $\ln \tau + d \ln \tau$ , the final general expression for the stress is

$$\sigma(t) = R_t \int_{-\infty}^{\infty} R(\tau) \cdot \tau [1 - e^{-t/\tau}] d \ln \tau \quad (4.10)$$

which can be rewritten in the form

$$\frac{\sigma(t)}{R_t} = \int_{-\infty}^{\infty} R(\tau) \cdot \tau [1 - e^{-\frac{t}{R_t \cdot \tau}}] d \ln \tau \quad (4.11)$$

One may note that  $\frac{\sigma(t)}{R_t}$  is a function of  $\frac{t}{R_t}$  only; hence, data obtained at different strain rates should form a single cumulative curve on a plot of  $\log \left( \frac{\sigma(t)}{R_t} \right)$  against  $\log \left( \frac{t}{R_t} \right)$ .

### 4.3 Time-Temperature Superposition

The analysis developed in the previous section modelled the linear viscoelastic performance of the material at a specific temperature. The principle of time-temperature superposition for temperatures varying from the glass transition temperature,  $T_g$  to  $T_g + 100^\circ\text{C}$  provides a way of consolidating the curves developed in the previous analysis to a single master characteristic curve at a reference temperature<sup>(5)</sup>. Assuming that all relaxation times have the same temperature dependence and that the modulus of each spring in the model is proportional to the absolute temperature, Ferry's reduced variable scheme<sup>(6)</sup> can be used to combine the data at different temperatures. At the molecular level, Ferry's assumptions reflect the fracture processes at that level. The molecular relaxations are shifted by the same time ratio ( $a_T$ ) by a change in temperature and can thus be represented at that temperature  $T$  by a single apparent activation energy<sup>(7)</sup>.

Williams, Landel and Ferry<sup>(8)</sup> derived an expression (WLF equation) which refines the relations in the second assumption, thus:

$$\text{Log } a_T = \frac{-C_1(T-T_g)}{(C_2+T-T_g)}$$

where  $a_T$  is the shifting factor and  $C_1 = 17.44$  and  $C_2 = 51.6^\circ\text{C}$  when the glass transition temperature is used as a reference in the WLF equation.

---

(5) Tobolsky, A.V., Op. Cit. (1)

(6) Williams, M.L., Landel, R.F. and Ferry, J.D., "The Temperature Dependence of Relaxation Mechanisms in Amorphous Polymers and other Glass-forming Liquids", J. American Chem. Soc., LXXVII, 3701, (1955).

(7) Tobolsky, A.V., Op. Cit. (1)

(8) Williams, M.L. et al, Op. Cit. (6)

For other reference temperatures, the constants  $C_1$  and  $C_2$  vary accordingly.

It is clear from the WLF equation that  $a_T$  as a function of temperature is calculated from the magnitude of the temperature shift. By introducing the assumption stated above into Equation (4.11), Smith<sup>(9)</sup> derived an equation by means of which the data could be reduced to a single master curve:

$$\frac{\sigma(t)T^q}{R_t Ta_T} = \int_{-\infty}^{\infty} R(\tau)\tau [1 - e^{-\frac{\epsilon(t)}{R_t a_T \tau}}] dL n \tau \quad (4.12)$$

where  $T$  is the temperature at which  $\sigma(t)$  and  $\epsilon(t)$  are measured. Thus, analysis of the data obtained at different temperatures and strain rates should yield a single master curve on a plot of  $\log \frac{\sigma(t)T^q}{R_t Ta_T}$  versus  $\log \frac{\epsilon(t)}{R_t a_T}$  providing the stated assumptions are valid.

#### 4.4 Stress Relaxation

If a real viscoelastic body of length  $L$  is pulled to a strain  $\epsilon_0$  and maintained at the length  $L(1+\epsilon_0)$  indefinitely, the equilibrium tensile force will not be a constant but a decreasing function of time  $t$ . In stress relaxation experiments, it becomes necessary to define a relaxation modulus  $E_r$  thus

$$E_r = \frac{\sigma(t)}{\epsilon_0} \quad (4.13)$$

---

(9) Smith, T.L., Op. Cit. (3).

Consider a single Maxwell element (a spring of elastic modulus  $E_i$  and a dashpot of viscosity  $\eta_i$ ) which is instantaneously deformed by a strain  $\epsilon_0$ . The initial stress is  $\sigma_i(0)$  and the time dependent stress  $\sigma_i(t)$  can be obtained from Equation (4.1).

$$\dot{\epsilon}_i(t) = \frac{1}{E_i} \dot{\sigma}_i(t) + \frac{1}{\eta_i} \sigma_i(t) \quad (4.1)$$

in which  $\dot{\epsilon}_i(t) = 0$

Thus

$$\frac{\dot{\sigma}_i(t)}{\sigma_i(t)} = -\frac{E_i}{\eta_i} = -\frac{1}{\tau_i}$$

where  $\tau_i$  is the relaxation time

$$\therefore d \ln \sigma_i(t) = -1/\tau_i \cdot dt \quad (4.14)$$

Integrating both sides of Equation (4.14)

$$\ln \sigma_i(t) = t/\tau_i + \ln C$$

at  $t = 0, \sigma_i(t) = \sigma_i(0)$

$$C = \sigma_i(0)$$

and  $\sigma_i(t) = \sigma_i(0) e^{-t/\tau_i}$  (4.15)

Equation (4.15) may be written in terms of the relaxation modulus

$$\begin{aligned} E_{ri}(t) &= \frac{\sigma_i(t)}{\epsilon_0} = \frac{\sigma_i(0)}{\epsilon_0} \cdot e^{-t/\tau_i} \\ &= E_i \cdot e^{-t/\tau_i} \end{aligned} \quad (4.16)$$

For the generalized Maxwell model which comprises  $n$  elements in parallel undergoing simultaneous stress relaxation, the response of the model is

the sum of the responses of each element:

$$E_r(t) = \sum_{i=1}^n E_i e^{-t/\tau_i} \quad (4.17)$$

As noted earlier, the stress relaxation modulus  $E_r(t)$  of a viscoelastic material is best represented by a Maxwell model in which the number of elements  $n$  is infinite. Thus,

$$E_r(t) = \int_0^{\infty} E(\tau) e^{-t/\tau} d\tau \quad (4.18)$$

where  $E(\tau)$  is the elastic modulus at time  $\tau$ .

Since experimental data are often plotted in terms of  $\log t$ , the integral is treated more readily in terms of  $dLnt = \frac{d\tau}{\tau}$ .

Equation (4.18) becomes

$$E_r(t) = \int_{-\infty}^{\infty} \tau \cdot E(\tau) \cdot e^{-t/\tau} dLnt \quad (4.18)$$

or in terms of stress

$$\frac{\sigma(t)}{\epsilon_0} = \int_{-\infty}^{\infty} \tau \cdot E(\tau) \cdot e^{-t/\tau} dLnt \quad (4.19)$$

It is evident from Equation (4.19) that  $\left(\frac{\sigma(t)}{\epsilon_0}\right)$  is a function of time only. (Note  $\sigma(t)$  represents true stress and an approximate value of  $\sigma(t)$  is obtained from nominal stress  $\sigma_t$  (in experimental data) by multiplying the nominal stress by the extension ratio  $\lambda = (1+\epsilon)$ ). It is to be expected, therefore, that relaxation data obtained at different strain levels should form a single cumulative curve on a plot of  $\log \left(\frac{\sigma(t)}{\epsilon_0}\right)$  versus  $\log (t)$  at a given temperature.

The basis of the analysis of stress relaxation tests for different temperatures is similar to that performed for tension test, i.e.,

it is based on the assumption that the effect of temperature on visco-elastic properties is to multiply the time scale at each temperature by a factor. The relaxation modulus  $E_{r,T}(t)$  at any temperature  $T$  and time,  $t$ , can be considered in terms of a relaxation modulus  $E_{r,T_0}$  at a given reference temperature multiplied by a function of  $(t/a_T)$  where  $a_T$  is a function which decreases as temperature increases. According to Tobolsky<sup>(10)</sup>, whose work on viscoelastic materials is extensive

$$E_{r,T_0}\left(\frac{t}{a_T}\right) = \frac{T_0}{T} E_{r,T}(t) \quad (4.20)$$

Thus, the function  $E_{r,T_0}\left(\frac{t}{a_T}\right)$  should be independent of temperature when plotted against  $(t/a_T)$  or  $\log(t/a_T)$ .

---

(10) Tobolsky, A.V., Op. Cit. (1)

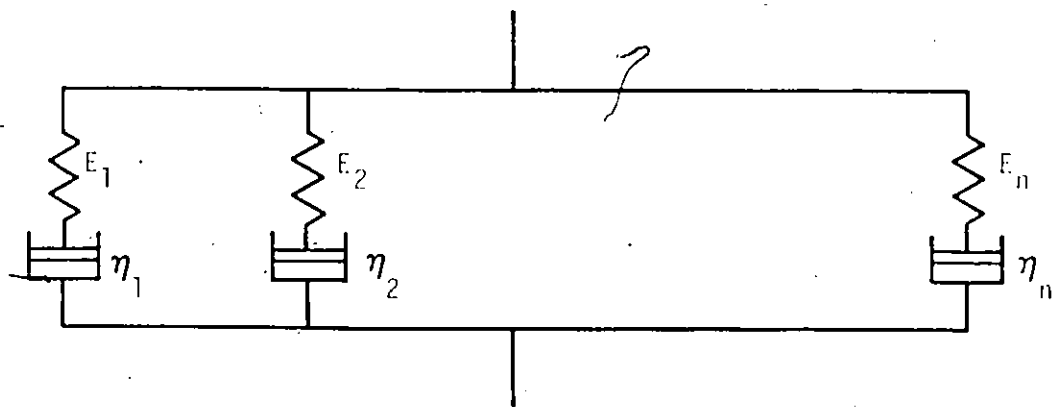


FIGURE 4.1 - Generalized Maxwell model for linear viscoelastic materials. A spring and dashpot system in parallel.



## CHAPTER 5

### TEST RESULTS: ANALYSIS AND DISCUSSION

#### 5.1 Introduction

In this chapter, the results of a test program on one-part urethane sealants (CGSB-19-GP-16M) is presented. As described in Chapter 3, the program comprises two sets of experiments, they are (i) tension tests and (ii) stress relaxation. The results of the tests and the subsequent analyses based on the mechanical model are presented graphically (Figures 5.1 to 5.32).

#### 5.2 Tension Tests

The objective of the tension tests is to study the properties of the urethane sealants in terms of the primary parameters (stress, strain, time and temperature) as well as other factors such as types of substrates and priming. In the set of tests, the load-deformation characteristics to failure are obtained at various temperatures, strain rates and for different conditions of substrate. It is important to note that failure occurs in the material (cohesive) or between the material and the substrate (adhesive) or in the substrate. Unlike the adhesive or substrate failure modes, cohesive failures are sometimes more difficult to determine. The criterion used to establish the point of failure is defined by the length of the crack. In these tests, failure is considered to have occurred when the crack length exceeds  $10 \text{ mm} \pm 1 \text{ mm}$ .

Tensile curves of the many tests performed with the one part urethane sealants are illustrated in Figures 5.1 to 5.14. In the range of strain rates investigated, the nominal stress-strain curves show a progressive increase in ultimate strength with increases in strain rate for all temperatures (Figs. 5.1 to 5.6). The strain at failure is generally greater the higher the strain rate except at low temperatures (i.e.,  $-20^{\circ}\text{C}$  to  $-40^{\circ}\text{C}$ ) where the strains at failure at high strain rates are noticeably smaller than those at low strain rates.

The tensile curves in Figures 5.1 to 5.6 are plotted again in different groupings in Figures 5.7 to 5.12. In the earlier set, each figure comprises a family of curves obtained at a specific temperature with each curve representing the nominal stress-strain relationship at the various strain rates. In Figures 5.7 to 5.12, each figure consists of the curves for a specific strain rate, the individual curves varying with temperatures. It is evident from the latter set that the ultimate strength increases with decrease in temperature (Fig. 5.15). No overall pattern can be discerned for the relationship between ultimate strain and temperature (Figure 5.16).

In general, the shape of the nominal stress-strain curves can be described as ideal elastic-plastic in form except at low temperatures and high strain rates. At low temperatures (Figures 5.5 and 5.6), two distinct elastic regions separated by a region with a loss in stress can be discerned. The initial "elastic" region is markedly linear up to the local maximum nominal stress and the second "elastic" region is also linear

but with a much reduced slope until failure. At high strain rates and temperatures (i.e., at room temperature and above) the shape of the curves are characterized by two linearly elastic regions, the slope of the second elastic region being much less than the initial one.

It is evident from an examination of the stress-strain graphs (Figures 5.1 - 5.6) that urethane sealants exhibit visco-elastic properties within the temperature range considered and the performance of the sealant with respect to the primary factors can best be explained by means of the viscoelastic model developed in the previous chapter. It is, moreover, possible to explain some aspects of the behaviour in terms of the kinetic theory of rubbery elasticity. At high strain rates, the elastic aspects of the deformations (in which the material has instantaneous response to strain) are more pronounced. Time-dependent deformations assume greater importance at lower strain rates for, unlike the deformations at high strain rates, the process that leads to equilibrium is a viscous flow which is superimposed on the elastic characteristics. This viscous flow at the higher temperatures is related to the breaking of secondary bonds enabling the chains or portions of them in the polymeric materials to slide on each other. With long term observations such as stress relaxation experiments, it is conceivable that the deformations reach the elastic equilibrium state which is maintained by the primary crosslinks. This aspect of the performance of the sealant is considered in greater detail in the discussion of the stress relaxation experiments.

Tobolsky<sup>(1)</sup> asserts that the effect of temperature on visco-elastic properties is to multiply or divide the time scale by a constant

---

(1) Tobolsky, A.V., "Properties and Structure of Polymers", Wiley and Sons, 1967.

factor at each temperature. This assertion is corroborated by the stress strain plots at different temperatures for different strain rates (Fig. 5.7 to 5.12). (The subsequent analysis based on this assertion is discussed at some length later in the chapter.) At high temperatures, the sealant approaches the viscous edge of the rubbery plateau (Fig. 2.2) and so the viscous properties become prominent. At low temperatures, however, the material is closer to the glassy edge of the rubbery plateau, and as such, the urethane sealant displays properties characteristic of hard, brittle materials.

The influence of substrate was investigated by using unprimed aluminium, redwood, unprimed cement mortar and glass (Fig. 5.13). These substrates, which are frequently used in buildings were not investigated in detail because the adhesive properties of sealants do not form a major part of this study. The influence of priming was also investigated in order to obtain information about its importance on sealant performance (Fig. 5.14).

With the wood substrate (Fig. 5.13), the failure is cohesive while with the unprimed aluminium and mortar, the failure is adhesive. It can be observed that when the failure is adhesive, the stresses and strains at failure are considerably lower than at cohesive failure. It is interesting to note that the stress-strain curves for the different substrates are almost identical and that the stress and strain at which the adhesive failure occurred is nearly the same for the aluminium and the mortar.

The failure in the glass substrate (Fig. 5.13) demonstrates the third kind of failure mentioned earlier. It is not possible, however, to draw any conclusions from this test because of the construction of the substrate which consists of a 5 mm thick piece of glass glued to a wood block. The failure occurred initially in the glue and finally with the breaking of the glass.

The influence of priming depends on the substrate. For aluminium, the effect is significant while for mortar it is negligible. In the case of aluminium, the failure of unprimed specimens was adhesive and it took place at much lower stress and strain levels than with primed specimens. This observation has provided a criterion for rejection of test results involving aluminium substrates in which the adhesive failure could be linked to inadequate priming. This differs from bad test results caused by air bubbles between the sealant and the substrate which create stress concentrations similar to those found at crack edges and invariably lead to adhesive failures. Observations about the age of the primer reinforce the manufacturer's admonishment not to use an old or opened primer because it would result in inadequate performance. It is reasonable to assert, however, that the use of deficient primer on aluminium substrates resulted in lower loads and elongations at failure than in the case without primer. The deficient primer provided a weak interface between the sealant and the substrate and this interface invariably failed before either the adhesive or the cohesive strengths were attained. (A whole batch of samples prepared with old primer was rejected during the test program because of this effect.) Rejection of test results, because of inadequate sample preparation has led to repetition of the tests. The tests which were repeated

have been identified in Tables 3.1 and 3.2. It is important to note that material variations from one batch to another can be significant making a reasonable assurance of the reproductibility of the general pattern of behaviour more difficult to attain with this material.

### 5.3 Analysis of Tension Tests

In the previous chapter, it was shown how the viscoelastic behaviour of materials could be modelled mechanically. The generalized Maxwell model developed there has proved to be especially useful in interpreting results from tension tests and has formed the basis of the analysis of the urethane sealants test results (Figures 5.17 and 5.22). The Equation (4.11) derived in the previous chapter is represented for convenience below:

$$\sigma(t)/R_t = \int_{-\infty}^{\infty} R(\tau)\tau \left[ 1 - e^{\frac{-\epsilon(t)}{R_t \tau}} \right] d \ln \tau \quad (5.1)$$

where

$\sigma(t)$  = "true" stress at time  $t$

$R_t$  = strain rate

$R(\tau)$  = relaxation spectrum

$\tau$  = relaxation time

$\epsilon(t)$  = strain at time  $(t)$

It was noted that  $\sigma(t)/R_t$  is a function only of  $\epsilon(t)/R_t$  (which is time  $t$ ) and so the curves of the tests as plotted in Figures 5.1 to 5.6 can be

superimposed on a cumulative curve by plotting  $\log (\sigma(t)/R_t)$  versus  $\log (t)$  (Figures 5.17 to 5.22).

It is evident from the cumulative curves that the material is temperature dependent. Furthermore, the "cumulative" curves obtained from the test results seem to replace the array of stress-strain curves obtained at each temperature adequately. Thus, the generalized Maxwell model seems to be applicable to urethane sealants at most temperatures investigated. For temperatures between 0°C and 40°C, the curves can be superimposed quite well thus validating the assumption that the material is linearly viscoelastic and so the sealant's behaviour can be represented by the Generalized Maxwell model. At 60°C and also at temperatures below 0°C, the modelling proves to be less suitable. This is probably because the assumption of linear viscoelasticity is less valid - a hypothesis which will be put to the test in the subsequent stress relaxation experiments.

The change in performance of the material with temperature is best explained by reference to the plot of relaxation modulus versus temperature (Fig. 2.2). At high temperatures (in this case, 60°C) the sealant tends to become viscous, while at lower temperatures, it tends towards more brittle and glassy behaviour.

#### 5.4 Glass Transition Temperature

The glass transition temperature,  $T_g$ , of the heat-aged unstrained sample was determined by means of differential thermal analysis to be

-60°C (Fig. 5.23). The shift in the base-line of the plot of change in temperature  $\Delta T$  versus sample temperature  $T$  is in the endothermal direction and may be due to either a decrease in thermal capacity or an increase in heat capacity or other experimental factors such as the sample falling away from the side of the tube and from the formation of voids<sup>(2)</sup>. In the case of the thermogram of the urethane sealant, there is an increase in heat capacity of the sample temperature compared to the reference and this is indicative of glass transition for amorphous polymeric materials<sup>(3)</sup>.

As explained earlier, a temperature dependent polymer can be characterized at each temperature by a three-dimensional coordinate system in terms of logarithms of stress-strain and time. The property surface, however, is too complex to characterize the material for practical use. Following Smith's example<sup>(4)</sup>, therefore, a master curve which characterizes the urethane sealant fully in terms of stress, strain, temperature and time was derived from the single curves at different temperatures. Assuming the reference temperature ( $T_0$ ) to be the glass transition temperature ( $T_g$ ) and the constants  $C_1$  and  $C_2$  to be 17.44 and 51.6°K (since these are generally applicable to a wide variety of polymers<sup>(5)</sup>), the shifting factor  $a_T$  was calculated from the equation

---

(2) DTA Manual

(3) Tobolsky, A.V., Op. Cit. (1)

(4) Smith, T.L., "Viscoelastic Behaviour of Polyisobutylene under Constant Rates of Elongation", J. Polymer Sci., Vol. XX, 1950, pp. 89-99:

(5) Williams, M.L., Landel, R.F. and Ferry, J.D., "The Temperature Dependence of Relaxation Mechanisms in Amorphous Polymers and other Glass-forming Liquids", J. American Chem. Soc., LXXVII, 3701 (1955).



$$\log a_T = \frac{-C_1(T-T_0)}{(C_2+T-T_0)} \quad (5.2)$$

The values of  $a_T$  for the range of temperatures considered in the test program are presented in Figure 5.24.

The master curve for urethane sealants is a "reduced stress" "reduced strain" logarithmic plot (Figure 5.25). On the ordinate, the reduced stress is calculated from the expression

$$\frac{\lambda \sigma_t T_g}{R_t T a_T}$$

where

$\lambda$  = extension ratio

$\sigma_t$  = nominal stress at time  $t$

$T_g$  = glass transition temperature

$R_t$  = strain rate

$a_T$  = shifting factor

$T$  = temperature

On the abscissa, the reduced strain is obtained from the expression

$$\epsilon(t)/R_t a_T$$

where  $\epsilon(t)$  = strain at time  $t$ .

The master curve plotted in Figure 5.25 is indicative of good agreement with the generalized Maxwell model and the time-temperature superposition principle. A regression analysis performed on the 286 points (7 points at the lower end were excluded) in the master curve

yielded the equation

$$\log(\sigma(t)T_g/R_t a_T) = 0.85 \log(\epsilon(t)/R_t a_T) + 2.65 \quad (5.3)$$

Statistical analysis of the data from both the single curves and the master curve is presented in Tables 5.1(a) and (b). Table 5.1(a) reveals that the cumulative curves obtained at different temperatures from a family of curves having different intercepts except at the temperatures below 0°C where the slopes are progressively lower than those for other temperatures. It is also possible to observe at these temperatures and also at 60°C significant deviations of the single curves from the cumulative curves (Figures 5.16 to 5.22).

Little, if any, physical significance can be attached to the master curve. One obvious conclusion is the time-temperature superposition principle holds for the urethane sealants. It is also reasonable to conclude from the master curve that the material is linearly viscoelastic but it must be noted that the curve is essentially a representation of the data in the cumulative curves at different temperatures in which the scale of the ordinate is multiplied by  $(T_g/a_T)$  and that of the abscissa by  $(1/a_T)$ . The effect of this is to extend the ordinate and reduce the abscissa such that data points have a more linear appearance. The observations made earlier regarding the non-linearity of the material at the temperatures 60° and below 0°C still hold.

### 5.5 Implications on Joint Design

In a digest on joint movement and sealant selection, Handegord and Karpati<sup>(6)</sup> have proposed a procedure for design which is, in essence followed. The maximum overall movement of the joint subjected to extremes of temperature on the panel surface is calculated. A check is then undertaken to ensure that the sealant can, in the joint width, accommodate the movement.

This simple design procedure is of necessity conservative. The dependence of the sealant on temperature and strain rate is ignored and in a climate (such as Montreal's) where extremes of weather are usual, this can have dire consequences. The procedure outlined below is derived from the experimental program undertaken here and from information available in the technical literature.

- a) Knowledge of the diurnal and seasonal movements of joints in buildings in various locations in Canada would provide the basis for information on temperature ranges and strain rates during the service life of the sealant. Such a study has been undertaken for Ottawa by Karpati and Gibbons<sup>(7)</sup> and for England by Ryder, J.F. and Baker, T.A.<sup>(8)</sup>.
- b) Knowledge of the sealant's behaviour when subjected to service conditions is essential. The technical information required would comprise the following:

- 
- (6) Handegord, G.O. and Karpati, K.K., "Joint Movement and Sealant Selection", CBD155, NPC 1973.
  - (7) Karpati, K.K., Gibbons, E.V., "Experimental Prediction of Joint Movements in Buildings", Materials Research and Standards, Vol. 10, No. 4, April 1970, p. 16, and, also NRC 11311.
  - (8) Ryder, J.F., Baker, T.A., "The Extent and Rate of Joint Movement in Modern Buildings", Building Research Station, CP2/71, Jan 1971.

- (i) the master curve which characterizes each sealant (e.g., Fig. 5.25)
- (ii) the failure criteria - essentially a plot of stress at failure versus temperature (e.g., Fig. 5.15)
- (iii) the shifting factor  $a_T$  variation with temperature (e.g., Fig. 5.24)
- and (iv) the glass transition temperature ( $T_g$ )

From the information about panel performance, the maximum strain at a particular temperature (having assumed a joint width) and the estimated strain rate can be calculated. The value of the shifting factor at a particular temperature can now be obtained and with these values it is possible to enter the master curve (Fig. 5.25). From the master curve the corresponding value of reduced stress is obtained. Knowing the glass transition temperature ( $T_g$ ), the shifting factor ( $a_T$ ), the extension ratio ( $\lambda$ ) and the strain rate  $R_t$ , the nominal stress can be calculated and magnified by a factor of safety; the value thus obtained is then checked against the lower bound of Figure 5.15 to ensure that the design is adequate. (See flow chart 5.1).

## 5.6 Stress Relaxation Experiments

The stress relaxation experiments were performed on 15 different samples, each specimen at a specific strain level and a specific temperature. Only one test (at strain level (0.2) and temperature (-20°C)

result was omitted from the plots (Figures 5.26-5.28) of nominal stress versus time. The experiment was conducted for a period of three hours which was deemed sufficient for the curve to stabilize.

The curves are identical in shape. The initial load and the load sustained by the specimen increases with imposed strain for each temperature. The equilibrium tensile load is also higher, for increasing imposed strain. Comparing the nominal stresses at a given imposed strain for different temperatures, it can be noticed that the stress levels decrease with increasing temperature, a phenomenon which validated the observations made previously and suggests that the time-temperature superposition principle is valid.

The shape of the stress-relaxation curves also suggest that the material is linearly viscoelastic. In that event, a logarithmic plot of  $\left(\frac{\sigma(t)}{\epsilon_0}\right)$  versus  $(t)$  should result in a single cumulative curve. The plot of Figures 5.29 - 5.31 is indicative of reasonable agreement between theory and experiment for the highest 3 strain levels. At strain levels 0.2 and 0.1 the curves cannot be superimposed except when each curve is multiplied by a constant factor. The reason for this discrepancy is not definitely known but it is thought that the actual strain levels are higher than the nominal at all levels by a constant value which affects the curves at the lower strain levels more than the others. This constant value of strain is likely the result of the experimental procedure followed, in which a small loading was applied to the specimen when setting up for testing and then tared out prior to

the start of the experiment. If a constant strain correction is now applied, the values of the 0.2 and 0.1 plots, the agreement between theory and experiment is virtually complete.

The cumulative plot for room temperature showed the best fit which demonstrated the linear-viscoelastic properties of the material at that temperature, while the deviations at the higher and lower temperatures can be attributed to changes in the structure of the material as the glassy phase and viscous phase respectively, are approached.

The master curve for all temperatures and strain levels (Figure 5.32) was obtained by means of the relationship suggested by Tobolsky, and the value of  $a_T$  was determined from Equation 5.2. The validity of the time-temperature principle is evident.

TABLE 5.1

STATISTICAL ANALYSIS OF RESULTS

(a)

°C Test temp.	n	r	a	b	Error in regression coefficient, b	Standard error
60	48	0.994	0.861	0.942	0.015	0.114
40	52	0.998	0.970	0.901	0.007	0.062
22.5	57	0.997	1.186	0.903	0.010	0.089
0	53	0.995	1.345	0.890	0.013	0.106
-20	50	0.992	1.586	0.970	0.015	0.128
-40	26	0.990	2.170	0.721	0.021	0.072
(b)						
overall	286	0.998	2.644	0.850	0.003	0.130

n Number of readings

r Correlation coefficient

a Intercept

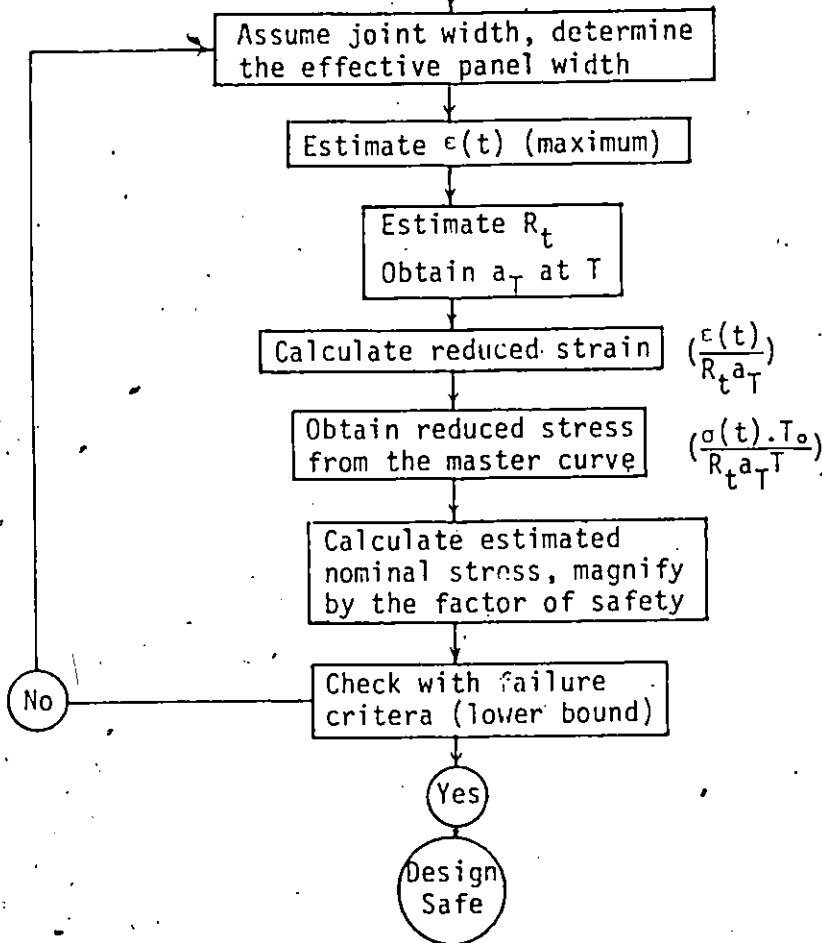
b Slope

FLOW CHART 5.1

SUGGESTED PROCEDURE FOR JOINT DESIGN

Design data required

- joint width variation due to diurnal and seasonal temperature changes, settlement wind load, etc.
- $\alpha$  - coefficient of thermal expansion
- $T_g$  - glass transition temperature
- $a_T$  versus  $T$  shifting factor curve (Fig. 5.24)
- the master curve (Fig. 5.25)
- the failure criteria (Fig. 5.15)



Factor of safety to account for unknowns such as:

- adhesive failure
- failure of substrate
- bad workmanship
- load cycling



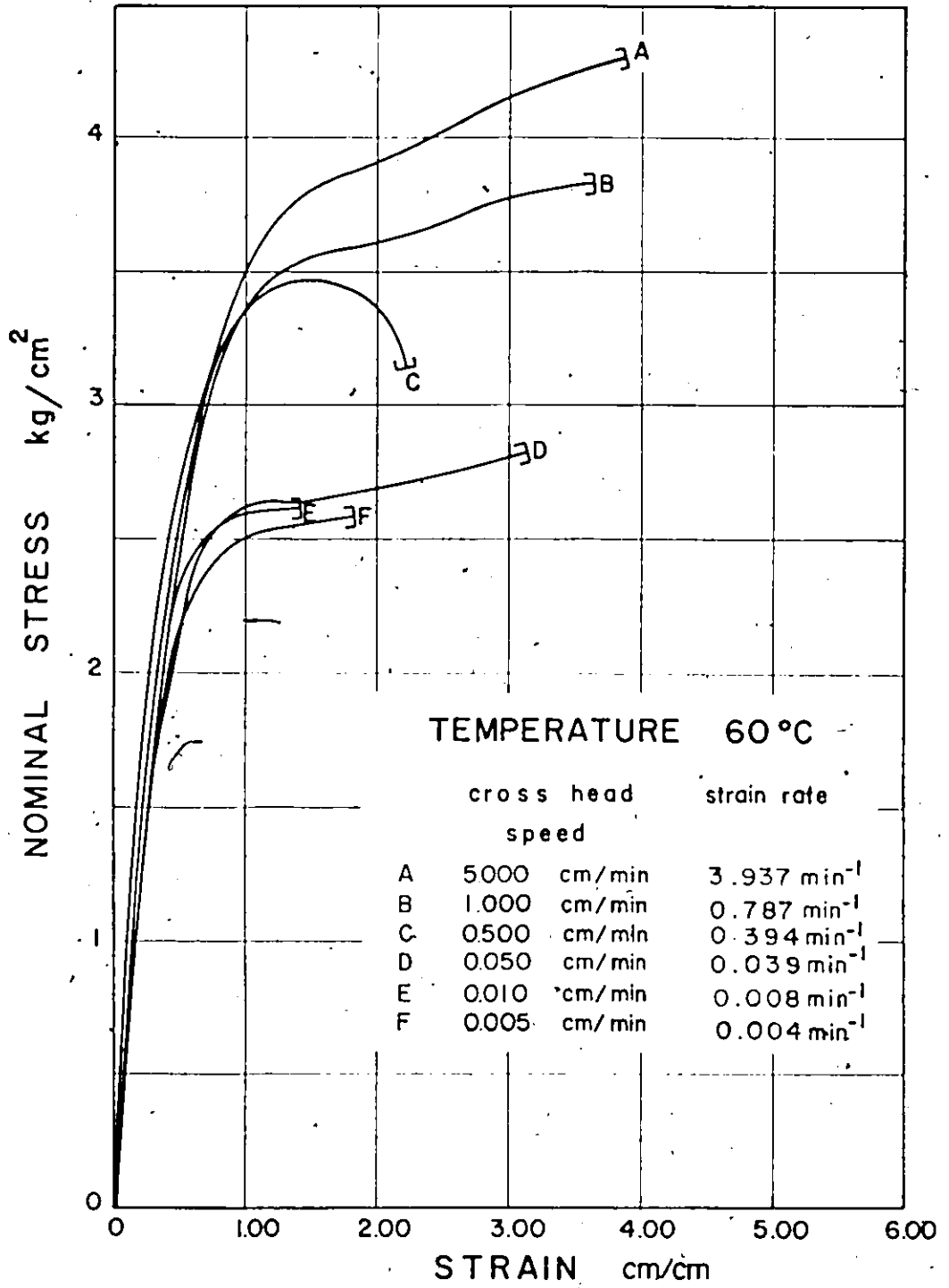


Figure 5.1 — Nominal stress-strain for one-part Urethane sealant at  $60^\circ\text{C}$

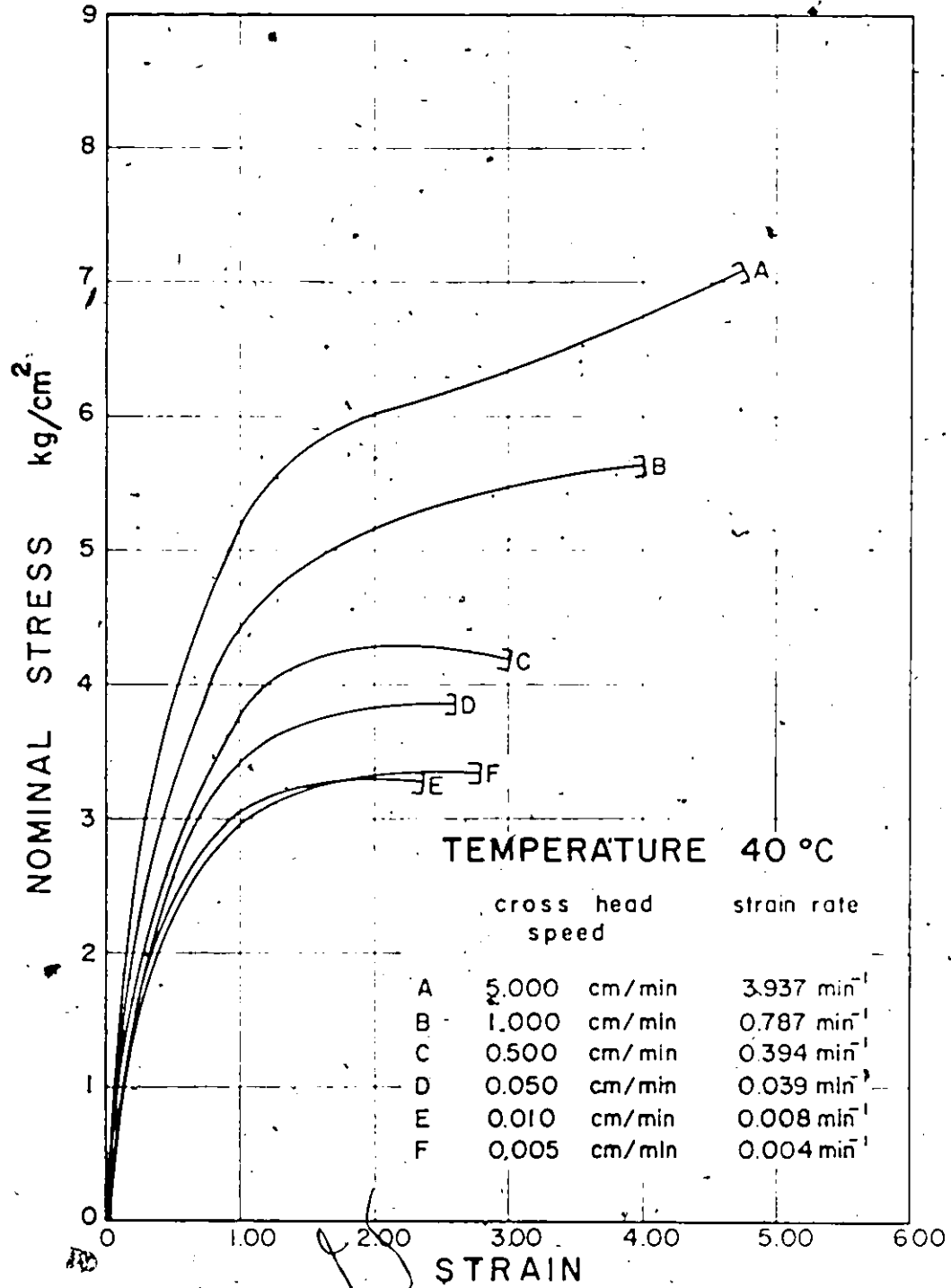


Figure 5.2. — Nominal stress — strain for one — part Urethane sealant at 40 °C

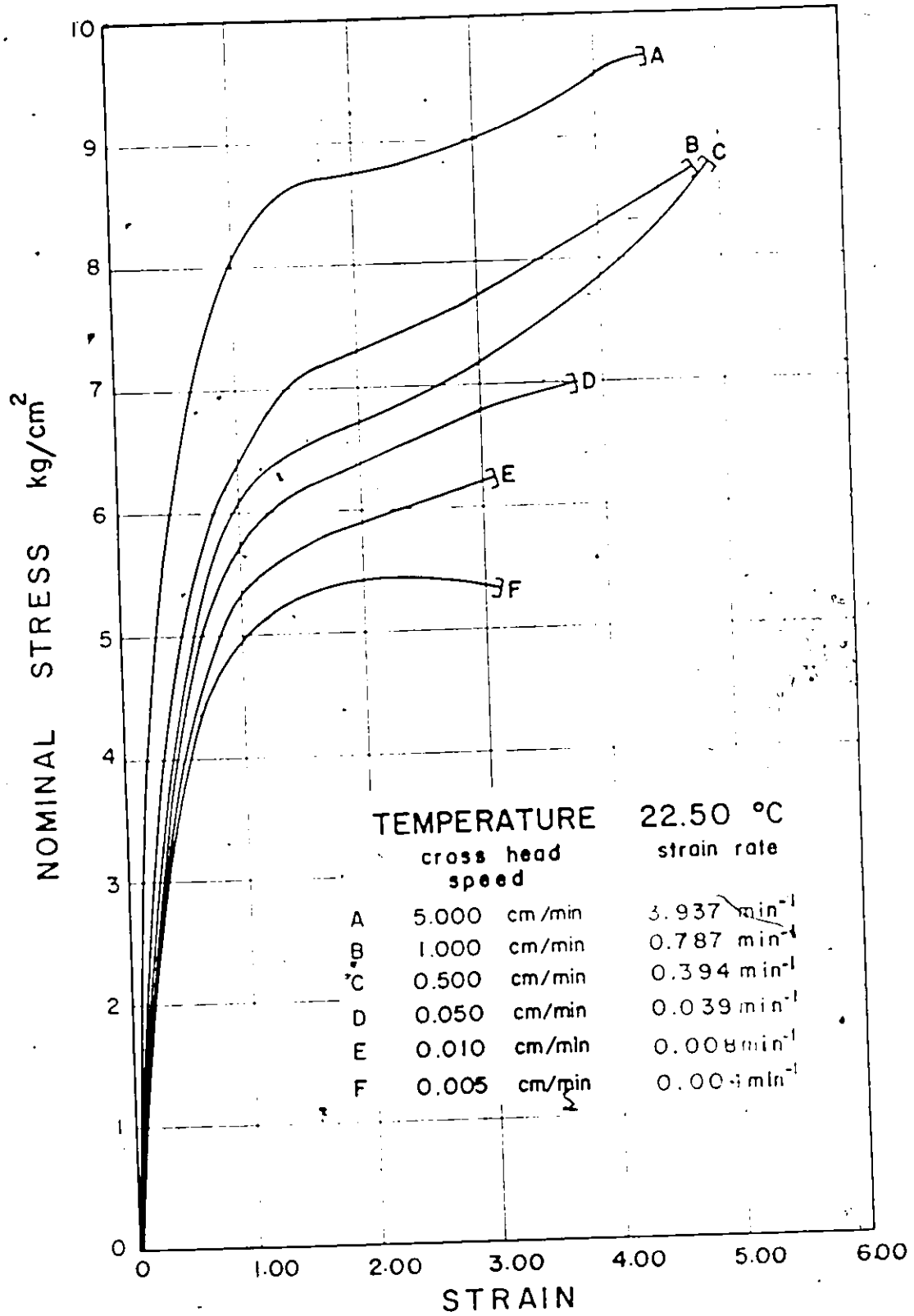


Figure 5.3 — Nominal stress-strain for one-part Urethane sealant at 22.50 °C

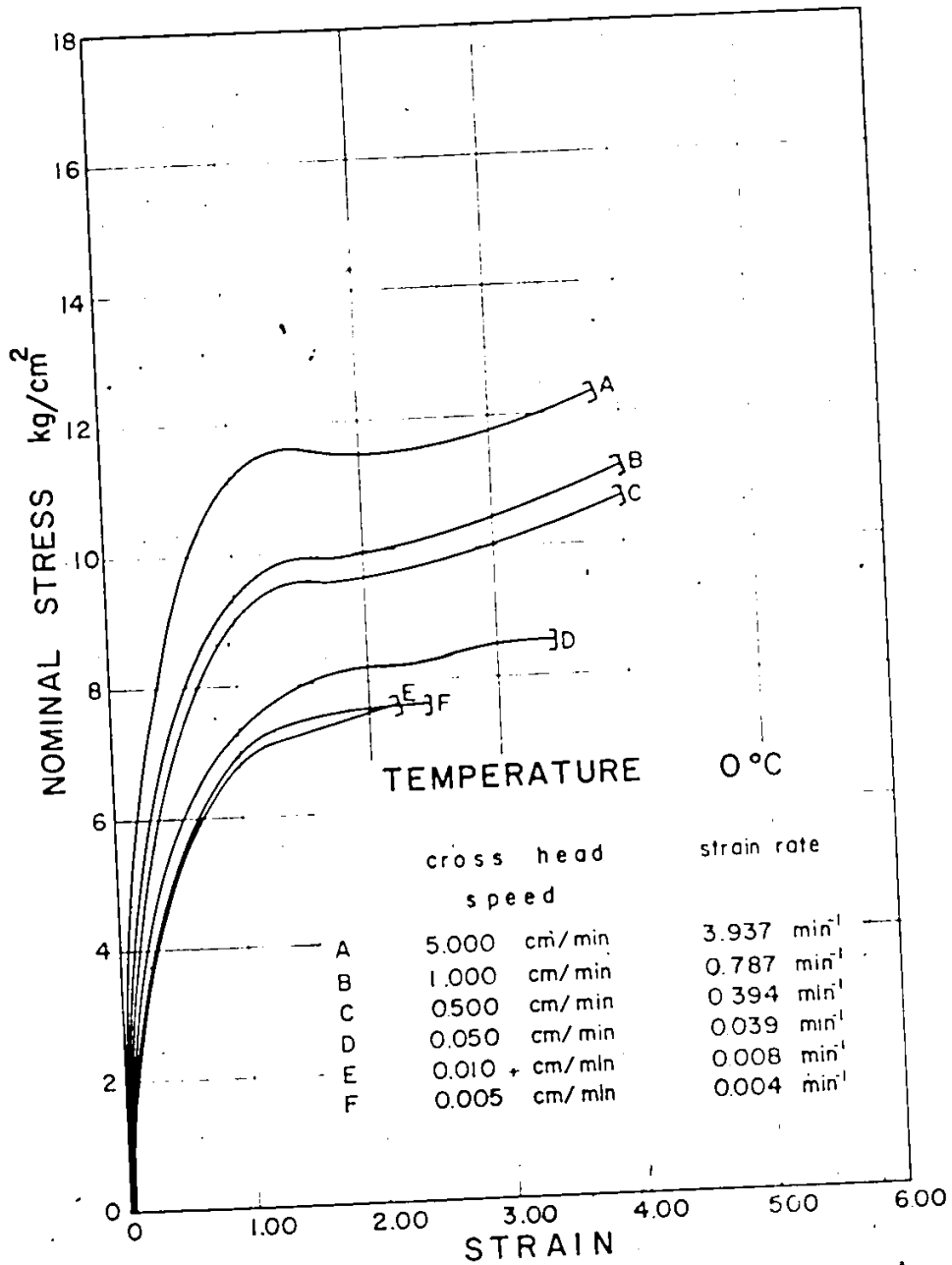


Figure 5.4 — Nominal stress-strain for one-part Urethane sealant at 0 °C

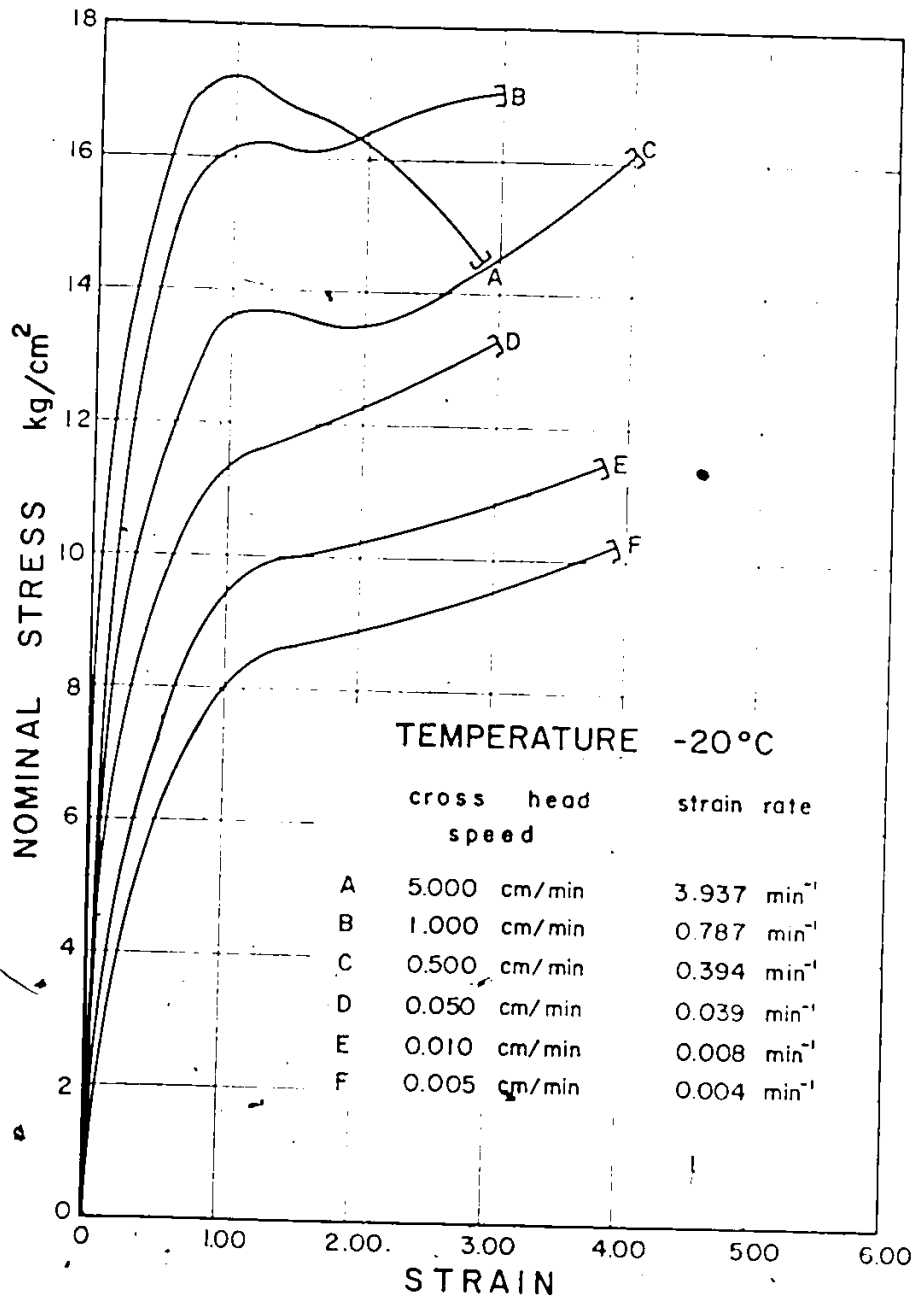


Figure 5.5 — Nominal stress — strain for one-part Urethane sealant at -20 °C

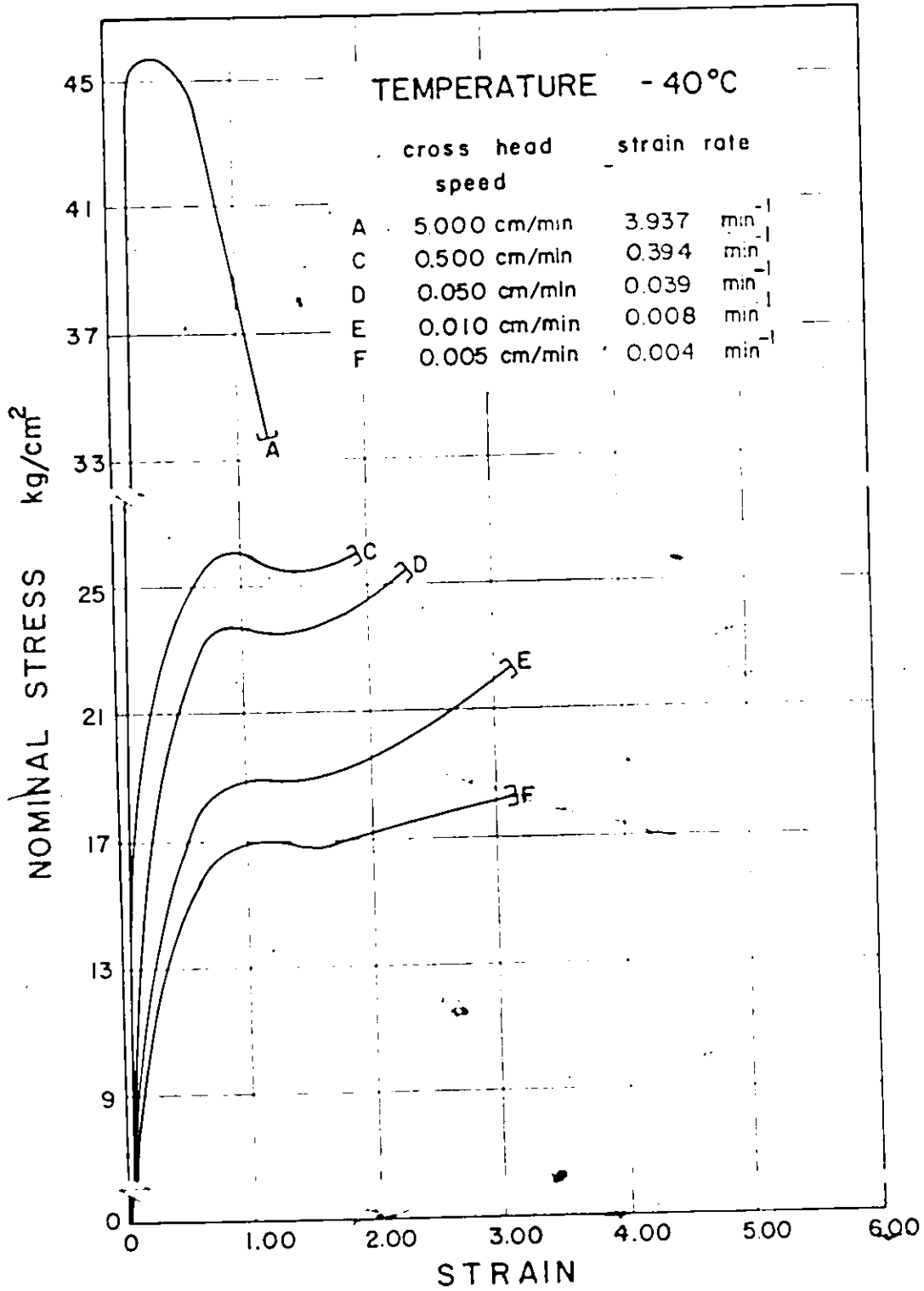


Figure 5.6 — Nominal stress-strain for one-part Urethane sealant at -40 °C

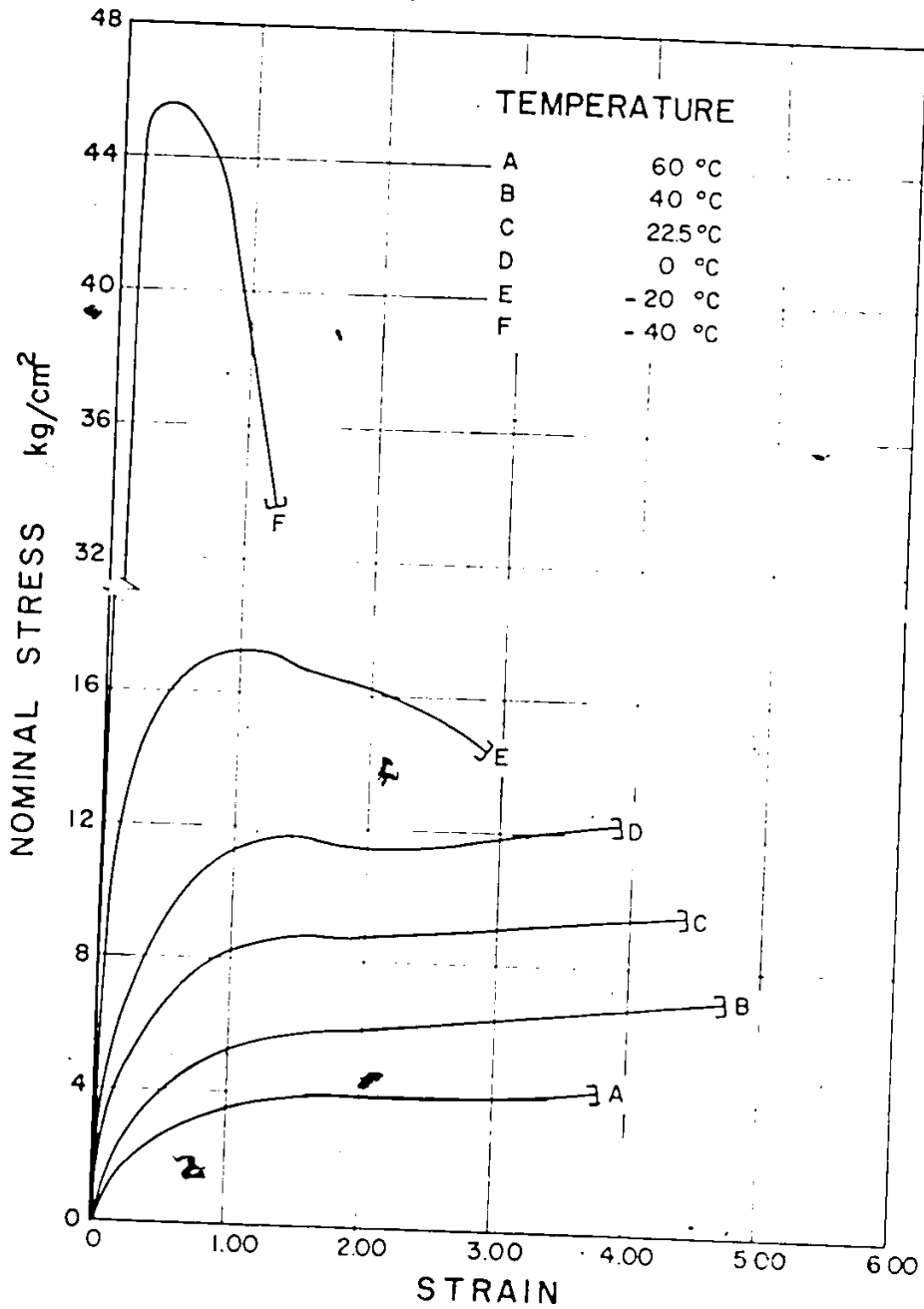


Figure 5.7 — Nominal stress-strain for one-part Urethane sealant at cross head speed 5 cm/min

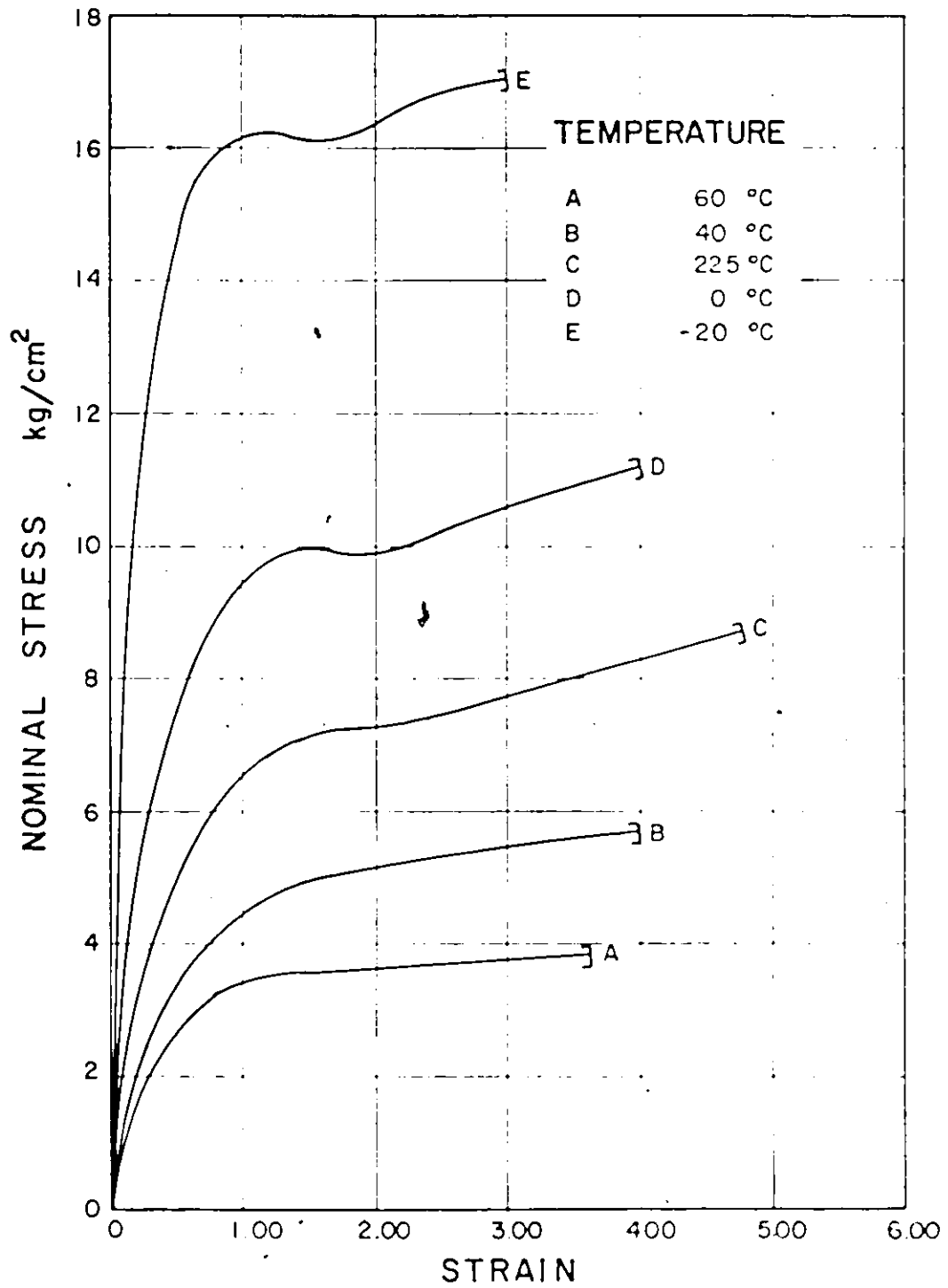


Figure 5.8 — Nominal stress-strain for one-part Urethane sealant at cross head speed 1 cm/min



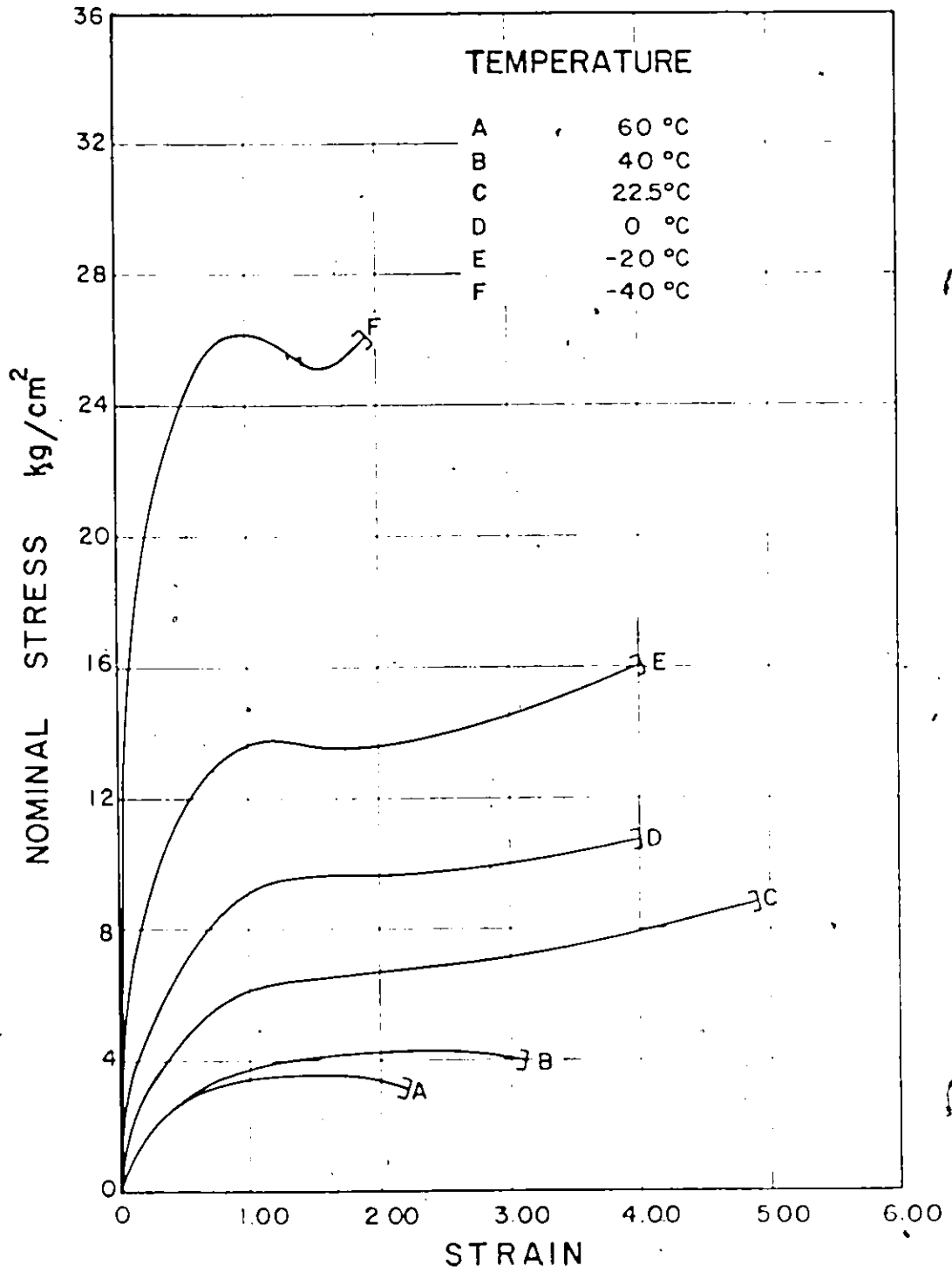


Figure 5.9 — Nominal stress - strain for one-part Urethane sealant at cross head speed 0.5 cm/min

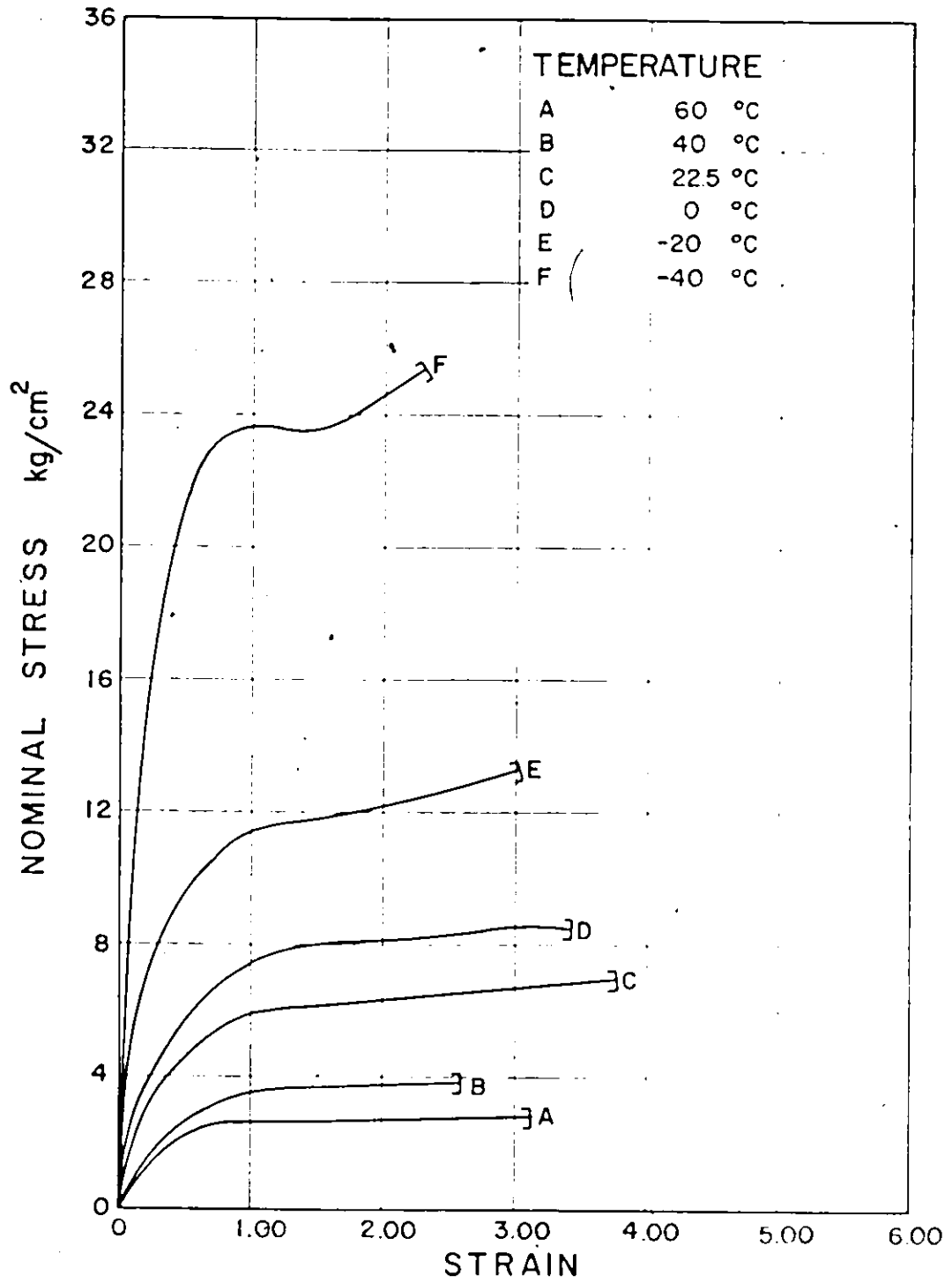


Figure 5.10 — Nominal stress - strain for one - part Urethane sealant at cross head speed 0.05 cm/min

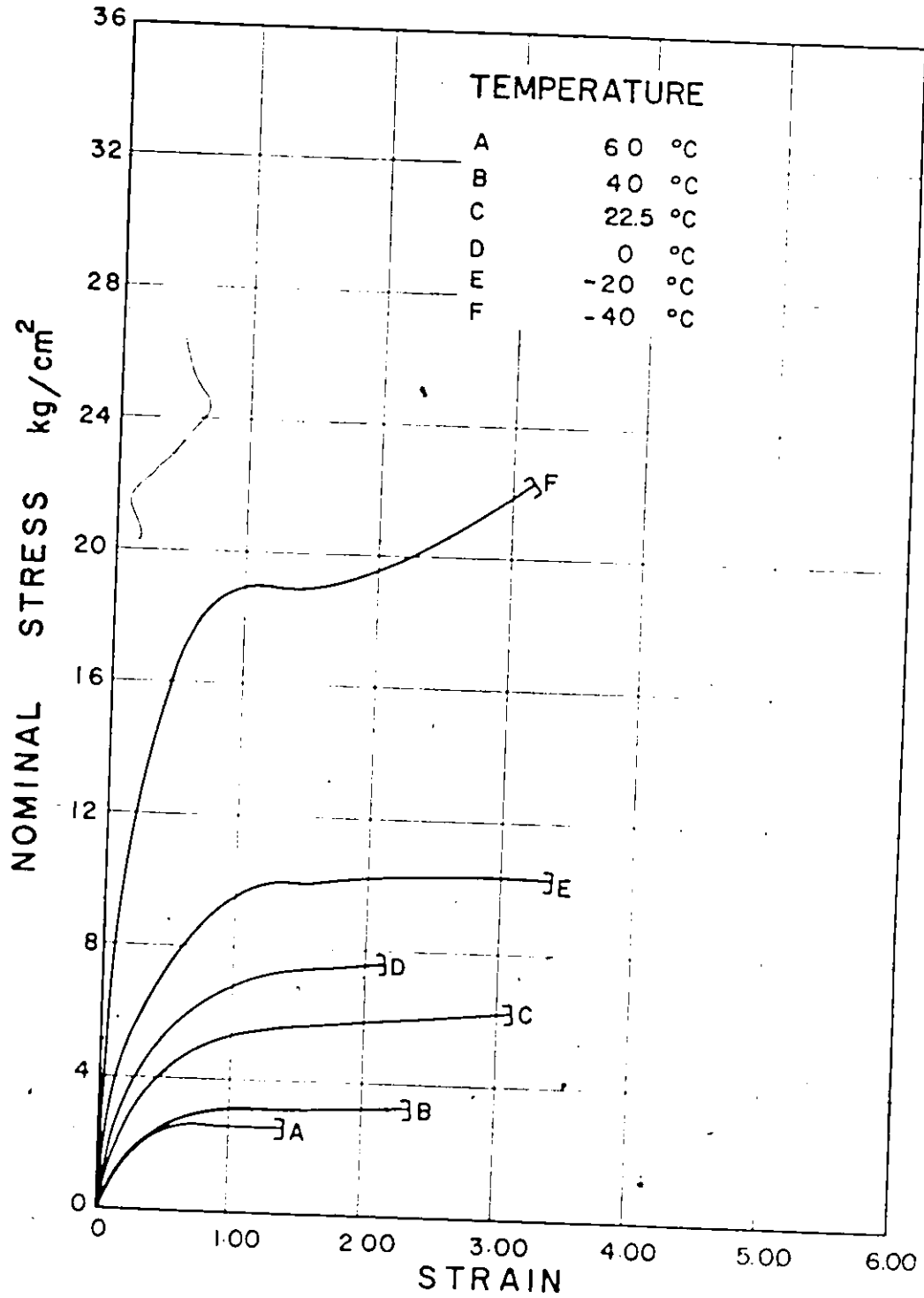


Figure 5.11 Nominal stress strain for one part Urethane sealant at cross head speed 0.01 cm/min

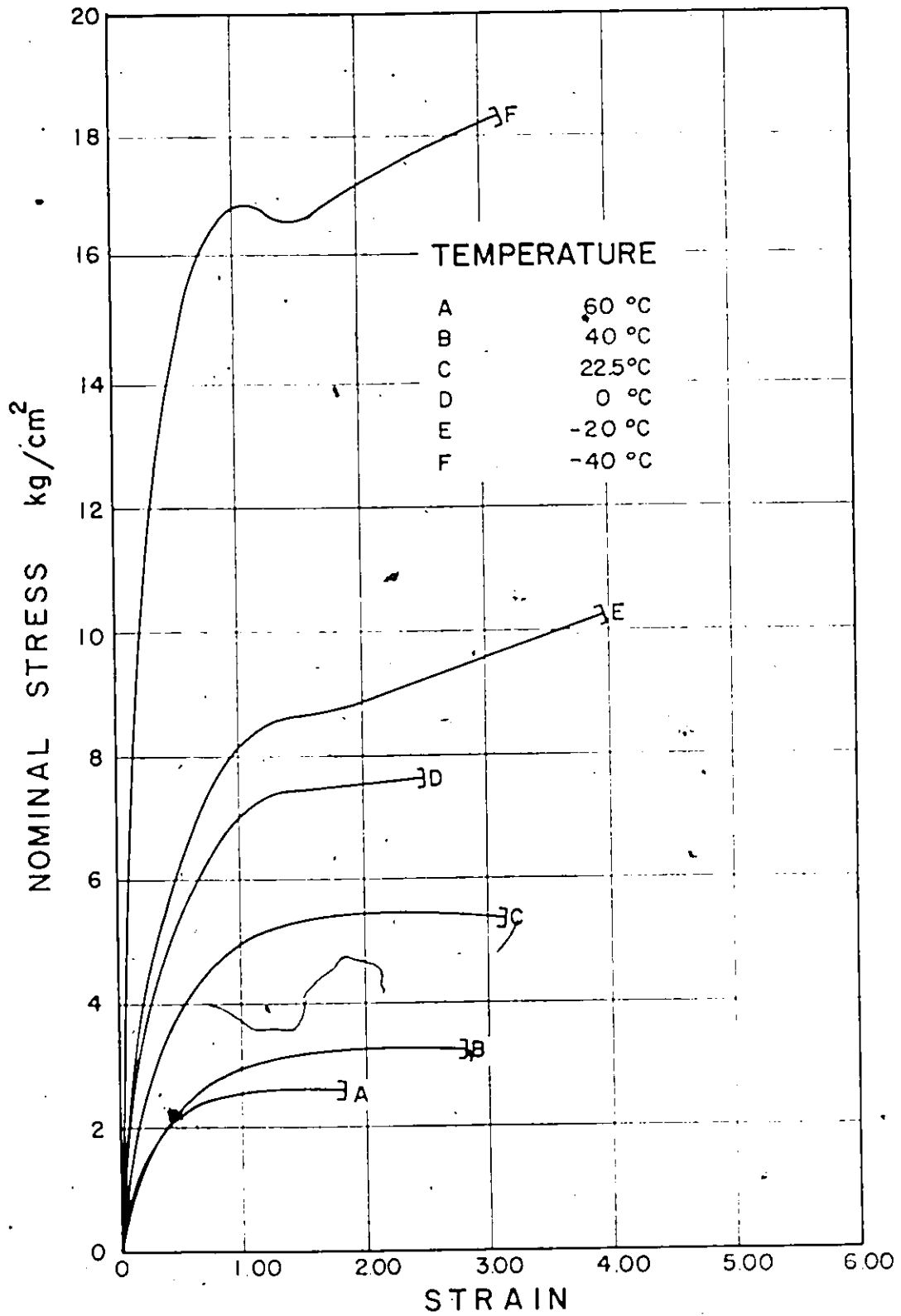


Figure 5.12 — Nominal stress - strain for one-part Urethane sealant at cross head speed 0.005 cm/min

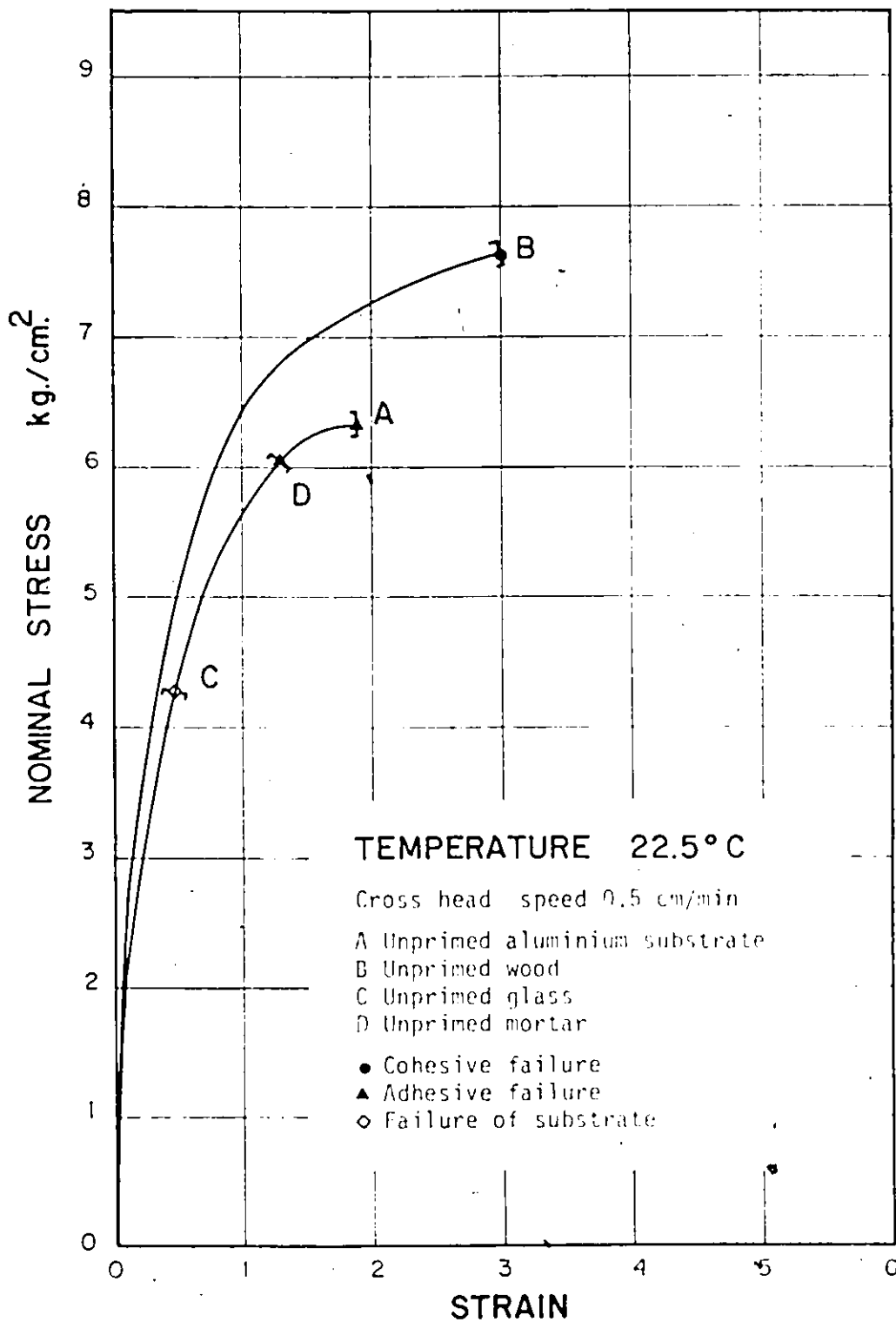


Figure 5.13 — Nominal stress - strain for one-part Urathane sealant at room temperature for different substrates.

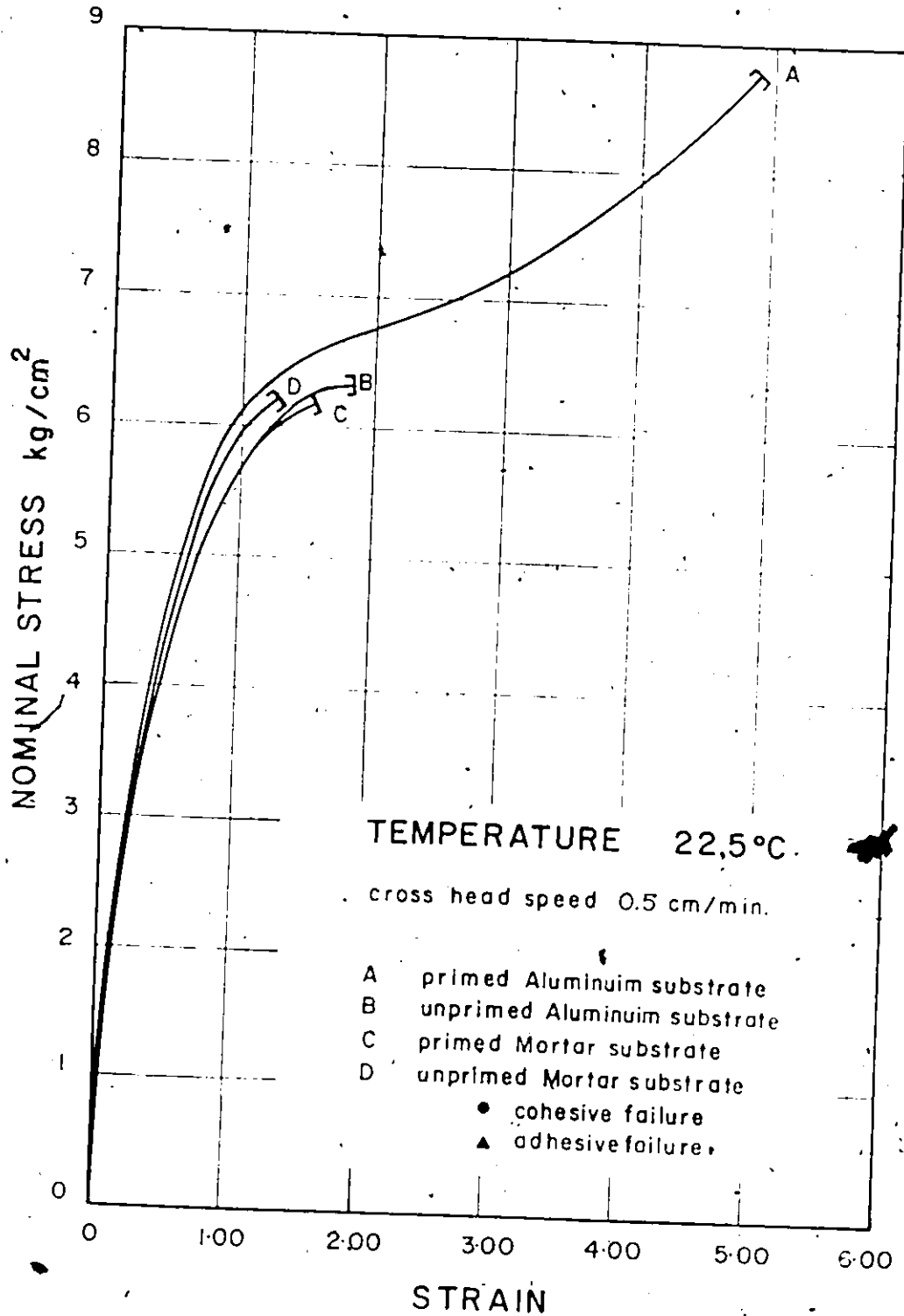


Figure 5.14 Nominal stress strain for one part Urethane sealant for primed and unprimed substrates

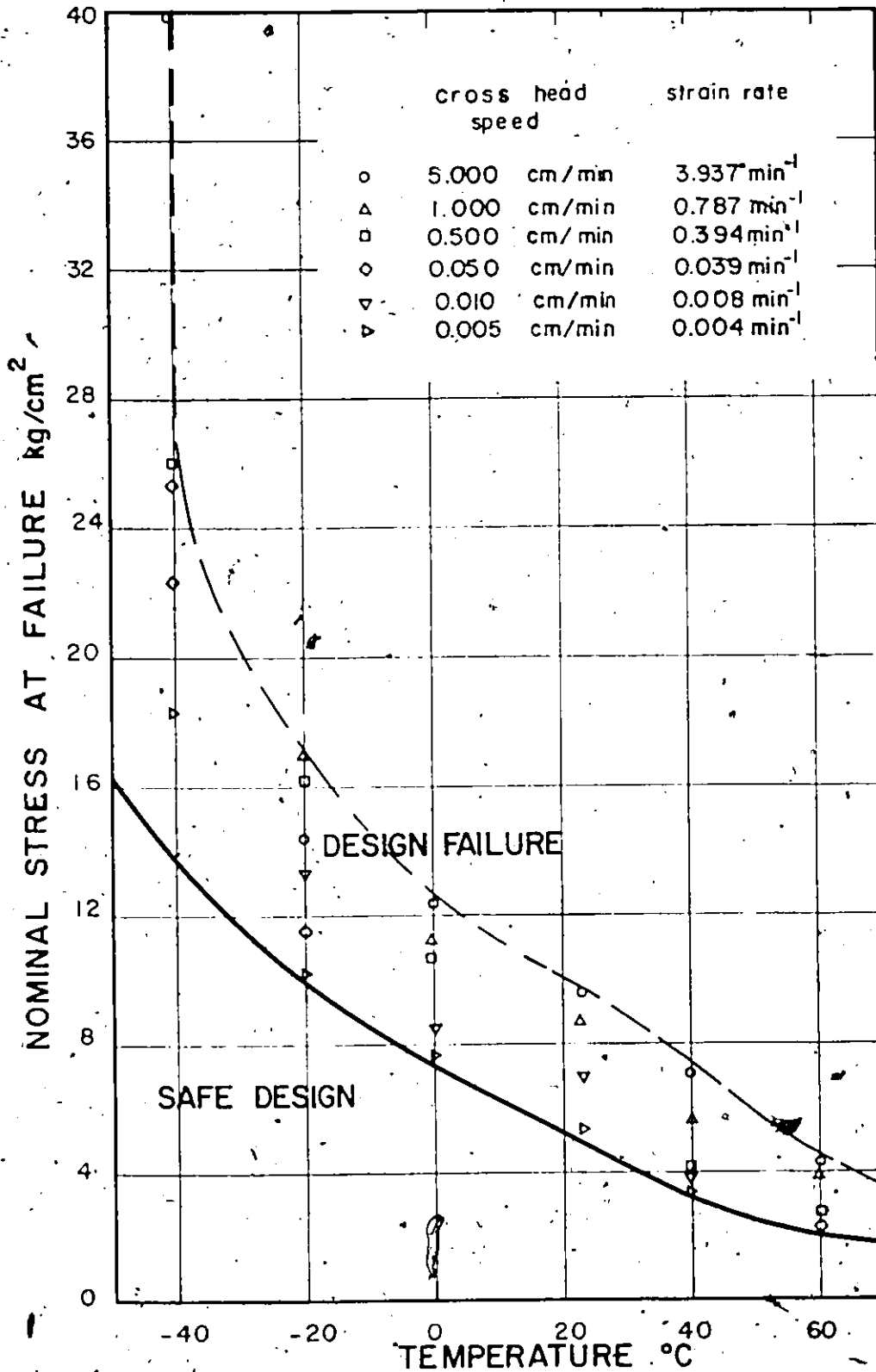


Figure 5.15\_Nominal stress at break - temperature

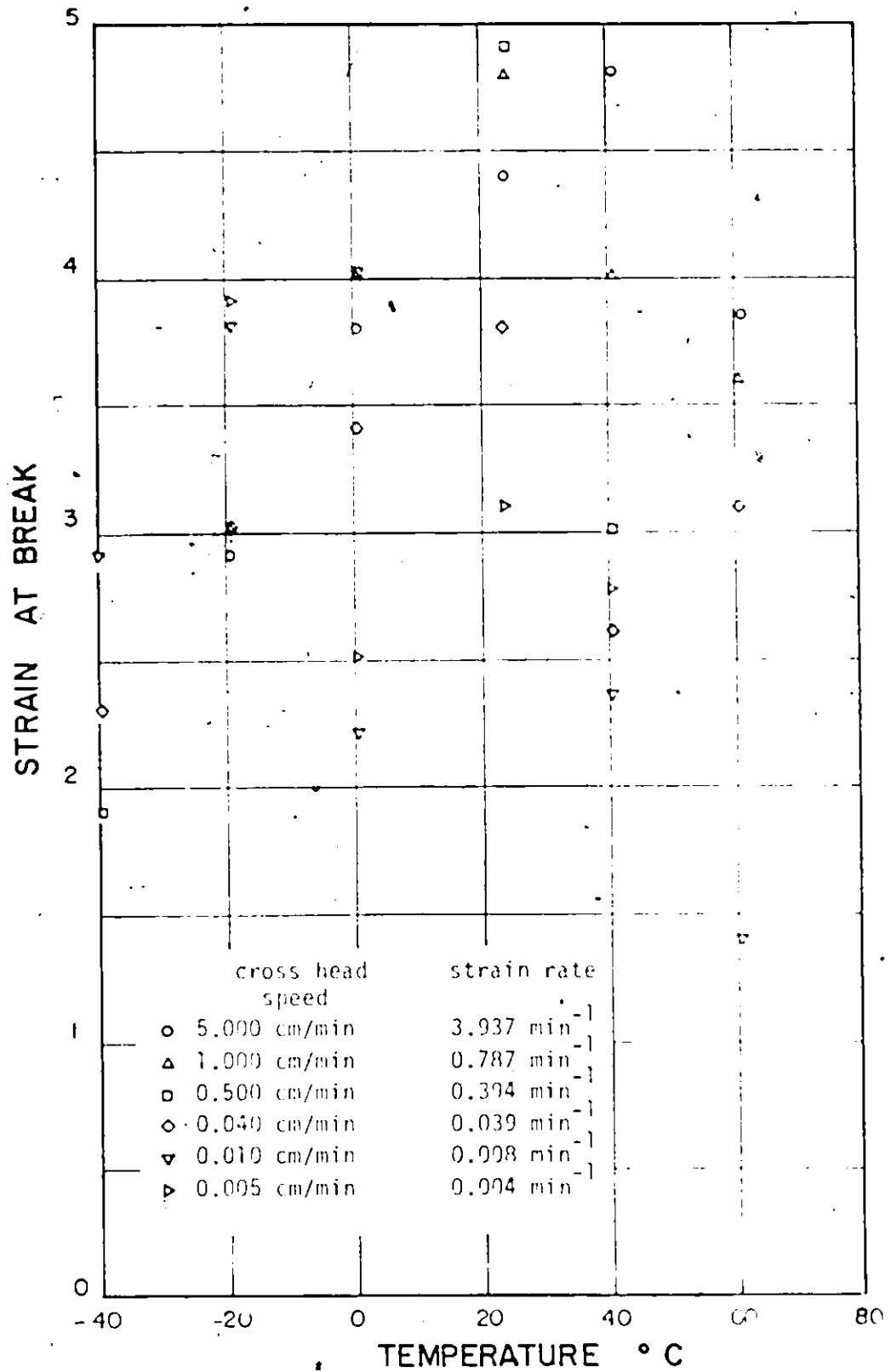


Figure 5.16 \_ Strain at break versus temperature



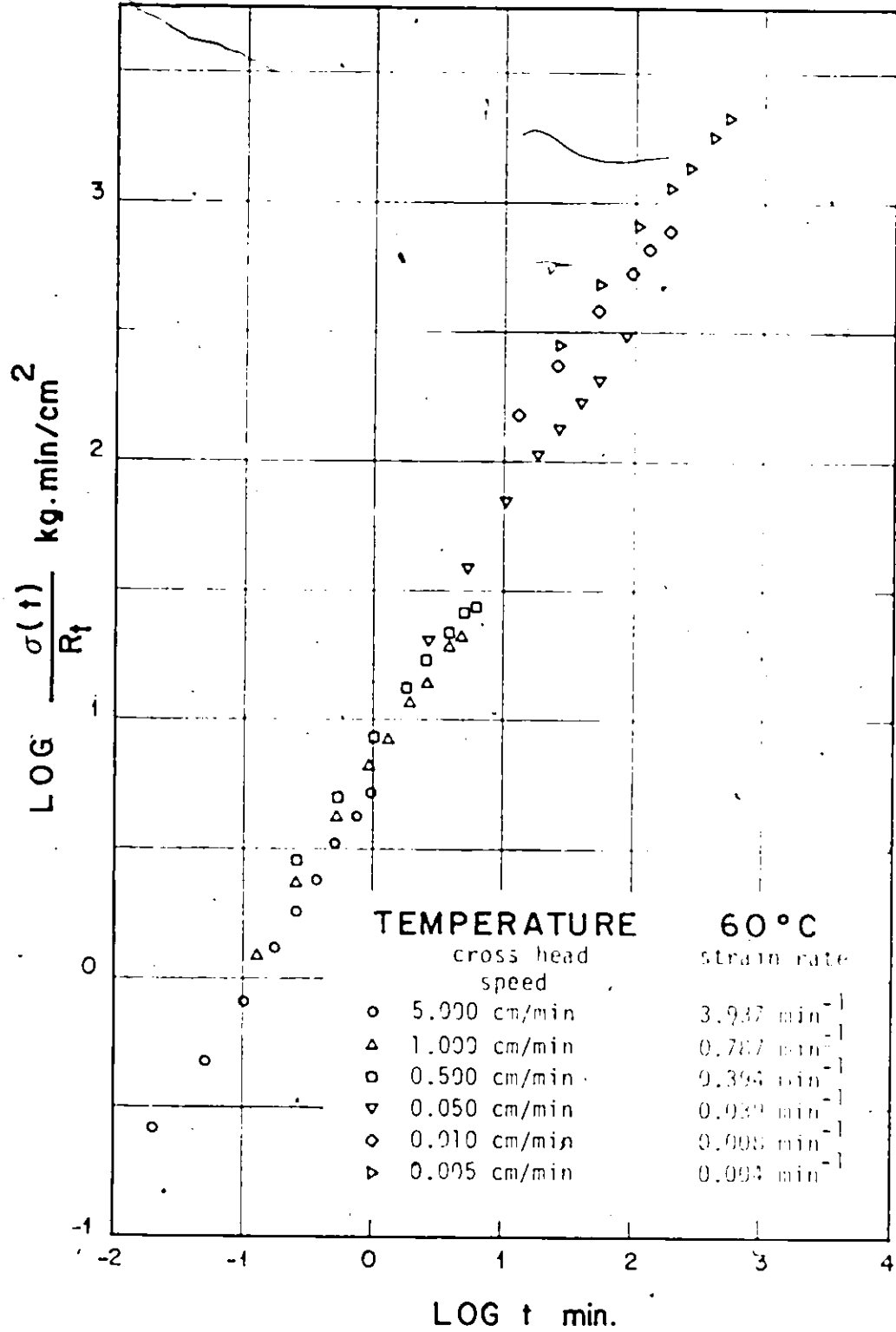


Figure 5.17\_ Nominal stress \_strain curves from figure 5.1 reduced to unit strain rate at 60 °C

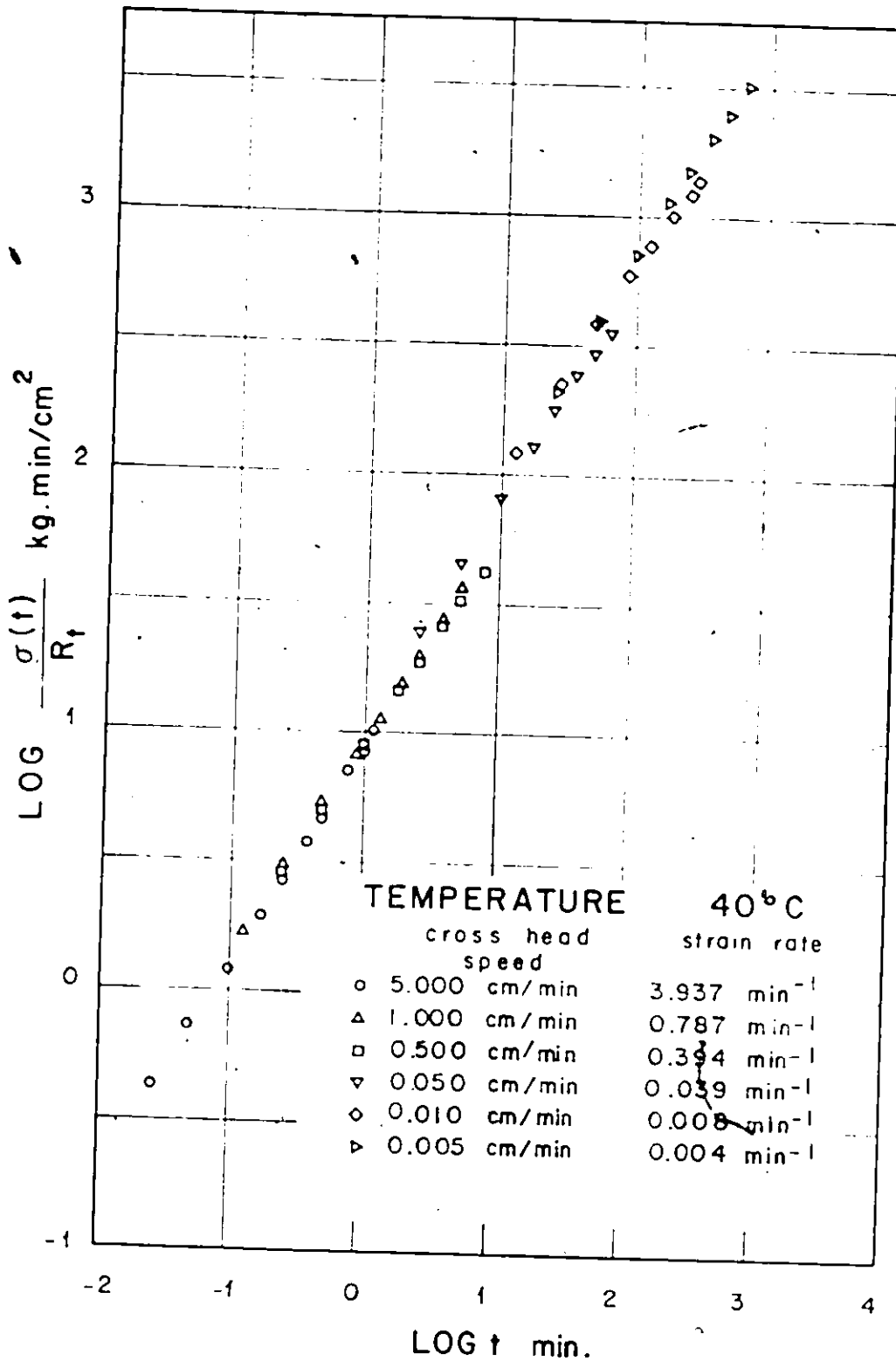


Figure 5.18 - Nominal stress-strain curves from figure 5.2 reduced to unit strain rate at 40 °C

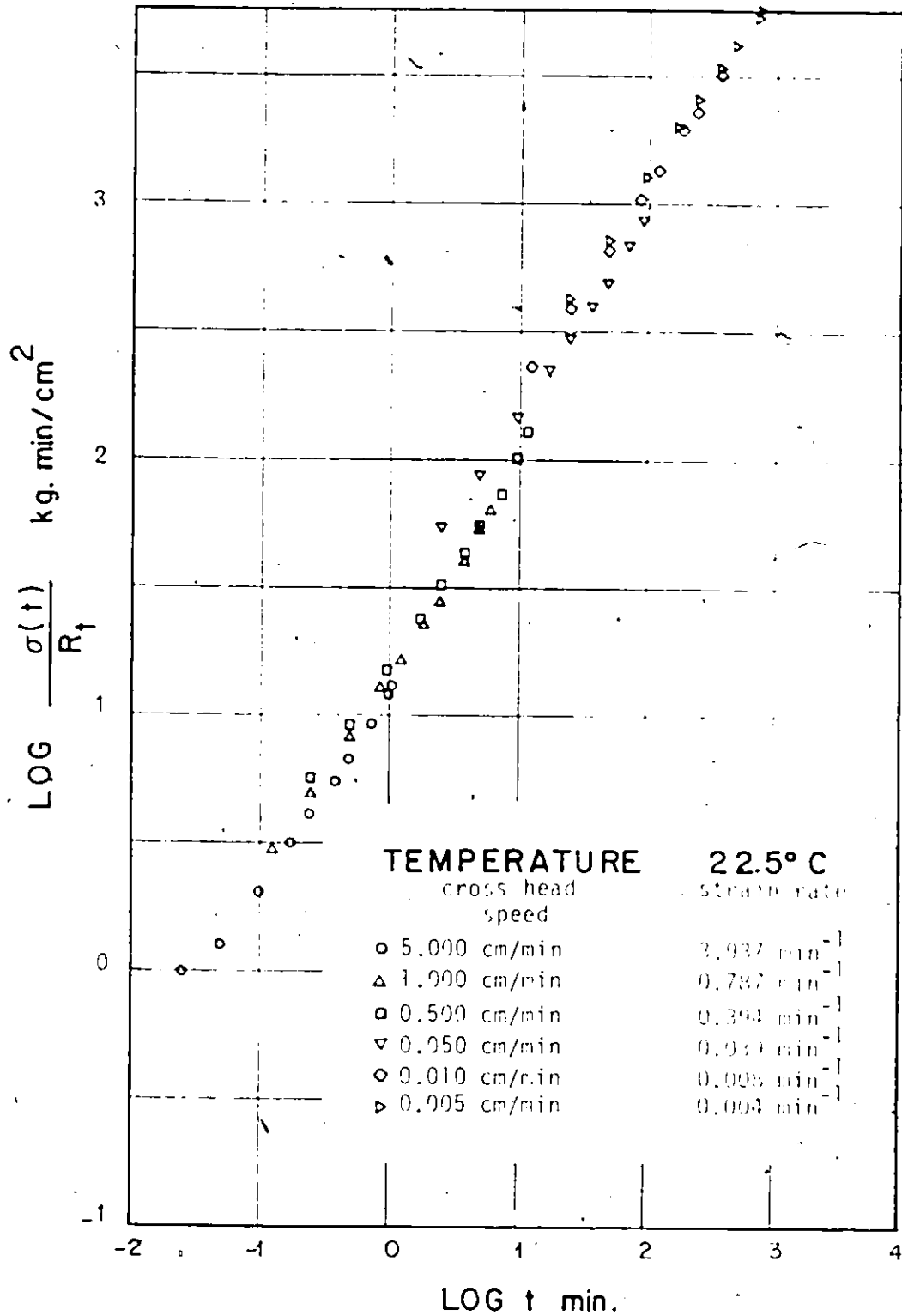


Figure 5.19 - Nominal stress-strain curves from figure 5.3 reduced to unit strain rate at 22.5 ° C

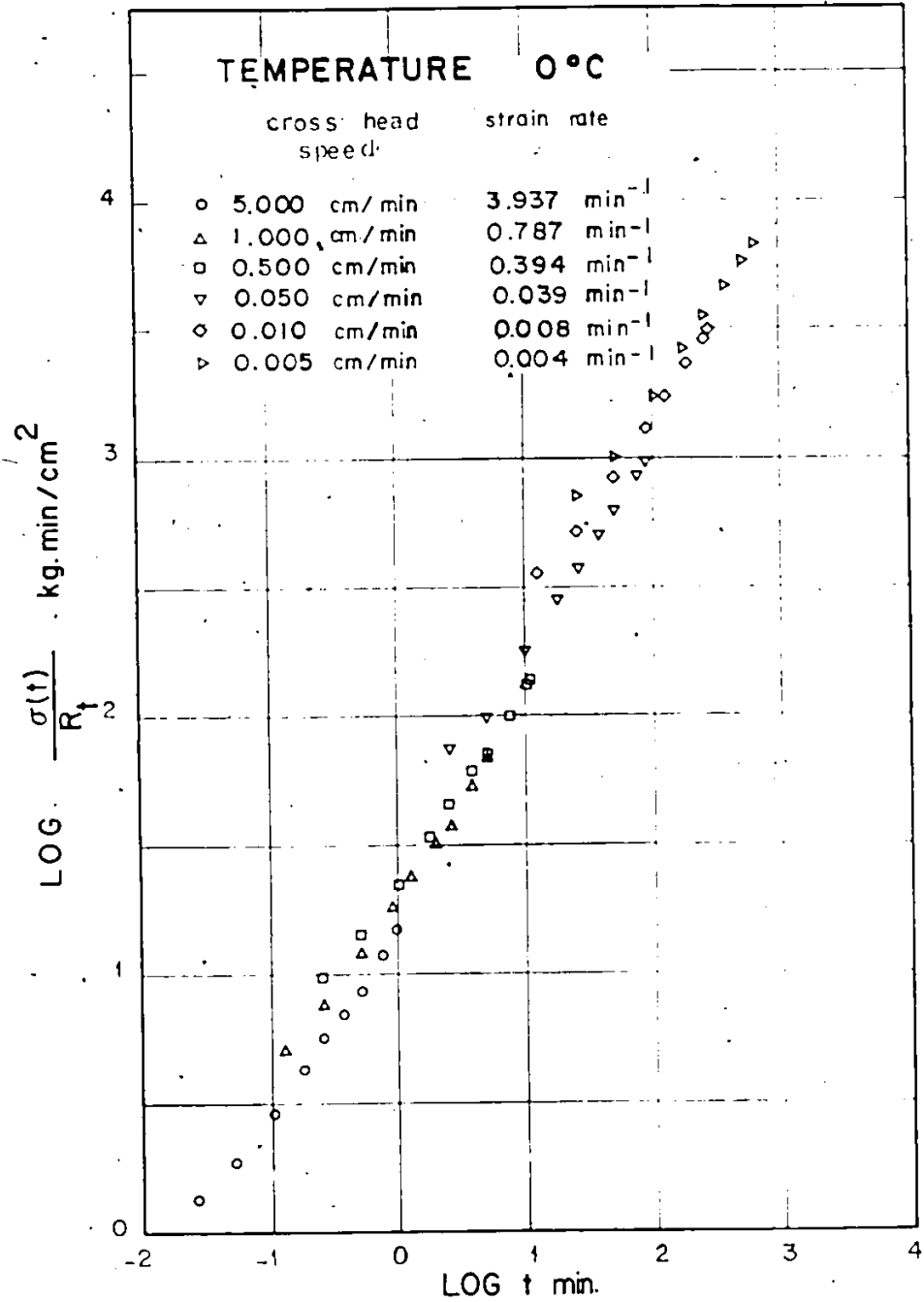


Figure 5.20 - Nominal stress strain curves from figure 5.4 reduced to unit strain rate at 0 °C

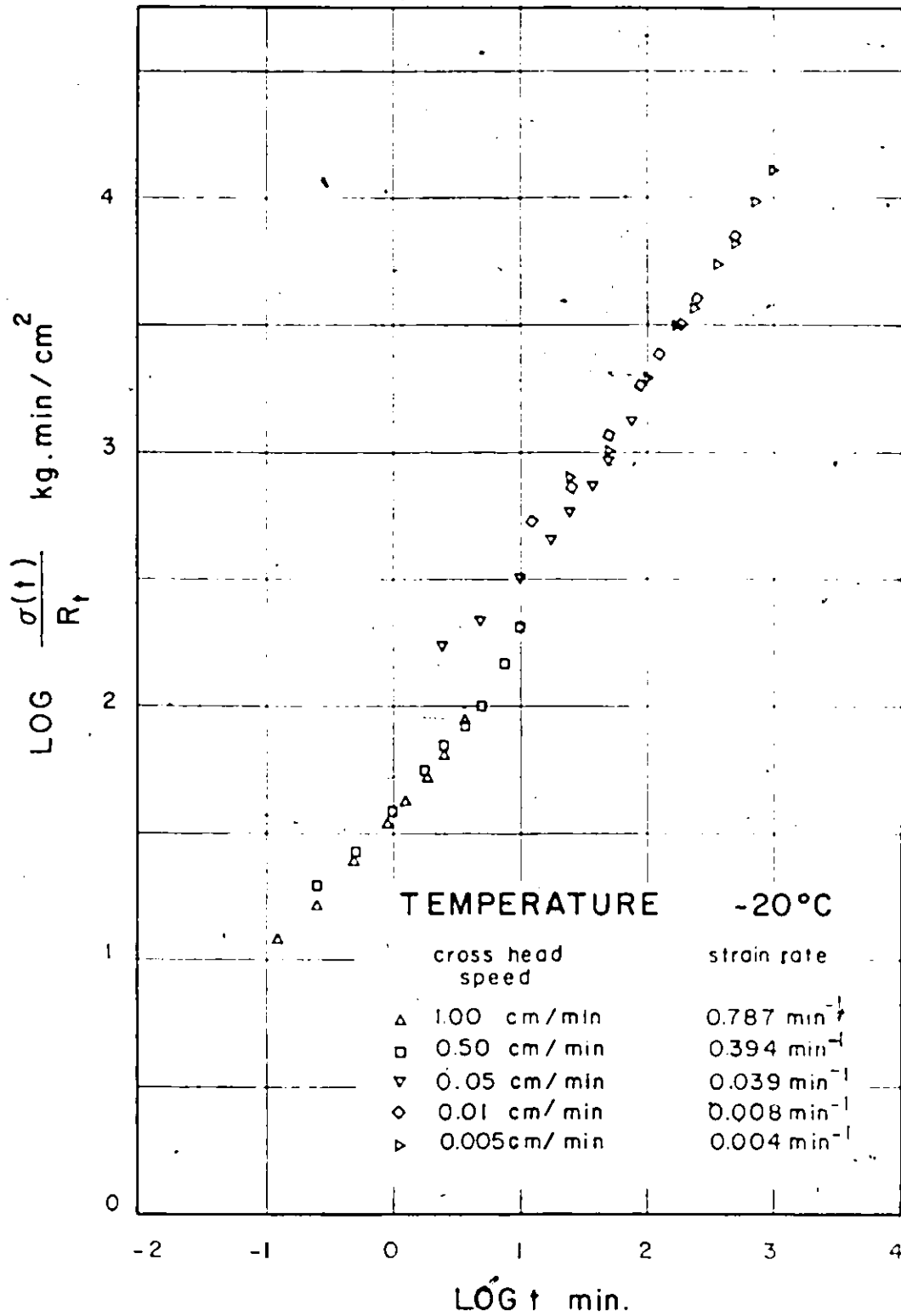


Figure 5.21 — Nominal stress-strain curves from figure 5.5 reduced to unit strain rate at -20°C

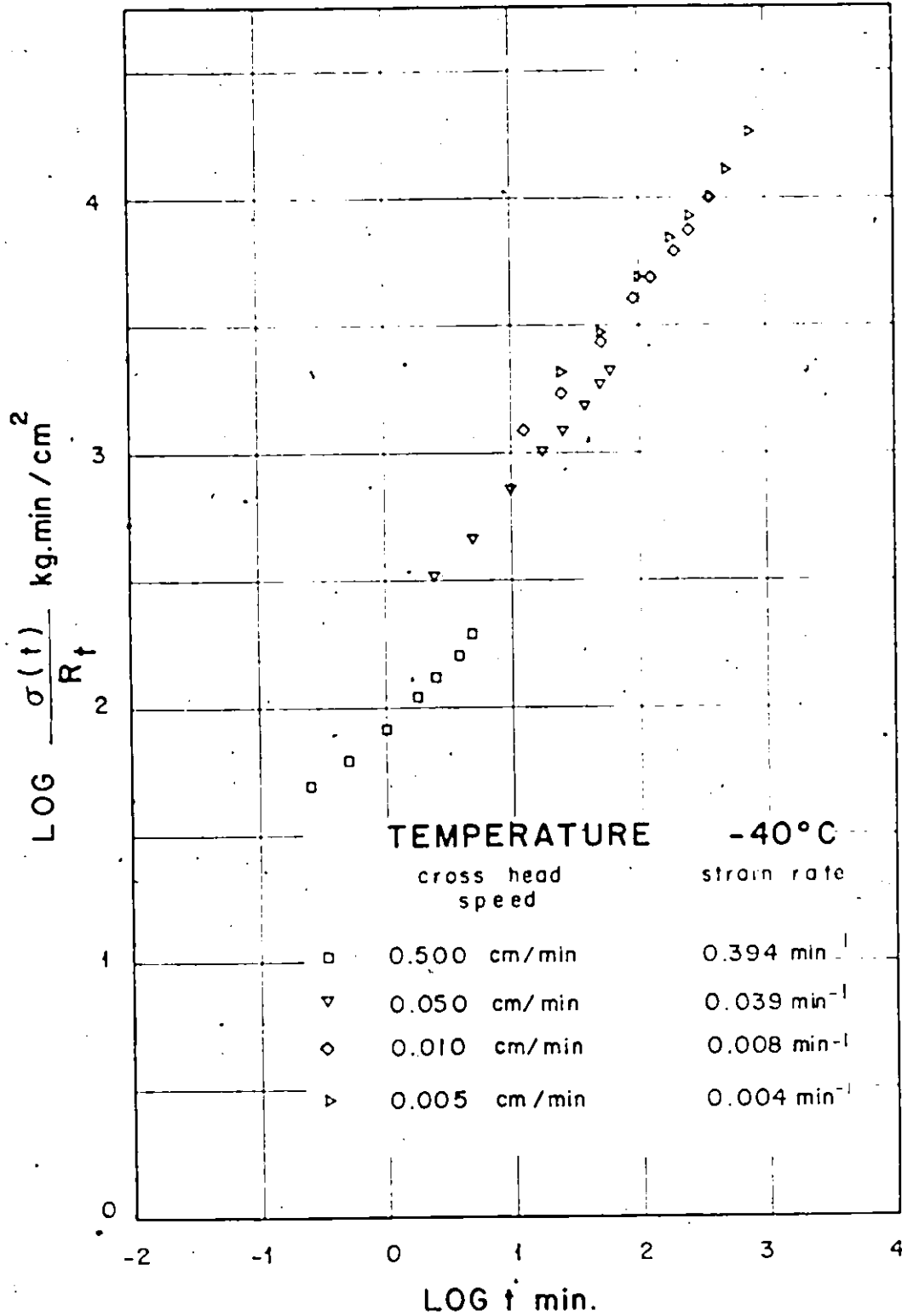


Figure 5.22 - Nominal stress strain curves from figure 5.6 reduced to unit strain rate at -40°C

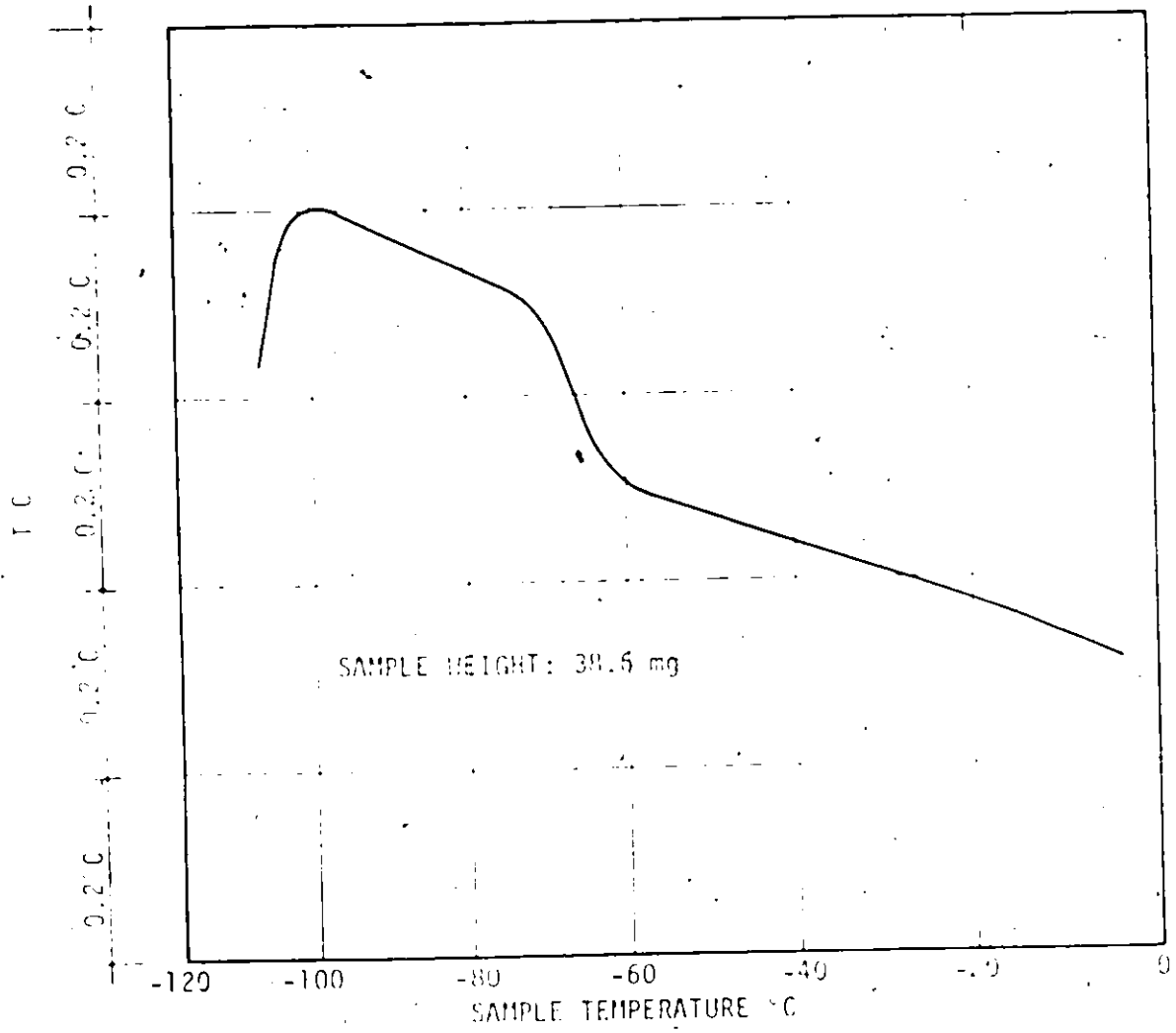


FIGURE 5.23 - Differential thermal analysis graph

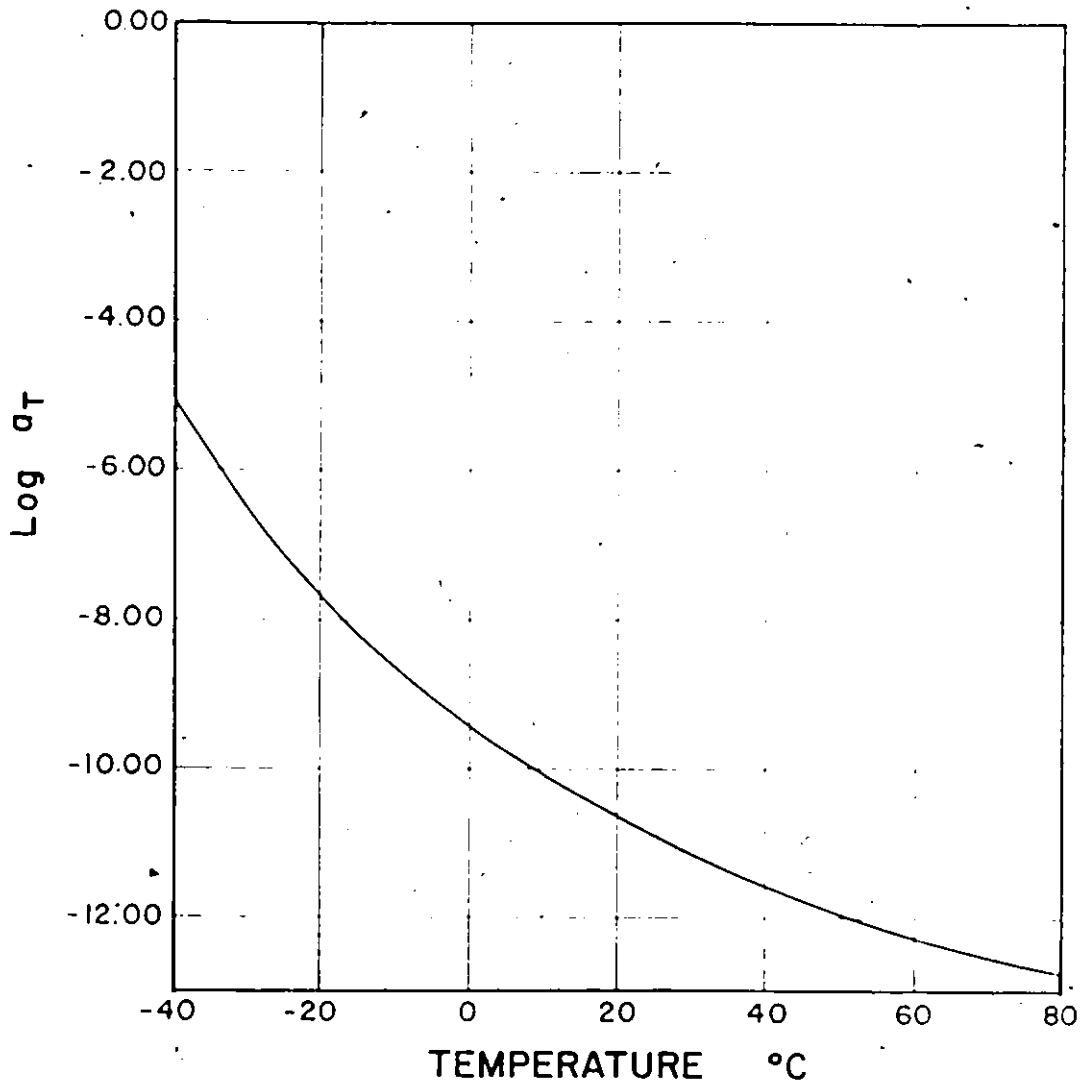


Figure 5.24—  $\text{Log } a_T$  vs. Temperature



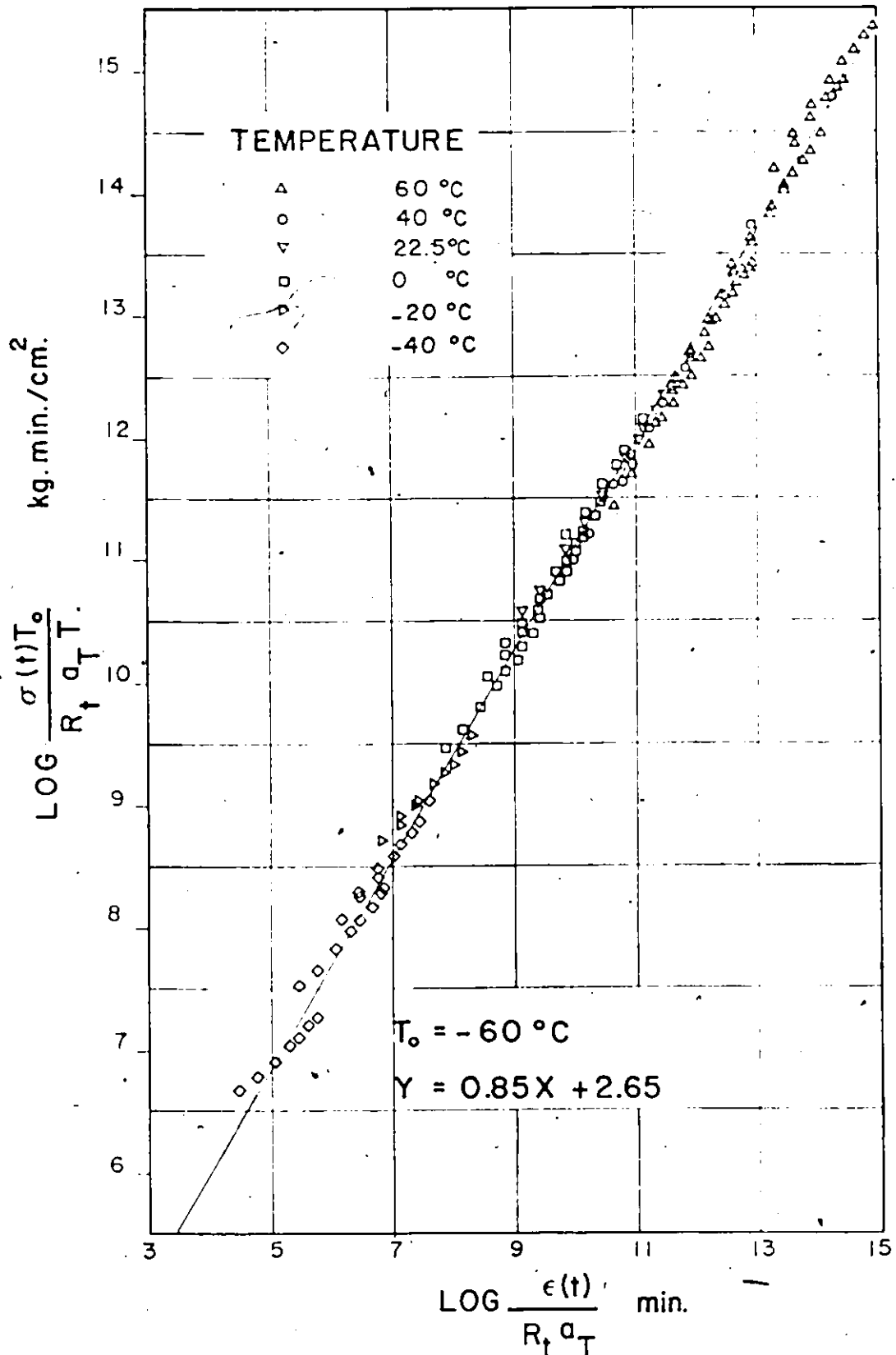


Figure 5.25 – Experimentally determined Master Curve from tensile test result.

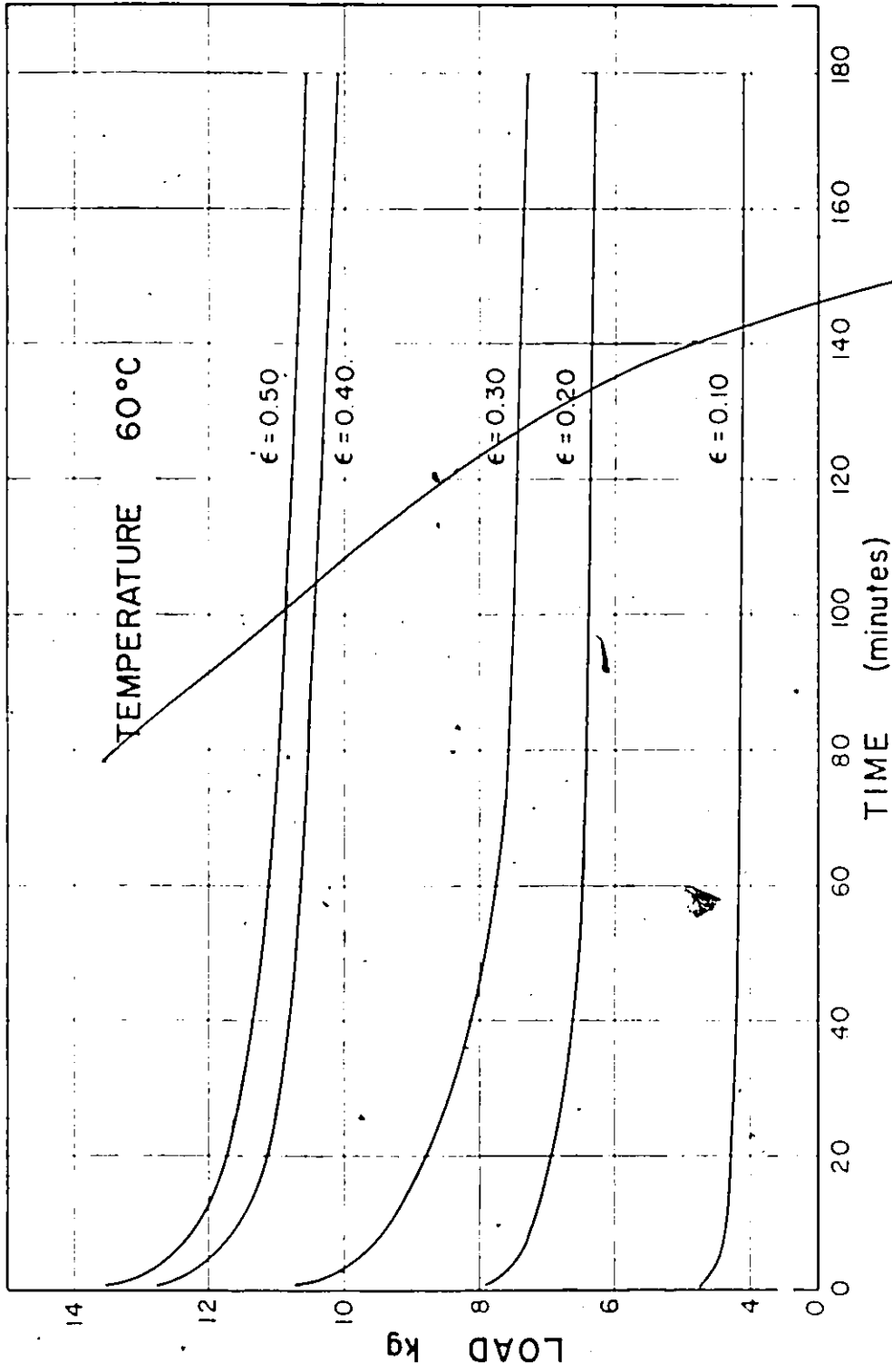


Figure 5.2.6 — Experimental relaxation curves of one part Urethane sealants at 60°C

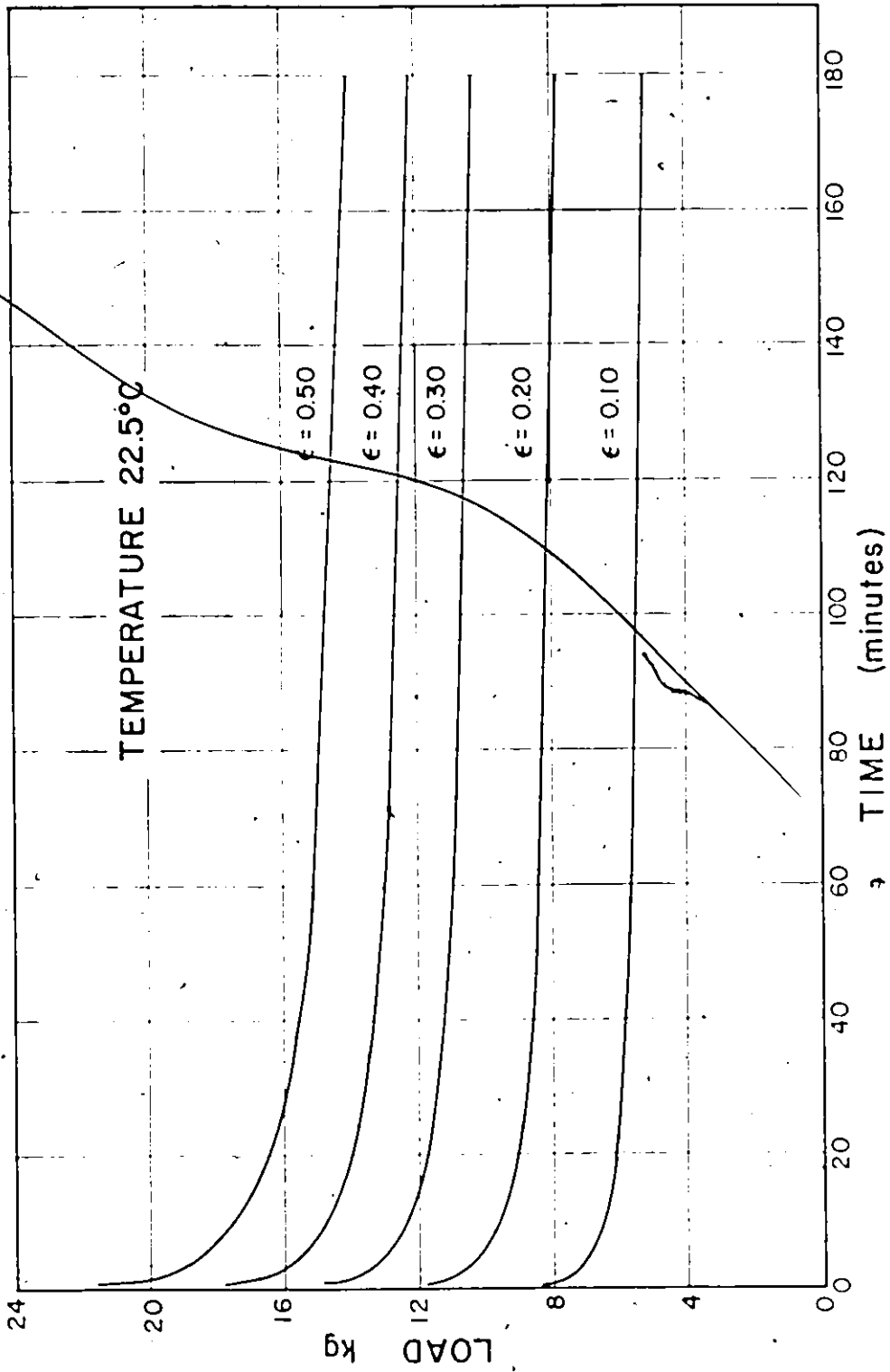


Figure 5.27 — Experimental relaxation curve of one-part Urethane sealants at 22.5°C

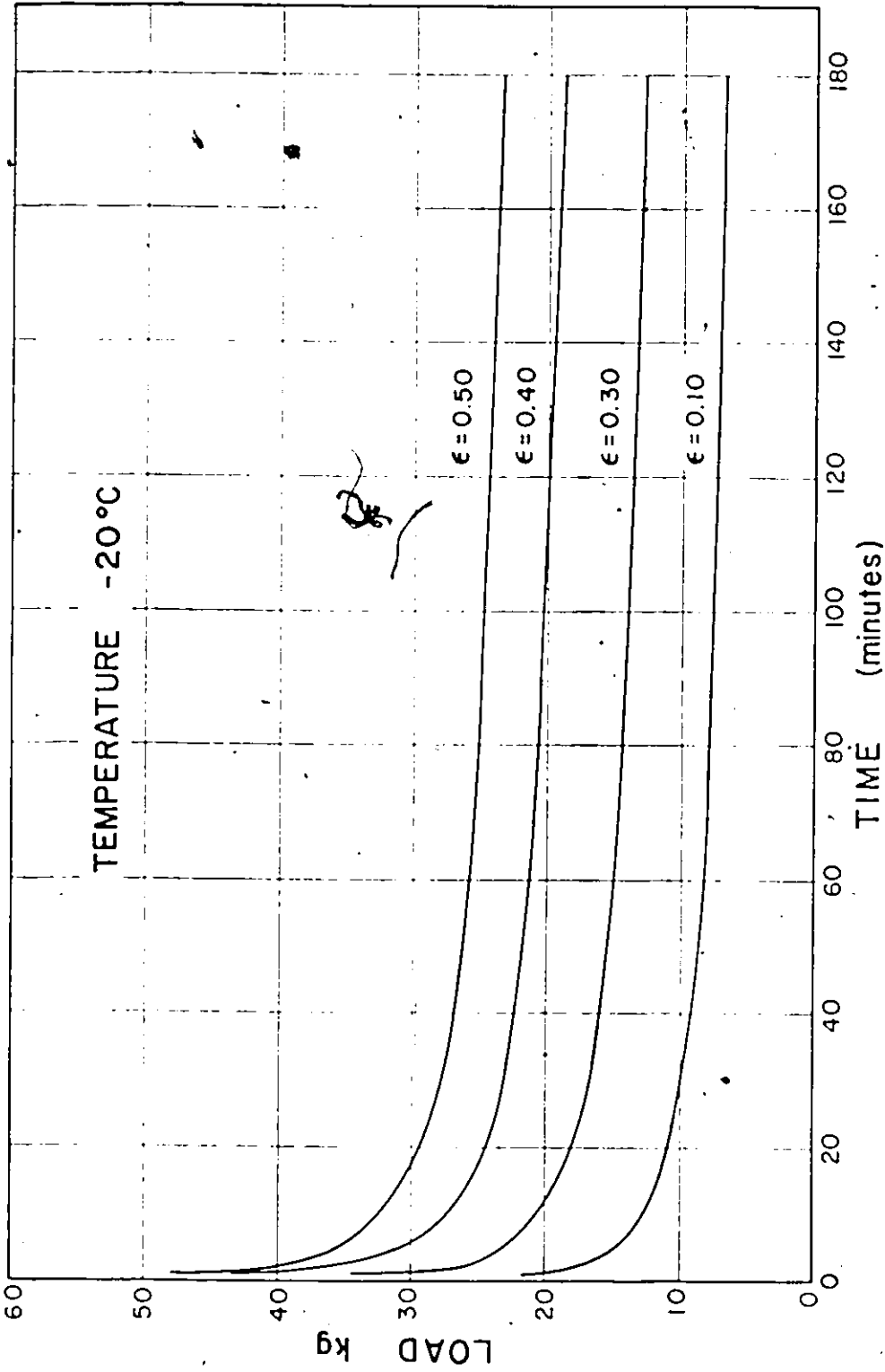


Figure 5.28 — Experimental relaxation curves of one-part Urethane sealants at -20 °C

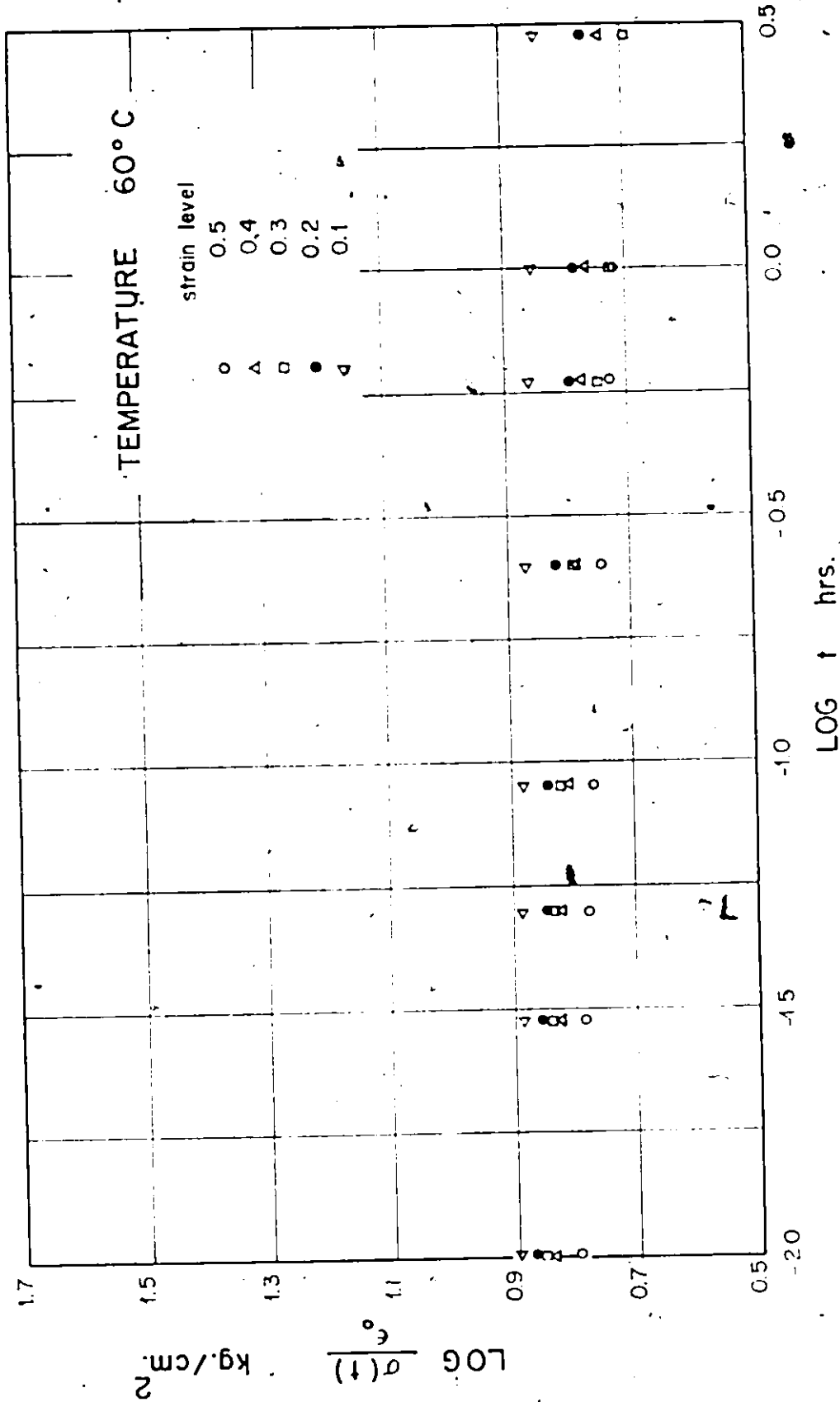


Figure 5.29 - Relaxation modulus versus time at 60°C.

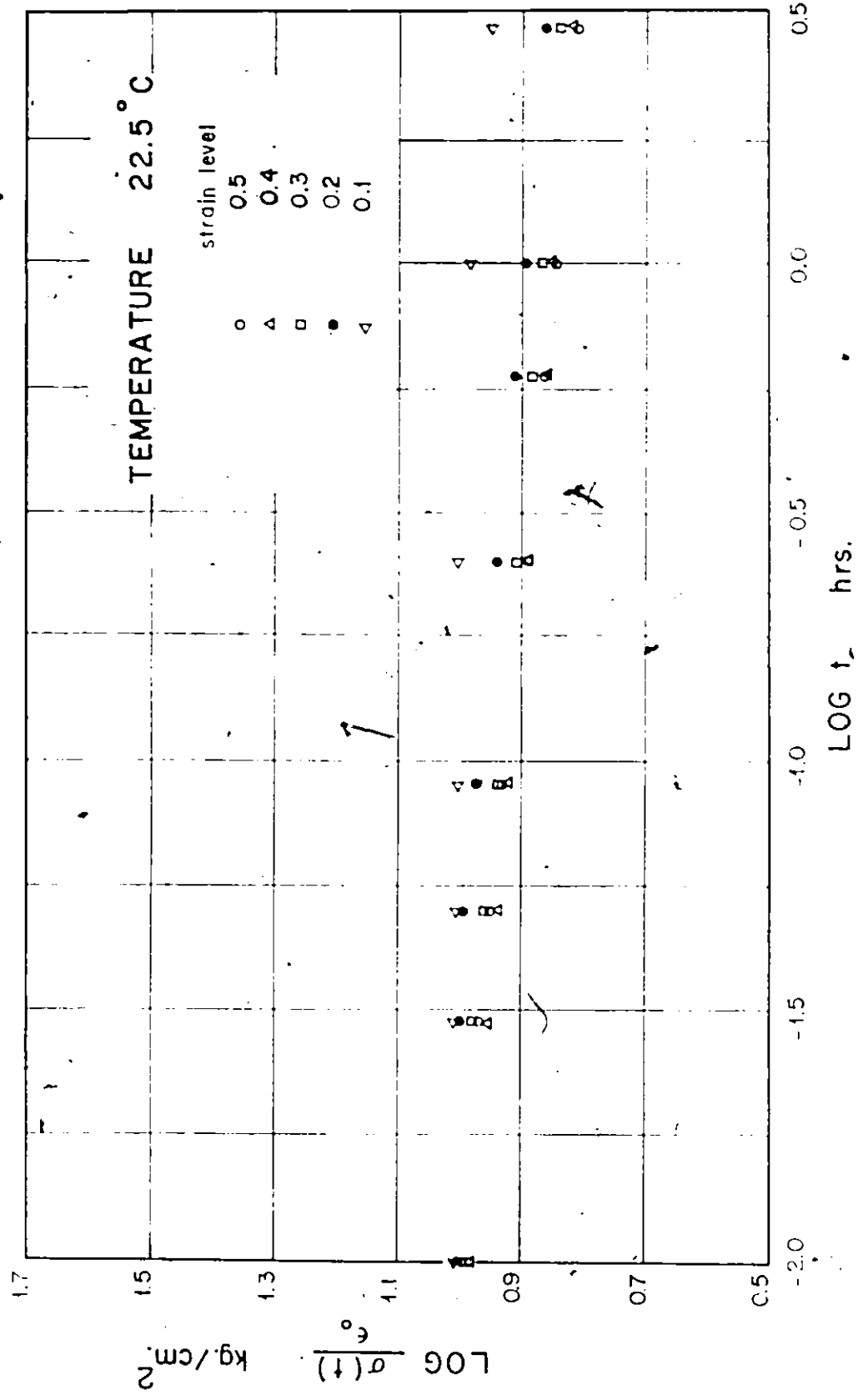


Figure 5.30 - Relaxation modulus versus time at 22.5°C



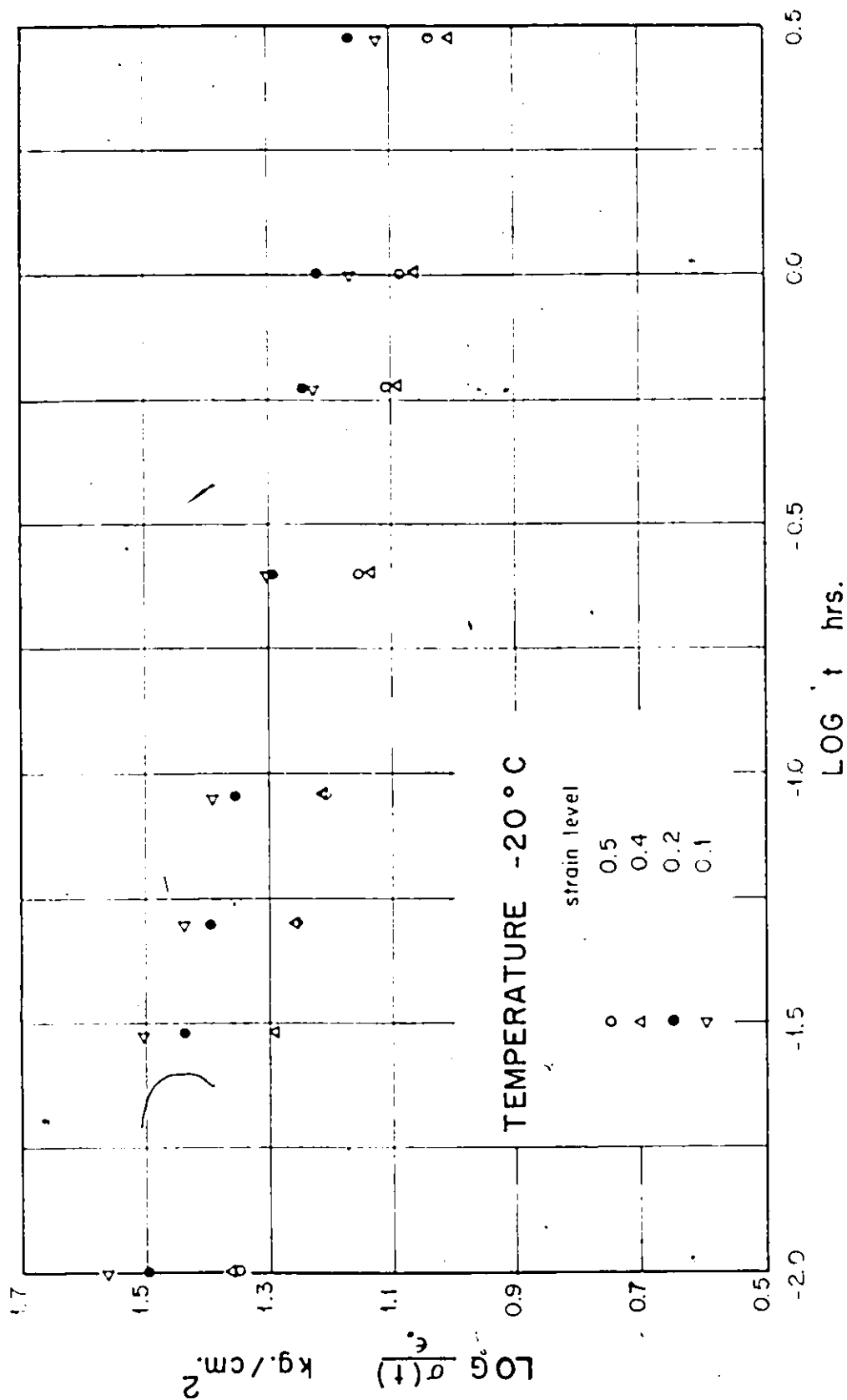


Figure 5.31 - Relaxation modulus versus time at -20°C

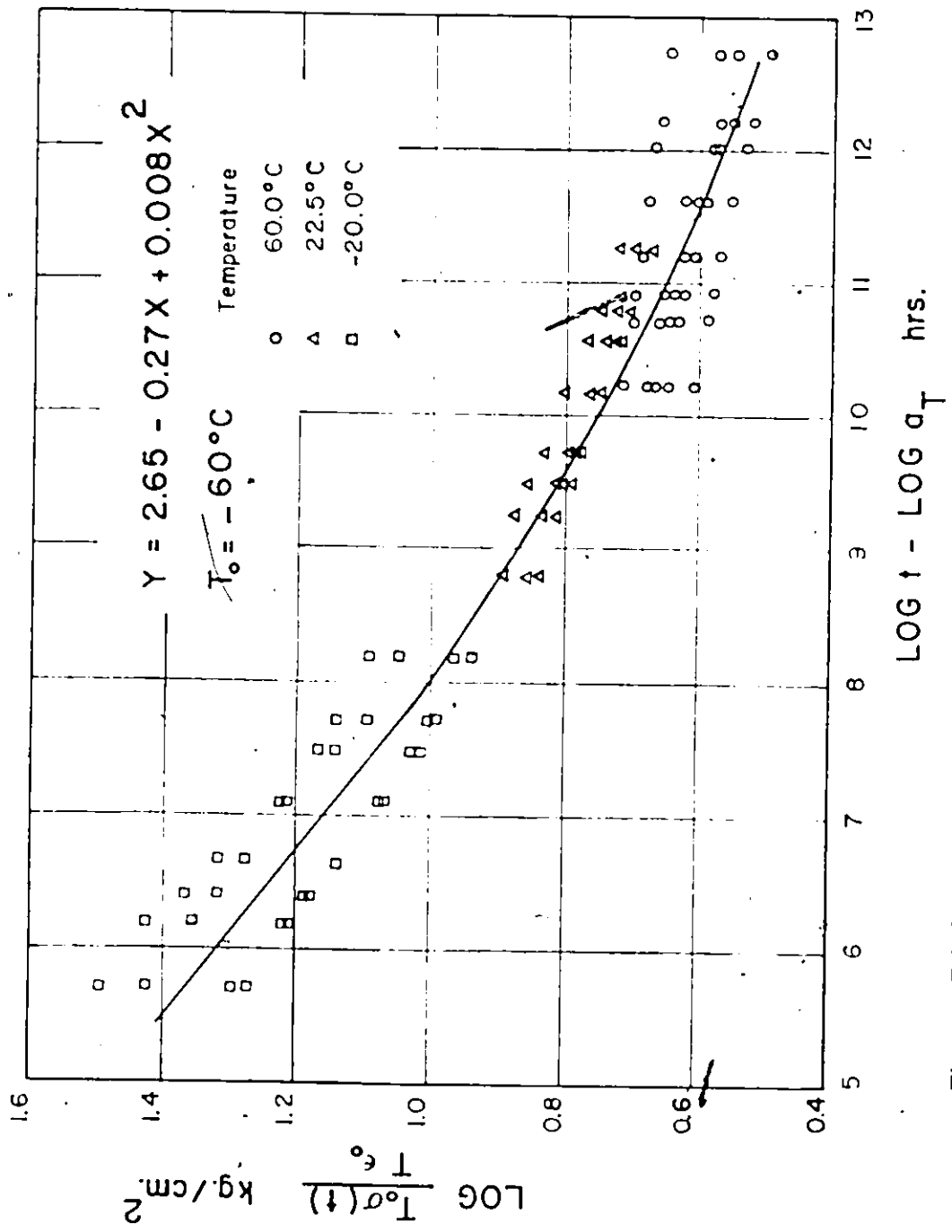


Figure 5.32 - Experimentally determined Master Curve from stress relaxation test results.



CHAPTER 6  
IN CONCLUSION

The study of the mechanical properties of urethane sealants has essentially been empirical for no adequate theory exists as yet which explains all the viscoelastic phenomena. The experimental program undertaken in this study was designed to characterize the mechanical properties of urethane sealants and the factors considered are as follows:

1. strain rate (tension tests)
2. temperature
3. priming
4. workmanship
5. strain level (stress relaxation tests)
6. substrate surface conditions

It is evident from the tests and analyses that the urethane sealants behave as viscoelastic materials for all temperatures and strain rates which are likely to be encountered in Canada. From this study, it can be concluded that urethane sealants which are one of the newest classes of materials to be used on joint fillers, are likely to prove satisfactory in service. However, *in situ* studies over a long period of time are required to confirm this initial assessment.

The tensile tests illustrate that strengths vary considerably with varying strain rates at constant temperature. The differences in the stress-strain curves at low strain rates were very small, below about 30%. At high strain rates, however, the curves differ considerably;

the higher the rate of elongation, the higher the ultimate tensile strength. Analysis of these curves on the basis of constant strain rate reveals that tensile strength decreases with increasing temperature.

The occurrence of failure points showed that these are arranged in a broad band, which for load at break as a function of temperature increases moderately for decreasing temperature until at about  $-40^{\circ}\text{C}$ , when larger increases are found. The implication of these findings is that the urethane can withstand large loads caused by excessive extensions due to lowering of temperature. This is a definite advantage since the material must undergo increasingly more extension, as the temperature decreases.

The tests on the effect of priming and of substrates were not extensive, therefore, the results presented here should be considered only as an indication of their effect upon sealant behaviour.

Adhesive properties were not considered here, however, some of the preliminary conclusions from this test program can be summarised. The urethane has sufficiently good adhesive properties when extruded on primed aluminium substrates or unprimed wood, but not on unprimed aluminium or mortar (no conclusions about glass substrates will be drawn at this point). If the lack of adhesion in the mortar and unprimed aluminium substrates is discounted, it does not seem to affect the tensile properties (such as shape of curve, etc.) unduly. As substrate, primed aluminium is adequate in determining the mechanical properties of the material because its strength is high enough and the type of failure in the sealant is not camouflaged by a failure in the substrate.

Closely allied to the problem of substrates is that of workmanship. It is possibly the most important factor affecting the performance of the material. It can be seen from the number of tests repeated because of poor priming, but more importantly, from the inclusion of bubbles, with the application of the sealant by means of the caulking gun. The bubbles, whether at the interface between the sealant and the substrate or within the material have the effect, which is often attributed to cracks, of concentrating stresses at their tips and causing premature failure (i.e., at lower than anticipated ultimate strength). A study of the occurrence of bubbles in actual joints as well as a more thorough study of their effect on material behaviour could prove to be beneficial to applicators and designers.

It has been demonstrated during the course of this study that the theoretical considerations developed for linear viscoelastic materials can be applied to urethane sealants with acceptable accuracy. The verification of this assertion was that individual tensile curves obtained with the specimens at different strain rates could be superimposed on a single cumulative curve at each temperature (Note: the regression analyses reported in the previous chapter.) Since urethane sealants have been shown to be temperature dependent, the superposition of the cumulative graphs to a single master curve verifies the assumption that temperature effects can be considered in terms of time is valid. The use of a shifting factor corroborates the findings of other researchers in this field.

The stress relaxation experiments confirm the conclusions drawn from tensile tests and demonstrate well a quality which is advantageous for sealants in actual use, that is, the diminution of stresses with time thus ensures adequate performance over a long period once the initial stresses imposed by deformation are resisted.

The increase in stress with increments in initial strain levels are to be expected as is the decrease in stress at specific strain levels with increase in temperatures. The superposition of the stress relaxation curves at different strain levels at given temperatures within tolerable ranges of accuracy confirm the validity of the generalized Maxwell model in modelling the performance of urethane sealants. The validity of time-temperature superposition principle is also confirmed by the development of the stress relaxation master curve.

The urethane sealants, in brief, display the most important characteristics which a sealant should possess, they are, capability of sustaining movement within a large range of temperature and deformation rates and adequate adhesive properties when properly applied. This observation has led to the proposition of an improved method of joint design in which use is made of the information generated here.

The proposal made in this study provides (i) a *raison d'être* for the present and similar research programs and (ii) the type of information which manufacturers should give and designers use if improvements in construction practice should follow the remarkable developments in modern sealant materials.

The design method outlined in the study makes use of predictions of the failure of sealants under practical conditions from the results of laboratory tensile testing. Predictions are possible because background information (such as joint movements, rates of deformation and temperature conditions) can be applied successfully to the model specimens. Information from the stress-strain curves at various temperatures and strain rates are represented in the form of a master curve which, together with the failure envelope (stress versus temperature plot) can be used to predict failure. Thus, the material properties can be characterized by the primary variables (stress, strain, time and temperature) as well as the failure envelope. The general applicability of the shifting factors (i.e., the WLF equation) to this and other sealants make the case for the improved design method more compelling yet.

CHAPTER 7

FURTHER RESEARCH

On the basis of the research work of this thesis, it is suggested that the following should be considered for further research.

- (A) Mechanical properties of other sealants. This is suggested in order to obtain a master curve and also failure envelope to be used for design purposes.
- (B) Response behaviour (macroscopic):
  - (i) Investigation of the effect of tensile load and cyclic temperatures upon sealants response; also the effects due to combined load and thermal cycling.
  - (ii) Investigation of workmanship, quality control etc., on the mechanical properties of sealants.
  - (iii) Investigation of batch difference.

Experimental work can be undertaken to simulate practical environment loading conditions. Tests can also be conducted to simulate complex states of stress. This may be achieved by superposition of simple stresses of various intensities. The dependence of material parameters such as elastic, shear, relaxation moduli on the state of stress and the temperature can also be determined.

- (C) Adhesion studies on sealants:
  - (i) A sealant-joint is quite complex and consists of at least five distinct areas, two adherents, two boundary layers, and a bulk sealant. A thorough study is required to understand the dependence of the macro-properties of the sealant-joint on the

inherent microstructure. Experimental and theoretical analyses are also required to investigate the nature of bonding that occurs at the interface between the sealant and the substrate.

It might be possible to incorporate agents capable of increasing the binding strength.

- (ii) A correlation between cohesive and adhesive failures is required, particularly in relation to the microstructure and test conditions. This will enable the prediction of time-dependent bond-rupture during specimen loading as well as final fracture.

BIBLIOGRAPHY

1. ASTM, "Test for Adhesion and Cohesion of Elastomeric Joint Sealants Under Cyclic Movements", Vol. 18, C719, 1977.
2. Canadian Government Specification Board, "Standard for: Methods of Testing Putty, Caulking and Sealing Compounds", 19-GP-OM, April 1976.
3. Castiff, E., Hoffman, R.F. and Kowalski, R.T., "Predicting Sealant Performance through Computers", Building Research, April/June 1974.
4. Cook, J.P., "The Effect of Specimen Length on the Laboratory Behaviour of Sealants", Highway Research Board, Jan. 1965.
5. Dietz, A.G.H., in Introduction to "Building Seals and Sealants", Panek, J. (Ed.), American Society for Testing and Materials, ASTM, STP606, 1976.
6. Distéfano, N., Todeschini, R., "Modelling, Identification and Prediction of a Class of Nonlinear Viscoelastic Material (I)", Int. J. Solids Structures, Vol. 9, 1973, pp. 805-818.
7. Dumasis, A., "Sealants", Reinhold Publishing Corp., 1967.
8. DTA Manual
9. Haddad, Y.M., "Mathematical Modelling in the Realm of Nonlinear Viscoelasticity", Proceedings of Conference . . . 1977, p. 847-857.
10. Handegord, G.O. and Karpati, K.K., "Joint Movement and Sealant Selection", CBD155, NRC 1973.
11. Karpati, K.K., "Literature Survey of Sealants", Journal of Paint Technology, Vol. 40, No. 523, August 1968, pp. 337-347 (also Technical Paper No. 287 of the Division of Building Research, National Research Council of Canada, NRC 10424).
12. Karpati, K.K., "Mechanical Properties of Sealants: I Behaviour of Silicone Sealants as a Function of Temperature", J. Paint Technology, Vol. 44, No. 565, Feb. 1972, pp. 55-62.
13. Karpati, K.K., "Mechanical Properties of Sealants: II Behaviour of Silicone Sealants as a Function of Rate of Movement", J. Paint Technology, Vol. 44, No. 569, June 1972, pp. 58-66.



14. Karpati, K.K., "Mechanical Properties of Sealants: III Performance Testing of Silicone Sealants", J. Paint Technology, Vol. 44, No. 571, Aug. 1972, pp. 75-85.
15. Karpati, K.K., "Mechanical Properties of Sealants: IV Performance Testing of Two-part Polysulphide Sealants", J. Paint Technology, Vol. 45, No. 580, May 1973, pp. 49-57.
16. Karpati, K.K., "Extension Cycling of Sealants", Proceedings, XII<sup>th</sup> FATIPEL Congress, May 1974, pp. 455-459.
17. Karpati, K.K., Gibbons, E.V., "Experimental Prediction of Joint Movements in Buildings", Materials Research and Standards, Vol. 10, No. 4, April 1970, p. 16, and, also NRCC 11311.
18. Karpati, K.K., Solvason, K.R. and Sereda, P.J., "Weathering Racks for Sealants", J. Coatings Technology, Vol. 49, No. 626, March 1977.
19. McClintock, F.A. and Argon, A.S. (Eds.), "Mechanical Behaviour of Material", Addison-Wesley, 1966.
20. Panel, J., "A Review of Sealant Specifications throughout the World", in Panek, J. (Ed.), "Building Seals and Sealants", American Society for Testing and Materials, ASTM, STP606, 1976.
21. Peterson, C.M., "Problems of Testing Sealants", in Damusis, A. (Ed.), "Sealants", Reinhold Publishing Corp. 1967.
22. Private discussion with technicians at DBR/NRC, April 1978.
23. Ralls, K.M., Courtney, T.H. and Wulff, J., "Introduction to Material Science and Engineering", John Wiley and Sons, 1976.
24. Ryder, J.F., Baker, T.A., "The Extent and Rate of Joint Movement in Modern Buildings", Building Research Station, CP2/71, Jan. 1971.
25. Smith, T.L., "Viscoelastic Behaviour of Polyisobutylene under Constant Rates of Elongation", J. of Polymer Science XX (1956), pp. 89-99.
26. Tobolsky, A.V., "Properties and Structure of Polymers, John Wiley and Sons, 1967.
27. Trelour, I.R.G., "The Physics of Rubbery Elasticity", Clarendon Press, Oxford, 1958.
28. Volterra, V., "Fonctions de Lignes", Gauthier-Villard, Paris, 1913.
29. Williams, M.L., Landel, R.F. and Ferry, J.D., "The Temperature Dependence of Relaxation Mechanisms in Amorphous Polymers and other Glass-forming Liquids", J. Am. Chem. Soc. LXXVII, 1955, pp. 3701-3707 (1955).